MULTI-ENZYME SYSTEM FOR THE RAPID METABOLISM OF ETHANOL: KINETICS AND CONJUGATION WITHIN pH-SENSITIVE HYDROGEL

by

Matthew W. Eggert

A thesis submitted to the Graduate Faculty of
Auburn University
in partial fulfillment of the
requirements for the Degree of
Master of Science

Auburn, Alabama
May 7, 2012

Keywords: Enzyme Conjugation, Enzyme Kinetics, Ethanol Metabolism, Biofunctional Polymers, Multiple Enzyme Microreactors, Therapeutic Enzyme Delivery

Approved by
Robert P. Chambers, Co-Chair, Professor of Chemical Engineering
Mark E. Byrne, Co-Chair, Daniel F. & Josephine Breeden Associate Professor of Chemical Engineering
Yoon Y. Lee, Uthlaut Family Professor of Chemical Engineering

ABSTRACT

Biohybrid materials, or materials utilizing biological molecules in their rational design, are prime therapeutic carrier candidates to perform detoxification processes. Specifically, catabolic processing of alcohol is a significant component of the glycolytic pathway to yield energy from alcohol. Moreover, the process is crucial to preventing toxic buildup of ethanol and its unstable, free-radical forming byproduct acetaldehyde. Our work introduces a biomimetic hybrid hydrogel structure capable of facilitating efficient ethanol conversion through enzymes delivered to the body. A multi enzyme system, composed of alcohol (ADH) and aldehyde (ALDH) dehydrogenases for conversion of ethanol to non-toxic acetate coupled with lactate dehydrogenase (LDH) for cofactor recycling, was kinetically defined by our research group with experimental data and simulations to provide rapid conversion of ethanol. The system at desired enzyme concentrations overcomes substrate and product inhibitions to metabolize ethanol at rates seven times faster than the human body.

A system involving the covalent attachment of ADH to a poly(MAA-co-PEG200MA-co-PEG200DMA) pH-sensitive network via UV free-radical polymerization following functionalization of the enzyme amino groups with acryloyl chloride was also thoroughly studied. After monitoring individual enzyme activity during each fabrication step, the enzyme-enhanced polymer system shows activity retentions up to 26%. Stability testing of the polymer-conjugated enzymes under pH cycles (pH 4.0-7.5)

demonstrates minor loss of activity and establishes protective capability of the hydrogel matrix against proteolytically harsh environments. This novel enzyme system and the demonstration of enzyme stability within a biocompatible hydrogel network emphasize the tremendous, emerging potential of multi-enzyme biofunctional gels.

ACKNOWLEDGEMENTS

I would like to thank foremost my graduate advisors, Dr. Robert Chambers and Dr. Mark Byrne, for their supply of knowledge, wisdom, guidance, and support throughout my academic career at Auburn University. From their creativity and passion, I have been enriched with experience and technical knowledge far beyond what I could hope to attain from just one advisor. They have been a wonderful inspiration in my academic pursuits, and I hope for continued collaboration with them well into the future. I would also like to thank Dr. Yoon Lee for his part in my committee. His background in bioprocess and enzyme technology was very helpful in the evaluation of my work. Additionally, I thank Dr. Thomas Hanley for his advice and input as well. I would like to extend gratitude to Dr. Christopher Roberts for his continual academic advice and direction and to the entire Auburn chemical engineering faculty and staff who have contributed greatly to my education.

I greatly appreciate all my Auburn graduate and undergraduate colleagues past and present, who have been a source of collaboration, encouragement, and motivation. I hope the time spent working (and playing) together may provide fruitful collaborations and joyful time spent reminiscing in the future. To my closest high school friends, and college friends at Tulane and beyond, I hope you understand how grateful I am for the friendship and support you have provided to me. All of you have helped me enjoy my education so much and so much more. I hope you know who you are. Also, to all my

friends in Auburn, you have made my time here more memorable than I could have ever imagined.

Most importantly, I would like to thank my parents and family. They are my true source of knowing God's blessings. I would not be the same person or in the position I am today without their constant, love, faith, support and encouragement. Mom and Dad, I appreciate *everything* you've done for me. Thanks for helping me always reach continually higher in education. Martin and Kathryn, I hope you're proud of your little brother, and I hope you know how important you are to me. I always miss spending time with you the most, but I know deep down you always understand. Grandma and Gramps, I dedicate this accomplishment to you. Thank you for always seeing the potential in me. I cannot think of any accomplishment I've achieved without thinking of you, Sabrina, Maw-Maw, and Pam-Paw. And to my youngest family member, my neice, Audrey, I hope my work can be an inspiration for you to pursue engineering, science (or math), and lofty educational goals.

Finally, I gratefully acknowledge funding and support from Auburn University and U.S. Department of Education GAANN Fellowship: Grant #P200A060184.

TABLE OF CONTENTS

Abstract ii

Acknowledgments iv

List of Figures x

1. Introduction 1

2. Literature Review 4

    2.1 The Human Impact of Ethanol 4

    2.2 Ethanol Detoxification 6

    2.3 Therapeutic Enzyme Carriers 10

    2.4 References 13

3. Impact of High Pyruvate Concentration on Kinetics of Rabbit Muscle Lactate Dehydrogenase 16

    3.1 Materials and Methods 17

        3.1.1 Chemicals and Enzymes 17

        3.1.2 Enzyme Activity and Kinetics 18

        3.1.3 Development of Kinetic Rate Expression 19

        3.1.4 Kinetic Expression Terms and Constant Determination 20

    3.2 Results and Discussion 20

        3.2.1 Substrate Inhibition of Lactate Dehydrogenase by Pyruvate and Pyrvate-Coenzyme Ternary Complex 20

3.2.2 Product Inhibition of LDH by L-lactate in Response to Pyruvate Concentrations 24

3.3 Conclusions....26

3.4 Figures....27

3.5 References....32

4. Kinetic Involvement of Acetaldehyde Substrate Inhibition on the Rate Equation of Yeast Aldehyde Dehydrogenase 34

4.1 Material and Methods 36

4.1.1 Chemicals and Enzymes 36

4.1.2 Enzyme Activity and Kinetics 36

4.1.3 Development of Kinetic Rate Expression....37

4.1.4 Kinetic Expression Terms and Constant Determination....38

4.2 Results and Discussion 38

4.2.1 Substrate Inhibition of Aldehyde Dehydrogenase by Acetaldehyde and Acetaldehyde-Coenzyme Ternary Complex....38

4.3 Conclusions....43

4.4 Figures....44

4.5 References....49

5. Analysis of the Three Dehydrogenase System 51

5.1 Materials and Methods....52

5.1.1 Chemicals and Enzymes 52

5.1.2 Enzyme Activity Assays....52

5.1.3 Multi-Enzyme Concentration Assay....53

5.1.4 Methods of Simulation....53

5.2 Individual Enzyme Kinetics....54
5.2.1 Alcohol Dehydrogenase Kinetic Studies....54
5.2.2 Aldehyde Dehydrogenase Kinetic Studies....55
5.2.3 Lacate Dehydrogenase Kinetic Studies....56
5.2.4 Single Enzyme Kinetic Analysis....57
5.3 Two Enzyme Kinetic Analysis....59
5.4 Three Enzyme Kinetics....60
5.4.1 Kinetic Analysis....60
5.4.2 Experimental vs. Simulation Comparison of Multi-Enzyme Kinetics and Three Enzyme Optimization....62
5.5 Conclusions....64
5.6 Figures....65
5.7 References....83
6. Incorporation of Alcohol Dehydrogenase by Convalent Conjugation into pH Sensitive PEG-g-MAA Hydrogel....84
6.1 Materials and Methods....85
6.1.1 Materials....85
6.1.2 Enzyme Activity Assays....86
6.1.3 Enzyme Functionalization....87
6.1.4 Enzyme Filtration....87
6.1.5 Hydrogel Formation....87
6.1.6 Gel Swelling....88
6.1.7 ADH Ultraviolet Exposure Testing....88
6.1.8 pH Cycling Activity....89

6.2 ADH Investigation 89
6.2.1 UV Influence on Activity of ADH 89
6.2.2 Hydrogel Formation Impact on ADH Activity 91
6.2.3 Swelling Studies 92
6.2.4 pH and Stability Testing of ADH Activity in Hydrogel 93
6.3 Conclusions 94
6.4 Figures 95
6.5 References 101
7. Conclusions and Future Direction 103
APPENDIX A – Detailed Assays and Standardizations 105
APPENDIX B – Visual Basic Three Enzyme Simulation 110

LIST OF FIGURES

Figure 3.1 Lactate Dehydrogenase – Classic kinetics of rate vs. substrate 27

Figure 3.2 Lactate Dehydrogenase – Effect of ternary complex conc. on rate.....28

Figure 3.3 Lactate Dehydrogenase – Linear relationship of rate to inhibition term.....29

Figure 3.4 Lactate Dehydrogenase – Effect of lactate product inhibition on rate 30

Figure 3.5 Lactate Dehydrogenase – Correlation of model and experimental values.....31

Figure 4.1 Aldehyde Dehydrogenase – Classic kinetics of rate vs. substrate.....44

Figure 4.2 Aldehyde Dehydrogenase – Effect of ternary complex conc. on rate.....45

Figure 4.3 Aldehyde Dehydrogenase – Effect of NADH product inhibition on rate 46

Figure 4.4 Aldehyde Dehydrogenase – Linear relationship of rate to inhibition term.....47

Figure 4.5 Aldehyde Dehydrogenase – Correlation of model and exper. values 48

Figure 5.1 Alcohol Dehydrogenase – Classic kinetics of rate vs. substrate 65

Figure 5.2 Alcohol Dehydrogenase – Classic kinetics of rate vs. inhibiting product.....66

Figure 5.3 Alcohol Dehydrogenase – Lineweaver-Burke for product inhibition.....67

Figure 5.4 Alcohol Dehydrogenase – Inhibited vs. basic modeled rate equation.....68

Figure 5.5 Modeled Substrate Inhibition of ALDH and LDH.....69

Figure 5.6 Modeled Substrate-Product Inhibition of ALDH and LDH 70

Figure 5.7 Two Enzyme Model – ADH and ALDH concentration profile of acetaldehyde intermediate at varying initial acetaldehyde concentrations.....71

Figure 5.8 Two Enzyme Model – ADH and ALDH concentration profile of ethanol at varying initial acetaldehyde concentrations.....72

Figure 5.9 Two Enzyme Model – ADH and LDH concentration profile of acetaldehyde at varying initial pyruvate concentrations 73

Figure 5.10 Three Enzyme Model – Concentration profile of acetaldehyde at varying initial acetaldehyde concentrations 74

Figure 5.11 Three Enzyme Model – Concentration profile of ethanol at varying initial acetaldehyde concentrations 75

Figure 5.12 Three Enzyme Model – Concentration profile of acetaldehyde at varying initial pyruvate concentrations 76

Figure 5.13 Three Enzyme System – Conversions w/ LDH at 30% of enzyme conc 77

Figure 5.14 Three Enzyme System – Conversions w/ LDH at 50% of enzyme conc 78

Figure 5.15 Three Enzyme Simulation – Ethanol conversion for various concentrations of enzyme using full kinetic equations 79

Figure 5.16 Three Enzyme Simulation – Ethanol conversion for various concentrations of enzyme using uninhibited kinetic equations 80

Figure 5.17 Three Enzyme Simulation – Acetaldehyde concentration for various concentrations of enzyme using full kinetic equations 81

Figure 5.18 Three Enzyme Simulation – Acetaldehyde concentration for various concentrations of enzyme using uninhibited kinetic equations 82

Figure 6.1 Effect of UV exposure on free ADH activity at different temperatures 95

Figure 6.2 Effect of UV exposure on free ADH activity for extended times 96

Figure 6.3 Recovered ADH enzyme from filtration following functionalization 97

Figure 6.4 Activity analysis of ADH for hydrogel conjugation 98

Figure 6.5 MAA/PEGMA hydrogel swelling studies 99

Figure 6.6 pH cycling activity of hydrogel conjugated ADH 100

Figure A.1 Standardization curve of 340nm absorbance vs. NADH conc 106

Figure A.2 Standardization curve of 280nm absorbance vs. ADH conc 107

Figure A.3 Rate activity determination for L-lactate dehydrogenase 109

CHAPTER 1

INTRODUCTION

While drinking alcoholic spirits has been common for over 10,000 years, ethanol and its metabolic product, acetaldehyde, are known to have adverse effects on the liver and the central nervous system. Today, the pervasive problem of driving under the influence of alcohol results in over 15,000 deaths and nearly 1.1 million injuries yearly, accounting for 37% of vehicular related accidents, according to the National Highway Transporation Safety Administration. Currently, no effective method for the reduction of systemic alcohol exists short of stomach aspiration and gastric lavage, charcoal absorption and/or blood or peritoneal dialysis, all of which are normally performed in a clinical environment by a skilled medical practitioner. There is a great need for a new approach that could provide effective, rapid lowering of ethanol blood levels for alcohol-impaired individuals prior to driving.

The general goals of this research project were as follows: (1) to determine the kinetics of a three enzyme system consisting of alcohol, aldehyde, and lactate dehydrogenases in vitro and assess the system's effectiveness in lowering a 22mM ethanol concentration within a therapeutically efficient time of 20-30 minutes; and (2) to fabricate a polymeric hydrogel carrier capable of retaining the three enzymes within the matrix structure, protecting the enzymes from harsh acidic environments, maintaining protein activity, and providing adequate loading to meet metabolic demands.

We hypothesized that we could meet the goals emphasized above by choosing a system involving commercially available enzymes, conduct individual enzyme kinetics to build a microreactor model, utilize the model for optimizing the quantity of enzyme required and for determining the effectiveness of the three enzyme combination at various critical component concentrations, and employing a poly(methacrylic acid-grafted-ethylene glycol) hydrogel that complexes and expands due to pH induced ionic interactions in aqueous buffer media.

The following chapters aim to provide analysis of the design and experimentation of the developed system. Chapter 2 is a literature review that details the biological impact and metabolism of ethanol, a look at enzyme candidates for use in the catabolism of ethanol, and an overview of polymeric supports that are used for immobilization of enzymes, specifically those that are more suited for biocompatible and therapeutic oral delivery. Chapters 3 and 4 contain the kinetic rate analysis of lactate dehydrogenase from rabbit muscle and aldehyde dehydrogenase from yeast, respectively. These enzymes exhibit unique forms of substrate inhibition that can potentially interfere in the rapid overall metabolism of ethanol. Chapter 5 presents reaction simulations based on the kinetic rate equations for the individual enzymes as well as the combined three enzyme microreactor. Additionally, the simulations are compared with in-vitro multi-enzyme experiments to evaluate the optimal concentrations and ratio of the necessary enzymes for the success of the system. Finally, Chapter 6 features the fabrication of a pH-responsive hydrogel with covalently bound alcohol dehydrogenase and details the functional activity of the hydrogel for converting ethanol.

The studies undertaken demonstrate the potential of responsive polymer structures

while also extending the functionality of a single hydrogel network. Novel enzyme polymer systems possessing concerted activity increase the promise of therapeutic designs for entire metabolic pathways.

CHAPTER 2

LITERATURE REVIEW

2.1 THE HUMAN IMPACT OF ETHANOL

Ethanol has been produced and consumed by humans in a diverse number of cultures for millennia, in the form of fermented and distilled alcoholic beverages. Commonly, alcohol plays a significant role in social interaction, but aside from pervasive use, chemically, ethanol is still a psychoactive drug that has a depressant effect reducing both attention and reaction speed at high alcohol blood content. Short-term effects of alcohol consumption include intoxication and dehydration. Long-term effects of alcohol include changes in the metabolism within the liver and brain and alcoholism (addiction).

Alcohol intoxication affects the brain, causing physical impairment in the form of slurred speech, clumsiness, and delayed reflexes. In the human body, ethanol affects the gamma-aminobutyric acid (GABA) receptors and produces a depressant (neurochemical inhibitory) effect. Ethanol is similar to other sedative-hypnotics such as barbiturates and benzodiazepines both in its effect on the $GABA_A$ receptor, although its pharmacological profile is not identical. It has anxiolytic, anticonvulsant, hypnotic, and sedative actions similar to many other sedative-hypnotic drugs. Ethanol is also cross-tolerant with benzodiazepines and barbiturates (1). Ethanol also binds to acetylcholine, serotonin, and NMDA receptors (2). Alcohol stimulates insulin production, which speeds up

glucose metabolism and can result in low blood sugar, causing irritability and (for diabetics) possible death.

Severe alcohol poisoning can be fatal. When compared to other alcohols, ethanol is only slightly toxic, with a lowest known lethal dose in humans of 1400 mg/kg (about 20 shots for a 100 kg person), and an LD_{50} of 9000 mg/kg (oral, rat), which is about six times the level of ordinary intoxication (0.08%). Nevertheless, accidental overdosing of alcoholic drinks, especially those containing a high percentage of alcohol, is risky, especially for women, lightweight persons, and children. These people have a smaller quantity of water in their bodies, so that the alcohol is less diluted. A blood alcohol concentration of 50 to 100 mg/dL (0.05 to 0.10% BAC) may be considered legal drunkenness (laws vary by jurisdiction). The threshold of effects is at 22 mg/dL (3). Vomiting or unconsciousness may occur much sooner in people who have a low tolerance for alcohol. The high tolerance of chronic heavy drinkers may allow some of them to remain conscious at levels above .40%, although serious health dangers are incurred at this level. Alcohol also limits the production of vasopressin (antidiuretic hormone) from the hypothalamus and the secretion of this hormone from the posterior pituitary gland. This is what causes severe dehydration when large amounts of alcohol are drunk. It also causes a high concentration of water in the urine and vomit and the intense thirst that goes along with a hangover.

Although at moderate usage, alcohol consumption has been known to reduce cardiovascular disease and increase longevity, significant overuse leads to a number of health issues ranging from alcoholism, dementia, diabetes, cancer, stroke, and ultimately death. A report of the United States Centers for Disease Control estimated that medium

and high consumption of alcohol led to 75,754 deaths in the U.S. in 2001. Low consumption of alcohol had some beneficial effects, so a net 59,180 deaths were attributed to alcohol (4). A study in Sweden found that 29% to 44% of "unnatural" deaths (those not caused by illness) were related to alcohol. The causes of death included murder, suicide, falls, traffic accidents, asphyxia, and intoxication (5). A global study found that 3.6% of all cancer cases worldwide are caused by alcohol drinking, resulting in 3.5% of all global cancer deaths (6).

2.2 ETHANOL DETOXIFICATION

In the human body, total alcohol removal from the bloodstream is by a combination of metabolism, excretion, and evaporation. The relative proportion disposed of in each way varies from person to person, but typically about 95% is metabolized by the liver. The remainder of the alcohol is eliminated through excretion in breath, urine, sweat, feces, milk and saliva (7). Ethanol is absorbed primarily by the tissues of the first part of the small intestine (duodenum) and to a lesser extent the tissue lining the stomach (gastric mucosa). The rate of ethanol absorption by the duodenum is between 7.5 and 85 times greater than the rate ethanol enters the blood from the stomach (8). Therefore, ethanol entering the duodenum is virtually instantaneously absorbed into the gastrointestinal tissues. Because ethanol does not bind proteins outside of enzymes in certain tissues, the alcohol quickly diffuses throughout the body's water fluid. For a 70kg male, the residence time of fluid within organ or system can be calculated based on water content (mL), blood flow (mL/min), and perfusion rate (blood flow rate/ H_2O volume = mL/min/mL H_2O), of which the inverse is residence time. These values are, respectively:

for stomach/intestine, 2400mL, 900mL/min, 0.375mL/min/mL H_2O, 2.67min; for liver, 1080mL, 1350mL/min, 1.25mL/min/mL H_2O, for blood, 2840mL, 5000mL/min, 1.76mL/min/mL H_2O, 0.57min; and brain, 1030mL, 700mL/min, 0.68mL/min/mL H_2O, 1.47min (9). It should be noted that total blood volume is typically 5.0L and total fluid volume is nearly 41L. Therefore, following retention time in each tissue, excretion into urine typically begins after about 40 minutes, whereas metabolism commences as soon as the alcohol is absorbed, and even before alcohol levels have risen in the brain.

As mentioned, the burden of metabolism falls on the liver by use of enzymes. In the liver, the enzyme alcohol dehydrogenase oxidizes ethanol into acetaldehyde, which is then further oxidized into harmless acetic acid by acetaldehyde dehydrogenase. Acetic acid is esterified with coenzyme A to produce acetyl CoA. Acetyl CoA carries the acetyl moiety into the citric acid cycle, which produces energy by oxidizing the acetyl moiety into carbon dioxide. Acetyl CoA can also be used for biosynthesis. Acetyl CoA is an intermediate that is common in the metabolism of sugars and fats; it is the product of glycolysis, the breakdown of glucose.

The removal of ethanol through oxidation by alcohol dehydrogenase in the liver from the human body is limited. Hence, the removal of a large concentration of alcohol from blood may follow zero-order kinetics. This means that alcohol leaves the body at a constant rate, rather than having an elimination half-life. Many physiologically active materials are removed from the bloodstream (whether by metabolism or excretion) at a rate proportional to the current concentration, so that they exhibit exponential decay with a characteristic halflife. This is not true for alcohol, however. Typical doses of alcohol actually saturate the enzymes' capacity, so that alcohol is removed from the

bloodstream at an approximately constant rate. This rate varies considerably between individuals; persons below the age of 25, women, persons of certain ethnicities, and persons with liver disease may process alcohol more slowly (10, 11). Many east Asians (for example, about half of Japanese) have impaired acetaldehyde dehydrogenase; this causes acetaldehyde levels to peak higher, producing more severe hangovers and other effects such as flushing and tachycardia. Conversely, members of certain ethnicities that traditionally did not brew alcoholic beverages have lower levels of alcohol dehydrogenases and thus "sober up" very slowly, but reach lower aldehyde concentrations and have milder hangovers. Rate of detoxification of alcohol can also be slowed by certain drugs which interfere with the action of alcohol dehydrogenases, notably aspirin, fumes of certain solvents, many heavy metals, and some pyrazole compounds. Also suspected of having this effect are cimetidine (Tagemet), ranitidine (Zantac), and acetaminophen (Tylenol). These drugs increase the toxicity of alcohol.

Because enzymatic conversion forms a bottleneck in the metabolic process, there are typically few alternatives to prevent alcohol intoxication or even poisoning. Concentrations of blood alcohol can easily accumulate after ethanol ingestion has ceased due to continued absorption from the intestines. Clinically, no medicine is available that reduces blood alcohol, and often physicians can only provide supportive care to the body’s natural means of eliminating ethanol through liver enzymes. This supportive care may be in the form of activated carbon, which binds to toxins through its large surface area and disrupts intestinal absorption, or gastric lavage, which involves physically pumping out the contents of the stomach. Additionally, intravenous fluids and oxygen

may be supplied to prevent dehydration and support aerobic respiration. Still, these methods only serve to prevent increasing blood alcohol concentrations and fail to actively reduce them.

Currently, the only known substance that can increase the rate of metabolism of alcohol is fructose. The effect can vary significantly from person to person, but a 100g dose of fructose has been shown to increase alcohol metabolism by an average of 80% (12). Alcohol absorption can be slowed by ingesting alcohol on a full stomach. Spreading the total absorption of alcohol over a greater period of time decreases the maximum alcohol level, decreasing the hangover effect. Also, alcohol in non-carbonated beverages is absorbed more slowly than alcohol in carbonated drinks (13). Even with very slow absorption rates, greater than 80% absorption is expected to occur within 100 min (14).

An alternative solution to rapidly reducing ethanol concentrations is the implementation of a multi-enzyme supplement. Pioneer work by David Whitmire and Robert Chambers showed large concentrations of alcohol dehydrogenase, aldehyde dehydrogenase, and lactate dehydrogenase could be used in canine duodenal fluid to convert ethanol to acetate by as much as 34% and prevent acetaldehyde accumulation (15). Other potential enzymes for ethanol oxidation include catalase; however, intravenous quantities of hydrogen peroxide can be deadly. Glycerol dehydrogenase is also a substitutable enzyme for cofactor nicotinamide adenine dinucleotide regeneration. Moreover, a wide variety of sources for these enzymes offers potential systems with improved activity and substrate binding.

2.3 THERAPEUTIC ENZYME CARRIERS

Overcoming biological barriers is a necessary part of delivering any sort of enzyme or protein therapeutic through oral means. Primarily, enzymatic degradation is a concern by means of hydrolysis in the gastric environment of the stomach or through digestion by other enzymes within the intestines.

The most common method for protecting many oral medications in the stomach is enteric coating. Enteric coating is a generalized term that means the coating is insoluble, non-dispersible in, and impermeable to stomach fluids, thus not degrading until it reaches the small intestine (16). This is accomplished by using materials that do not degrade in acidic environments, but are degraded in higher pH 5-9 environments. Enteric coating usage has been proven numerous times to effectively deliver medications through the stomach. Generic enzyme supplements to aid in digestion of the intestinal track using lyophilized enzymes and enteric coating are available on the market; however, the effectiveness of the enzymes in remaining active are often unstudied. Specifically, for chronic pancreatitis, studies have shown tablet forms of enzymes to be effective in pancreatic pain relief while capsule forms were not, presumably due to intestinal region of release (17).

A more effective approach involves the use of biocompatible polymer carriers. Polymer carriers offer a large versatility in both structures and properties that may be exhibited. A major reason for this versatility is the wide variety of monomers that may be used to form the polymer architectures. Furthermore, certain polymers contain chemical groups that have the ability to adapt accordingly to its current environment resulting in a change of properties in the overall polymer itself. These polymers are

referred to as responsive or “smart polymers” (18). This corresponding change in properties results in the release of therapeutics. These polymers may be ideal for protein transport through the stomach.

Specifically, pH sensitive hydrogels, in reference to oral drug delivery, are hydrophilic polymers that have the ability to stay tightly bound in gastric (acid) conditions and expand in intestinal (pH 5-8) conditions. The underlying principle behind the majority of pH sensitive hydrogels for the purpose of drug delivery via enteric routes includes two different monomers; one monomer having an atom that contains free electrons that readily form hydrogen bonds (electronegative atoms) and the other containing an acidic group with a pKa in the range of 3.5-5. In gastric conditions, the acidic group is protonated, carrying a slight positive charge, where the chained monomers can form a hydrogen bond keeping a tightly bound structure throughout the polymer. While in intestinal conditions, the acidic group is not protonated, causing the group to be partially electronegative, which causes separation between the polymer chains. Water is attracted to the unprotonated acidic group and will increasing swelling of the hydrogel. Numerous publications show that this technology is effective at transporting proteins through the stomach and into the small intestine (19, 20). Furthermore, the number of repeating ethylene glycol units in the PEG chains, as well as methacrylic acid:ethylene glycol monomer ratio, crosslinker fraction and solvent fraction may be changed to create a controlled release profile from the hydrogel (21, 22). If a faster release profile is desired, a poly(methacrylic acid-*co*-*N*-vinyl pyrrolidone) system has shown to have 90% release of growth hormone after 45 min under simulated intestinal pH, whereas the

P(MAA-g-PEG) system takes around 180 minutes to achieve the same percent release (23).

Aside from structural material for use in delivery of the bioactive element, there are many methods, such as adsorption, entrapment, covalent binding, etc., for enzyme immobilization (24–26). Covalent binding to an insoluble support is an attractive enzyme immobilization methodology because it combines the high selectivity of the enzymatic reactions with the desirable chemical and mechanical properties of the support (27, 28) When the support contains the relevant functional groups, covalent immobilization of enzymes becomes feasible. These functional groups include amino, hydroxyl, carboxyl and phenolic groups (29).

2.4 REFERENCES

1. Galanter, Marc; Kleber, Herbert D. (2008). The American Psychiatric Publishing Textbook of Substance Abuse Treatment United States of America. 4th ed. American Psychiatric Publishing Inc., p. 114.

2. Eckardt, M. J., File, S. E., Gessa, G. L., Grant, K. A., Guerri, C., Hoffman, P. L., Kalant, H., Koob, G. F., Li, T.-K. and Tabakoff, B. (1998). Effects of Moderate Alcohol Consumption on the Central Nervous System. Alcoholism: Clinical and Experimental Research, 22, 998–1040.

3. Stewart, S. (1996). Alcohol abuse in individuals exposed to trauma: A critical review. Psychological Bulletin, 120, 83-112.

4. Bouchery EE, Harwood HJ, Sacks JJ, Simon CJ, Brewer RD. (2011). Economic costs of excessive alcohol consumption in the United States, 2006. Am J Prev Med, 41, 516–24.

5. Sjögren, H., Eriksson, A., Ahlm, K. (2001). Role of alcohol in unnatural deaths: a study of all deaths in Sweden. Alcoholism, clinical and experimental research, 24(7), 1050-6.

6. Schütze M, Boeing H, Pischon T, *et al*. (2011). Alcohol attributable burden of incidence of cancer in eight European countries based on results from prospective cohort study. Br Med J, 342, 1584.

7. Baselt, R.C. (2011). Disposition of Toxic Drugs and Chemicals in Man, 9th edition, Biomedical Publications.

8. Wilkinson, P. K., Sedman, A. J., Sakmar, E., Kay, D. R., & Wagner, J. G. (1977). Pharmacokinetics of ethanol after oral administration in the fasting state. J. Pharmacokinet Biopharm., 5, 207–224.

9. Rowland, M., Tozer, T. N., & Rowland, R. (1995). Clinical Pharmacokinetics: Concepts and Applications (3rd ed.). Lippincott, Williams & Wilkins, Philadelphia.

10. Thomasson, H. (2002). Gender Differences in Alcohol Metabolism: Physical Responses to Ethanol. Recent Developments in Alcoholism, 12 (2), 163-179.

11. Xiao, Q., Weiner, H., Crabb, DW. (1996). The mutation in the mitochondrial aldehyde dehydrogenase (ALDH2) gene responsible for alcohol-induced flushing increases turnover of the enzyme tetramers in a dominant fashion. J. Clin. Invest. 98 (9): 2027–32.

12. Mascord, D., Smith, J., Starmer, G.A., Whitfield, J.B. (1991). The effect of fructose on alcohol metabolism and on the [lactate]/[pyruvate] ratio in man. Alcohol 26: 53–59.

13. Roberts, C., and Robinson, S.P. (2007). Alcohol concentration and carbonation of drinks: The effect on blood alcohol levels. Journal of Forensic and Legal Medicine 14 (7): 398–405.

14. Levitt, M. D., Li, R., DeMaster, E. G., Elson, M., Furne, J., & Levitt, D. G. (1997). Use of measurements of ethanol absorption from stomach and intestine to assess human ethanol metabolism. Am J Physiol 273(4 Pt 1), 951–957.

15. Whitmire, D. R., Chambers, R. P., Dillon, A. R. (1991). Multi-enzyme catalyzed rapid ethanol lowering in vitro. Alcoholism: Clin. and Exper. Res., 15(5), 804-807.

16. Clymer, H.A. (1951). Enteric Coating. US Patent 2,540,979.

17. Warshaw, AL, Banks, PA, Fernández-Del Castillo, C. (1998). AGA technical review: treatment of pain in chronic pancreatitis. Gastroenterology, 115 (3), 765–76.

18. Schmaljohann, D. (2006). Thermo- and pH-responsive polymers in drug delivery. Adv. Drug Del. Reviews. 58, 1655-1670.

19. Wu, D.Q., Sun, Y.X., Xu, X.D., Cheng, S.X., Zhang, X.Z., and Zhuo, R.X. (2008). Biodegradable and pH-Sensitive Hydrogels for Cell Encapsulation and Controlled Drug Release. Biomacromolecules, 9, 1155–1162.

20. Carr, D.A. and Peppas, N.A. (2010). Assessment of poly(methacrylic acid-co-N-vinyl pyrrolidone) as a carrier for the oral delivery of therapeutic proteins using Caco-2 and HT29-MTX cell lines. Journal of Biomedical Materials, Feb, 504-512.

21. Peppas, N.A., Keys, K.B., torres-Lugo, M., and Lowman, A.M. (1999). Poly(ethylene glycol)-containing hydrogels in drug delivery. J. Control. Release, 62, 81-87.

22. Peppas, N.A., Huang. Y., Torres-Lugo, M., Ward, J.H., and Zhang, J.(2000). Physicochemical Foundations and Structural Design of Hydrogels in Medicine and Biology. Annu. Rev. Biomed. Eng., 9-29.

23. Carr, D.A., Gomez-Burgaz, M., Boudes, M.C., and Peppas, N.A. (2010). Complexation Hydrogels for the Oral Delivery of Growth Hormone and Salmon Calcitonin. Ind. Eng. Chem. Res., 49, 11991–11995.

24. Woodward, J. (1985). Immobilized enzymes: adsorption and covalent coupling. In: Immobilized Cells and Enzymes: A Practical Approach, Oxford, UK, 3–17.

25. Soni, S., Desai, J.D., and Devi, S. (2001). Immobilization of yeast alcohol dehydrogenase by entrapment and covalent binding to polymeric supports. J Appl Polym Sci, 82: 1299–1305.

26. Mateo, C., Palomo, J.M., Fernandez-Lorente, G., Guisan, J.M., Fernandez-Lafuente, R. (2007). Improvement of enzyme activity, stability and selectivity via immobilization techniques Enzyme Microb Technol, 40, 1451–1463.

27. Elvira, C., Gallardo, A.; Roman, J., Cifuentes, A. (2005). Covalent Polymer-Drug Conjugates. Molecules, 10, 114-125.

28. Hoffman, A.S., Stayton, P. (2007). Conjugates of stimuli-responsive polymers and proteins. Prog. Polym. Sci., 32, 922.

29. Brena, B.M., Batista-Viera, F. (2006). Immobilization of enzymes: a literature survey. Methods in Biotechnology, 22, 15-30.

CHAPTER 3

IMPACT OF HIGH PYRUVATE CONCENTRATION ON KINETICS OF RABBIT MUSCLE LACTATE DEHYDROGENASE

(Published online May 31, 2011 in Applied Biochemistry and Biotechnology, 165 (2), 676-686, DOI: 10.1007/s12010-011-9287-y under authorship of Matthew Warren Eggert, Mark E Byrne, and Robert P. Chambers)

The interconversion of pyruvate and lactate is an integral part of energy formation. During anaerobic respiration in muscle, the conversion of pyruvate to lactate by L-lactate dehydrogenase maintains energy production and regeneration of co-enzyme nicotinamide adenine dinucleotide (NAD^+) from its reduced form (NADH). LDH can participate in many multi-enzyme metabolic systems as an effective enzyme for regenerating NAD^+ from NADH. LDH is also potentially useful in the commercial production of poly(lactic acid). Kinetics play a critical role in enzyme activity, defining the concentrations of substrate and product at which binding processes occur and subsequently accounting for speed of conversion. Specifically, a comprehensive analysis of L-lactate dehydrogenase kinetics is studied here to investigate viability in larger enzymatic processes. By determining all inhibition factors present, a kinetic rate expression can be utilized to describe and understand concentration barriers that limit the overall reaction rate at high pyruvate concentrations.

Substrate inhibition of LDH, at pyruvate concentrations in excess of its Michaelis constant, is common characteristic in multiple sources and tissues. In the bi-substrate conversion of pyruvate and NADH to lactate and NAD, as pyruvate concentration

surpasses a certain minimum, a simultaneous decline in rate occurs. This inhibition was initially suggested to be caused by formation of a dead-end, "ternary" complex involving enzyme, pyruvate, and the oxidized cofactor (1). Subsequent studies indicated that inhibition is created when enzymatic coupling of the substrates leads to covalent joining of the C2 carbon of pyruvate with the C4 carbon on the oxidized nicotinamide ring, before it is released from the enzyme. The ternary formation has become better known as an E-NAD^+-Pyr adduct complex (2-5). Additional work promoted the idea of simple enzyme-pyruvate binary complexes and other inhibiting ternary complexes involving only cofactors (6, 7). Recently, the substrate binding has been examined with extremely small timescales to better understand the enzyme's intricate mechanics (8). Furthermore, genetic engineering has led to mutant LDH with substrate inhibition knockouts that can endure higher pryuvate concentrations but sometimes diminish substrate binding and turnover rate (9). In any instance, the presence of simple and complex substrate and product inhibitors necessitates the use of additional terms to a simple bi-substrate enzyme kinetic rate expression especially if large amounts of pyruvate are required for effective use of the enzyme. By creating a kinetic rate expression capable of accounting for each of the inhibiting complexes, our kinetic equation can be used to simulate systems that involve, and possibly require, the inhibiting pyruvate and/or lactate concentrations.

3.1 MATERIALS AND METHODS

3.1.1 Chemicals and Enzymes

All chemicals were purchased at the purest grade available from Sigma-Aldrich (St. Louis, MO) and Fluka (Milwaukee, WI). Lyophilized enzyme L-lactate

dehydrogenase (LDH, EC 1.1.1.27) from rabbit's muscle was also obtained from Sigma-Aldrich (St. Louis, MO). Purity of the enzyme was listed on the label as having a specific activity of 891 U/mg (pH 7.5, 37°C).

3.1.2 Enzyme Activity and Kinetics

L-lactate dehydrogenase activity was assayed spectrophotometrically at 340nm and 22 °C using a concentration of 2.3mM pyruvate and 0.12mM β-nicotinamide adenine dinucleotide, reduced disodium salt (NADH; $\varepsilon_{340} = 6.22\ mM^{-1}\ cm^{-1}$) as substrate and co-factor, respectively, in 200 mM-sodium, 90 mM potassium, 150mM phosphate buffer pH 7.8, which is a modification of a published procedure (10). One unit of LDH activity was defined as the amount of enzyme converting 1.0 μmol of pyruvate per minute. The volumetric activity ($mM\ min^{-1}$) was defined as the enzyme activity per ml of enzyme solution for the free enzyme.

For kinetic determinations, a variety of substrate (pyruvate and NADH) and product (lactate and NAD) concentrations using the aforementioned buffer and temperature were investigated. All kinetic experiments were designed for the conversion of pyruvate to lactate. The kinetic experiments were divided into four sets wherein only two concentrations were varied per set while the intial concentration of the other components remained constant or zero. Pyruvate was varied against lactate to determine both lactate inhibition and pyruvate inhibition with lactate inhibition. Pyruvate was then also studied in the presence of different concentrations of reduced and oxidized cofactor to understand correlating effects: i) Pyruvate and cofactor substrate NADH concentrations were varied; ii) NADH and NAD variants were tested at an non-inhibiting concentration of pyruvate; and iii) pyruvate and cofactor product NAD were studied to

investigate inhibition of the adduct. A total of 85 different kinetic experiments were produced and repeated several times to eliminate possible error. Pyruvate concentrations up to 40mM and L-lactate concentrations as high as 100mM were studied. Cofactor concentrations exceeding common biological amounts were also employed since higher concentrations are often more relevant for biotechnical catalysis. Concentrations of NADH ranged from 0.1-0.45mM well above reported Michaelis-Menten constants of NADH from multiple LDH sources (11), while NAD concentrations ranged from 0 to 4mM. The rates of oxidation of NADH were carried out for 5 minutes, and the linear portion of the reaction progress curve was used to analyze the kinetics. Typically, the rates reported are from the first 15 seconds to 105 seconds, with concentrations from the median time (one minute) of the rate determination being used for kinetic analysis.

3.1.3 Development of Kinetic Rate Expression

In order to produce an accurate LDH kinetic rate expression for reacting pyruvate and NADH to lactate and NAD, kinetic parameters were necessary for all enzymatic steps over the concentrations of interest. For an enzymatic reaction mechanism involving two substrates, in which both interact with the enzyme before any product is released, a simple rate equation is obeyed (12):

$$\mathbf{v} = \frac{\mathbf{V_{max}(AB)}}{\mathbf{K_{ia}K_b + K_bA + K_aB + AB}} \tag{3.1}$$

where A is reduced cofactor concentration, B is the substrate concentration, and K_{ia}, K_a, and K_b are kinetic parameters, with K_{ia} denoting the dissociation of the substrate with enzyme. The mechanism of reaction also initially involves cofactor binding. The K_a and K_{ia} parameters were obtained from literature as kinetic experimental conditions were

typically above the cofactor saturating concentrations, i.e. nearly ten times the concentration of the binding constant. These values are 0.0107mM and 0.00842mM, respectively (13).

3.1.4 Kinetic Expression Terms and Constant Determination

Determination of kinetic terms was first approached by utilizing traditional plotting techniques, measuring inverse rates vs. substrate and/or inhibitory concentrations, in Microsoft Excel to verify linear or non-linear relationships. When possible, least square regressions of the linear plots were used to extract Michaelis-Menten constants or grouped terms that would fit into the general rate expression (detailed in later equations). Subsequently, multiple linear regressions were generated using JMP (version 8) statistical software from SAS Institute, Inc. (Cary, NC) using the rate data collected. Similarly, initial estimates of inhibition constants for terms were found by using the kinetic data at concentrations where that term had the most weighted significance in the kinetic rate expression.

3.2 RESULTS AND DISCUSSION

3.2.1 Substrate Inhibition of Lactic Dehydrogenase by Pyruvate and Pyruvate-Coenzyme Ternary Complexes

Preliminary experiments in our laboratory indicated that the enzyme is inhibited markedly by large pyruvate concentrations. Therefore, we determined the effect of increasing concentrations of pyruvate on LDH. Experimental results indicate the highest rate is at approximately 4.3mM pyruvate. At concentrations significantly above 4.3mM pyruvate, activity is less than 50% of the maximum (Figure 3.1A). In addition, inhibition

effects are observable above a 1mM pyruvate concentration. The K_b value, without substrate inhibition effects, determined by double reciprocal plots of the initial reaction velocity against the concentration of pyruvate is 0.216mM. The value matches well with literature (13) and is among the lowest pyruvate kinetic constant of various vertebrate sources (11, 14). While the effect of pyruvate alone is apparent on the reaction rate, the inhibition is also dependent on the cofactor binding and formation of ternary complexes.

To investigate the effect of ternary complexes formed by the pyruvate substrate, L-lactate dehydrogenase, and both coenzymes, kinetic experiments at non-inhibiting pyruvate concentrations as well as higher inhibiting pyruvate concentrations were analyzed. NADH cofactor concentrations were studied against inhibiting pyruvate concentration up to 40mM. Below saturating cofactor substrate concentrations, first order rate increases are expected to be observed for increasing NADH concentrations at lower pyruvate concentrations, 0.2mM up to 4mM pyruvate. However, at the experimental concentrations of NADH, overall effect of NADH on reaction rate was minimal, given that NADH concentrations were ten times the concentration of K_a. Even with inhibiting pyruvate conditions above 4mM, the effect of NADH concentration was minimal (Figure 3.1B).

Complexity of the pyruvate substrate and NAD product inhibition was evaluated similarly. NAD concentration was varied from 0.25mM to as high as 4.0mM, while NADH concentration was held constant at 0.333mM. Kinetic experiments at lower concentrations of pyruvate, 1.0mM or less, experienced little change in kinetic rate as the initial NAD concentration increased. Despite the possibility that co-factor NAD presence can cause a reversal of reaction as L-lactate product builds up, this phenomenon does not

occur at the lower pyruvate / high NAD initial conditions despite conversion of substrate to near equimolar concentrations of pyruvate and lactate. This effect could be attributed to the saturation of the enzyme by NADH. Again, however, with inhibiting initial concentrations of pyruvate, the kinetic rate was affected significantly by the presence of high levels of NAD (Figure 3.2A). The impact of the ternary complex, where NAD does not properly unbind from the enzyme and instead binds with a pyruvate intermediate, becomes elucidated by the hampered rates. While pyruvate alone (40mM) as an inhibiting factor yields a relative rate around 46% of the maximum experimental rate, the result with 1mM initial NAD is 33% of the maximum experimental rate and further declines to 14% at 4mM NAD. The decline in catalytic rate with NAD can be directly observed against the higher pyruvate concentrations (Figure 3.2B). Additionally, the initial cofactor ratio becomes of consequence to the reaction rate at higher NAD concentrations. Whereas the saturating NADH does not notably affect the rate in relation to pyruvate, increasing NADH in relation to NAD decreases any onsetting inhibition (Figure 3.2C).

The inhibition effects noted illustrate the necessity for additional terms in the kinetic rate expression. Multiple linear modeling in the statistical software becomes a powerful tool for evaluating these new kinetic constants from the data. High concentrations of pyruvate have been shown to form a complex with the free enzyme, such that another kinetic parameter ($K_{I\text{-}Pyr}$) was added as a squared substrate term to the general equation (Eq. 3.1). Additionally, the high pyruvate and high NAD inhibition effects suggest the presence of a ternary complex and the added kinetic parameter is $K_{I\text{-}Pyr\text{-}NAD}$.

$$\mathbf{v} = \frac{\mathbf{V_{max}(AB)}}{\mathbf{K_{ia}K_b + K_bA + K_aB + AB + \frac{B^2A}{K_{I\text{-}Pyr}} + \frac{B^2Q}{K_{I\text{-}Pyr\text{-}NAD}}}} \tag{3.2}$$

The $K_{I\text{-}Pyr}$ has been used in analysis of LDH from other sources (11); however, the $K_{I\text{-}Pyr\text{-}NAD}$ seen here is explored in detail.

Inversion of the rate expression allowed for a multiple linear regression against the assayed concentrations:

$$\frac{\mathbf{V_{max}}}{\mathbf{v}} = \frac{\mathbf{K_{ia}K_b}}{\mathbf{AB}} + \frac{\mathbf{K_a}}{\mathbf{A}} + \frac{\mathbf{K_b}}{\mathbf{B}} + \mathbf{1} + \frac{\mathbf{B}}{\mathbf{K_{I\text{-}Pyr}}} + \frac{\mathbf{BQ}}{\mathbf{AK_{I\text{-}Pyr\text{-}NAD}}} \tag{3.3}$$

The presence of saturating amount of NADH cofactor means the pyruvate binary complex effect is linear with the pyruvate concentration (Figure 3.3A). The degree of enzyme-pyruvate-NAD^+ ternary complex, however, is demonstrated to be a combination of the pyruvate concentration and cofactor oxidized to reduced ratio. This may be accounted for by the competition of NADH and NAD for the binding site.

Because values of the first four terms where known or easily evaluated, the remaining factors were regressed upon, using the JMP statistical software package, initially at experimental concentrations where the accompanying term of the kinetic factor carried the greatest weight. The linear nature of the term expressing pyruvate-cofactor complex is demonstrated (Figure 3.3B). Subsequent regressions utilizing the expanded data sets in JMP provided final kinetic constants of 0.301mM for Kb, 29.91mM for $K_{I\text{-}Pyr}$, and 97.47mM for $K_{I\text{-}Pyr\text{-}NAD}$.

3.2.2 Product Inhibition of Lactic Dehydrogenase by L-Lactate in Response to Pyruvate Concentrations

The inverse rate vs. lactate product Dixon plots demonstrate rates that are 67% and 52% relative to the maximum experimental rate for concentrations of 50mM and 100mM L-lactate respectively at the lowest pyruvate concentration tested (Figure 3.4). For similar lactate conditions involving high pyruvate substrate, the lactate effect is less apparent to the forward reaction giving rise to the flat lines. Lineweaver-Burk double reciprocal plots of the initial reaction velocity against the concentration of pyruvate for several concentrations of L-lactate indicated that the product inhibition is predominately noncompetitive. At concentrations on pyruvate conducive to V_{max}, the slope of inverse velocity relative to lactate suggests a lactate product inhibition K_i estimate value of 126 mM for the rabbit muscle LDH enzyme.

Lactate also creates the potential for a reversible reaction. For reversible mechanisms such as that with LDH, an ordered bi-bi model with cofactor binding first and accounting for product inhibitions in each reaction direction can be generated (15) in correlation with the new terms:

$$\mathbf{v} = \frac{\mathbf{V_{max}}\left(\mathbf{AB} - \mathbf{PQ/K_{eq}}\right)}{\mathbf{K_{ia}K_b} + \mathbf{K_bA} + \mathbf{K_aB} + \mathbf{AB} + \frac{\mathbf{K_{ia}K_bQ}}{\mathbf{K_{iq}}} + \frac{\mathbf{K_{ia}K_bK_aP}}{\mathbf{K_{iq}K_p}} + \frac{\mathbf{K_{ia}K_bPQ}}{\mathbf{K_pK_{iq}}} + \frac{\mathbf{K_bK_qAP}}{\mathbf{K_{iq}K_p}} + \frac{\mathbf{K_pBQ}}{\mathbf{K_{iq}}} + \frac{\mathbf{ABP}}{\mathbf{K_{ip}}} + \frac{\mathbf{K_{ia}K_bBPQ}}{\mathbf{K_pK_{iq}K_{ib}}} + \frac{\mathbf{B^2A}}{\mathbf{K_{I\text{-}Pyr}}} + \frac{\mathbf{B^2Q}}{\mathbf{K_{I\text{-}Pyr\text{-}NAD}}}} \quad (3.4)$$

where P indicates product concentration, and Q is the oxidized cofactor concentration. At the experimental reaction conditions, negligible reverse reaction occurred.

Initial modeling using Eq. 3.4 demonstrated little significance of several NAD terms that are evident at lower concentrations of NADH. The terms are important to the enzymatic reaction of lactate to pyruvate, but have little contribution at the conditions in this study. JMP analysis of the full equation 4 indicated that having multiple lactate terms is not statistically significant. The final forward reaction rate including the remaining L-lactate product inhibition can be expressed inversely as:

$$\frac{\mathbf{V_{max}}}{\mathbf{v}} = \frac{\mathbf{K_{ia}K_b}}{\mathbf{AB}} + \frac{\mathbf{K_a}}{\mathbf{A}} + \frac{\mathbf{K_b}}{\mathbf{B}} + \mathbf{1} + \frac{\mathbf{P}}{\mathbf{ABK_{I\text{-}Lac}}} + \frac{\mathbf{B}}{\mathbf{K_{I\text{-}Pyr}}} + \frac{\mathbf{BQ}}{\mathbf{AK_{I\text{-}Pyr\text{-}NAD}}} \qquad (3.5)$$

in which the remaining lactate terms simplify to one term.

The linear nature of the term expressing lactate inhibition is provided, and the subsequent value for $K_{I\text{-}Lac}$ following all regressions is $487.33 mM^{-1}$ (Figure 3.3C).

The final overall correlation coefficient between experimental and model kinetic expression rates (Eq. 3.5) is 97.5%. The correlation coefficient is 98.9% for experiments at higher enzyme concentration and is 91.5% for the larger data set at lower LDH protein concentrations (Figure 3.5).

In 62 of the experimental assay experiments, the simulations exhibit less than 10% error of difference. In the instances of higher error, only six experimental conditions exceed 15% error. The regions of error occurred with the lowest levels of substrate where the binding constants were not fully investigated and literature values were utilized in their place. At these conditions, the simulation tended to produce slightly slower rates comparative to measurement. In nearly all the highest inhibition scenarios, the simulation provided excellent replication of the data.

3.3 CONCLUSIONS

Statistical software was a valuable tool in analyzing the three primary inhibiting factors effecting pyruvate to lactate conversion by rabbit skeletal muscle lactate dehydrogenase. For the first time, the substrate-cofactor product ternary complex is accounted for at high concentrations of pyruvate and NAD. The protein activity is seen to drop as much as 50% with pyruvate inhibition alone and, with ternary complexes involved, can further diminish to nearly a twelth of optimal rate. The provided kinetic rate expression supplies a solid basis to evaluate use of lactate dehydrogenase in a large scale enzymatic system requiring cofactor regeneration or lactate production.

3.4 FIGURES

a)

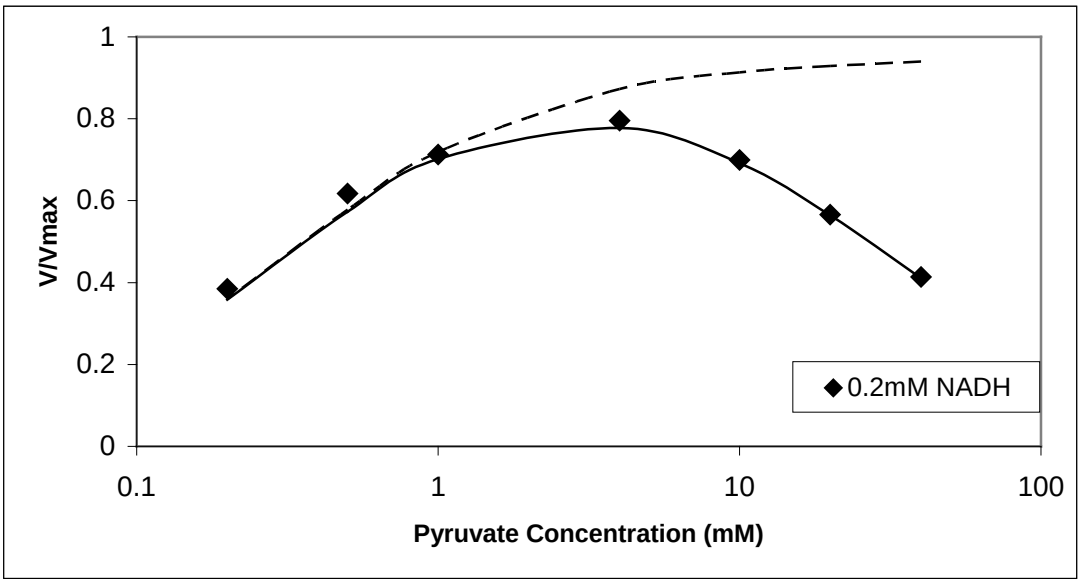

b)

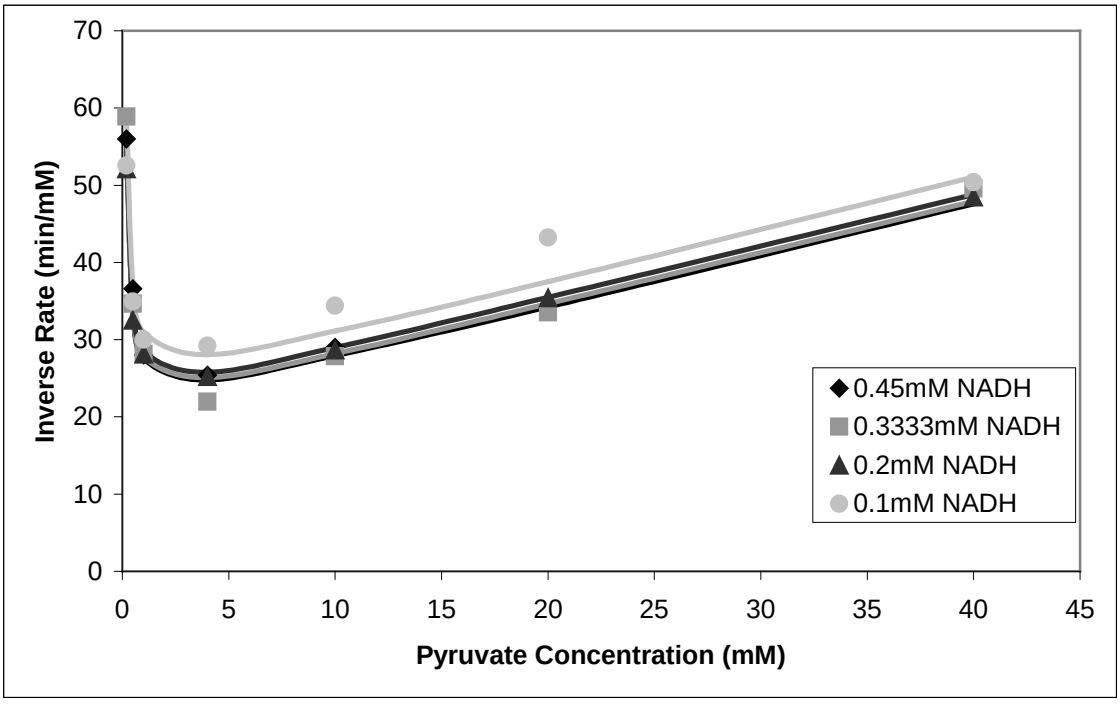

Figure 3.1 (a) Classic example of relative velocity versus pyruvate demonstrating substrate inhibition. (b) Reciprocal rate vs. pyruvate concentration plot demonstrating substrate inhibition. At high concentrations of pyruvate, a linear relationship exists in relation to the $K_{I\text{-}Pyr}$ term. Enzyme assay volumetric activity: 0.0485 Units/mL. Lines of similar shading to experimental points depict kinetic rate expression (Eq. 3.5) predictions. Dashed line in Fig. 3.1a depicts basic model (Eq. 3.1) predictions.

a)

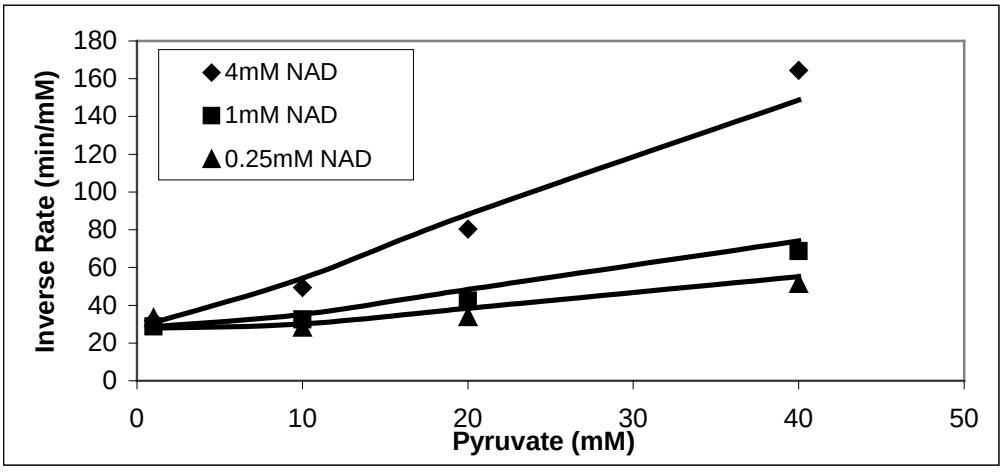

b)

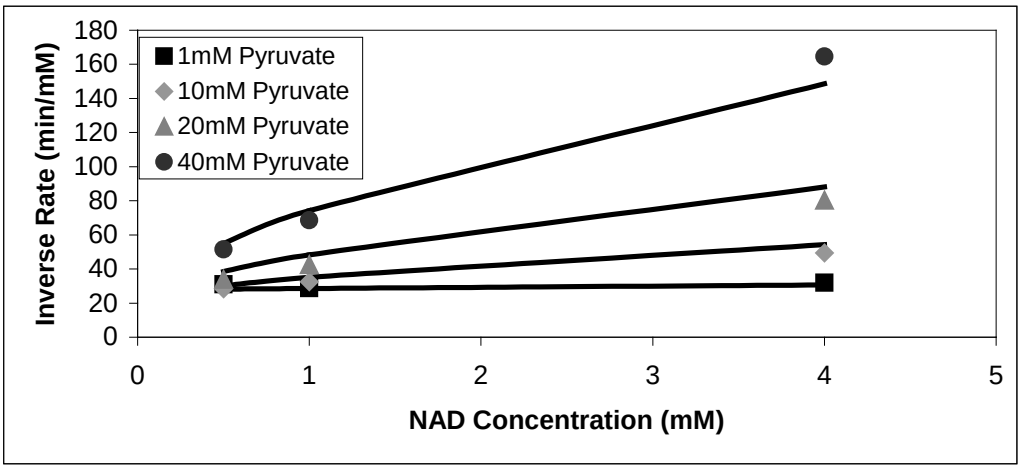

c)

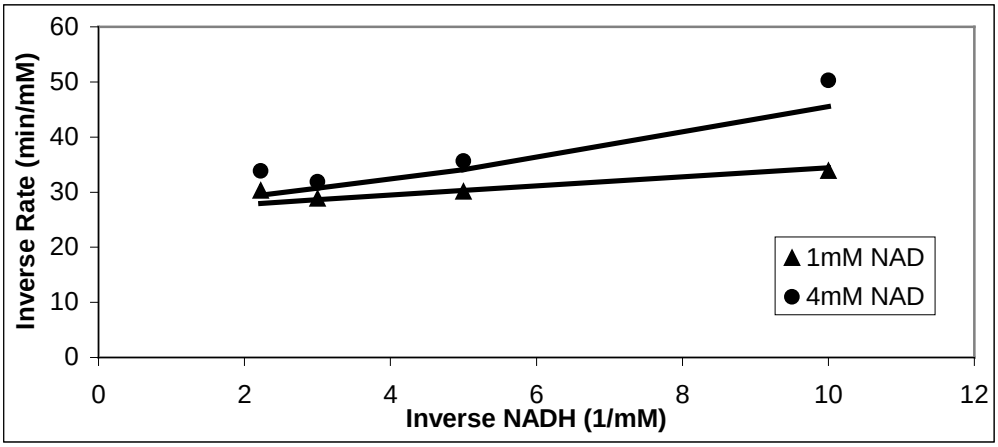

Figure 3.2 (a)Inverse rate vs. concentration of pyruvate in the presence of product cofactor. (b) Replot of Fig. 2a depicting increasing NAD concentration. Initial NADH concentration: 0.35±0.013mM. (c) Inverse rate vs. inverse NADH at elevated NAD concentrations. Initial pyruvate concentration: 1mM. Enzyme assay volumetric activity: 0.0485 Units/mL in each graph. Solid lines depict kinetic expression (Eq. 3.5) predictions.

a)

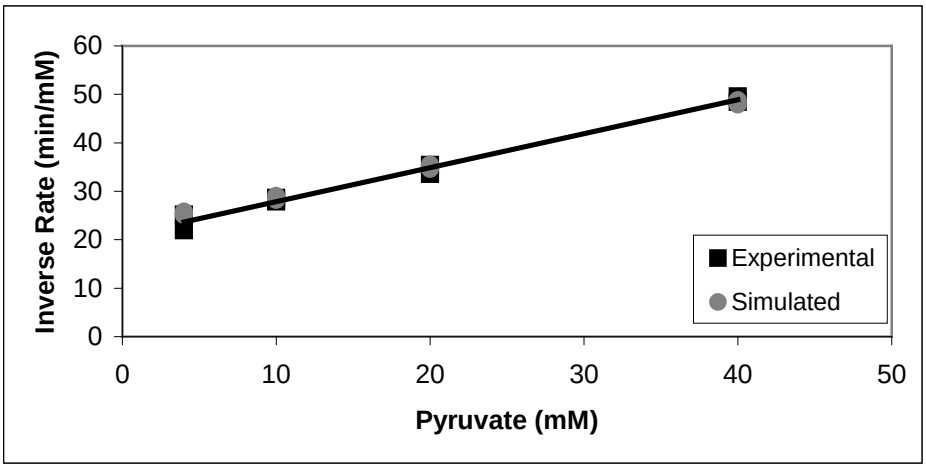

b)

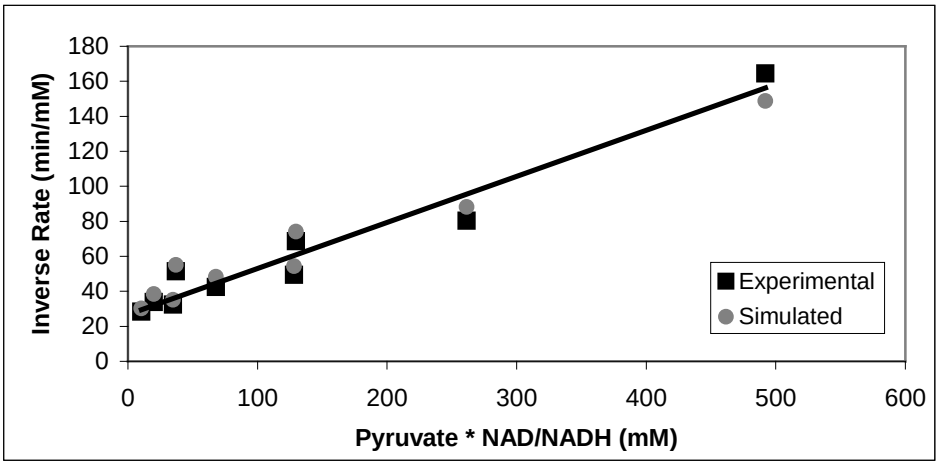

c)

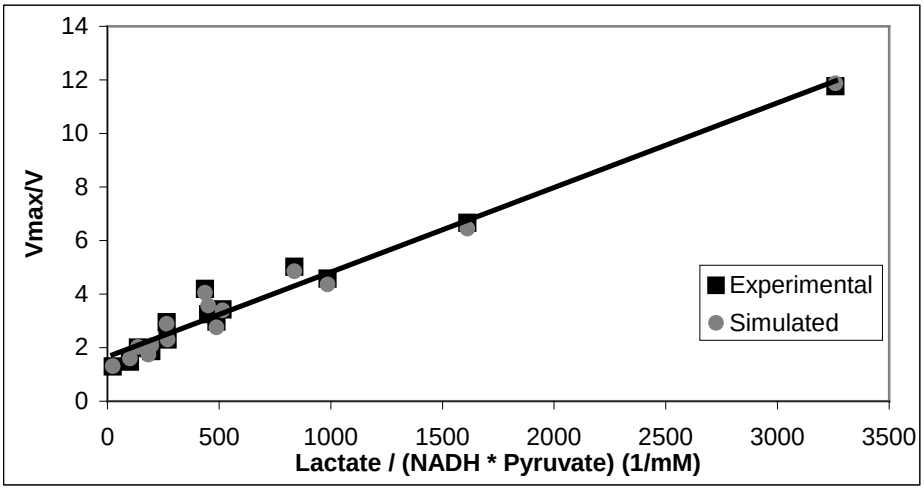

Figure 3.3 Linearity of inverse rate with respect to concentrations of inhibition terms. Approximations of kinetic constants can be drawn from linear least squares regression for (a) $K_{I\text{-}Pyr}$ using data from Fig. 3.1, (b) $K_{I\text{-}Pyr\text{-}NAD}$ using data from Fig. 3.2, and (c) $K_{I\text{-}Lac}$ featuring data from Fig. 3.4a.

a)

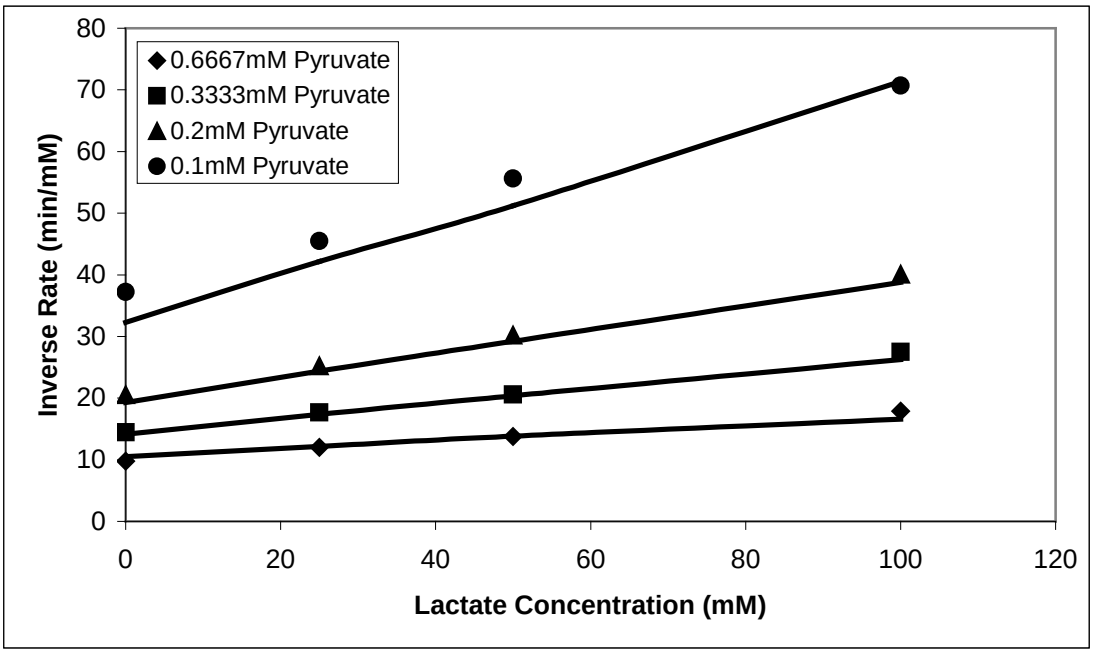

b)

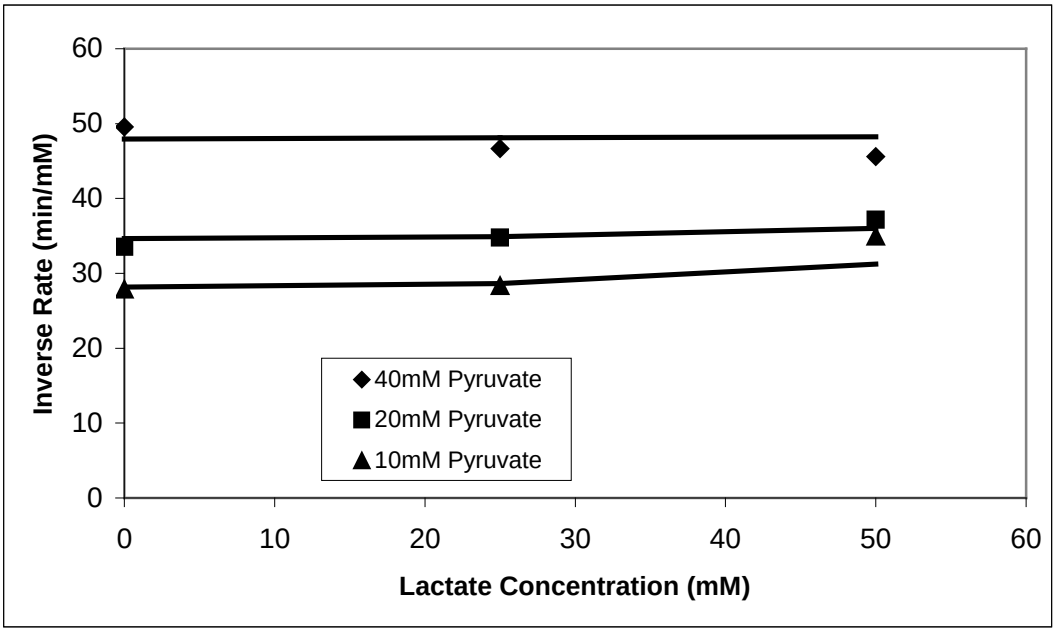

Figure 3.4 Inverse velocity linearity to lactate concentrations. (a) At lower concentrations of pyruvate, lactate demonstrates inhibition at high concentration. Enzyme assay volumetric activity: 0.1663 Units/mL. (b) In the presence of large pyruvate concentrations, lactate has a diminished effect. Enzyme assay volumetric activity: 0.0499 Units/mL. Initial NADH Concentration in both plots: 0.335±0.025mM. Solid lines depict model (Eq. 3.5) predictions.

a)

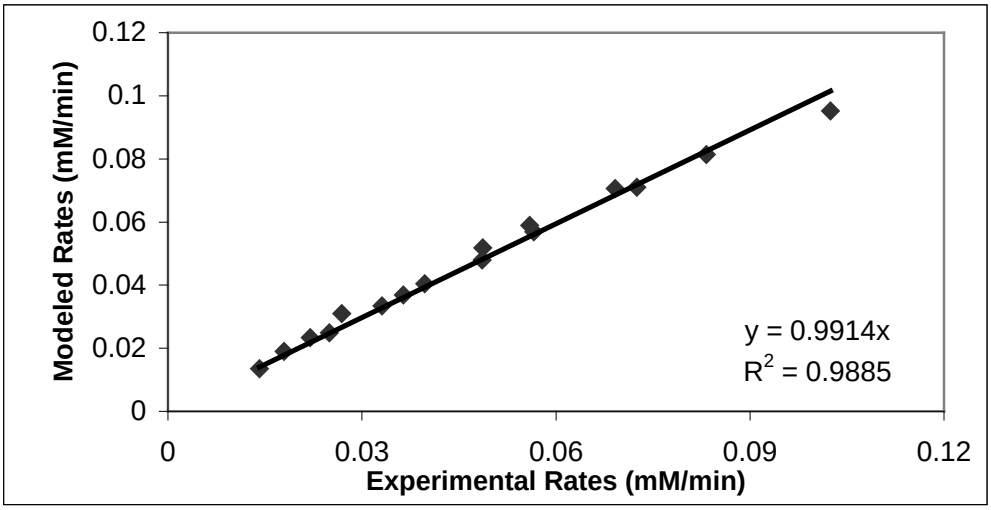

b)

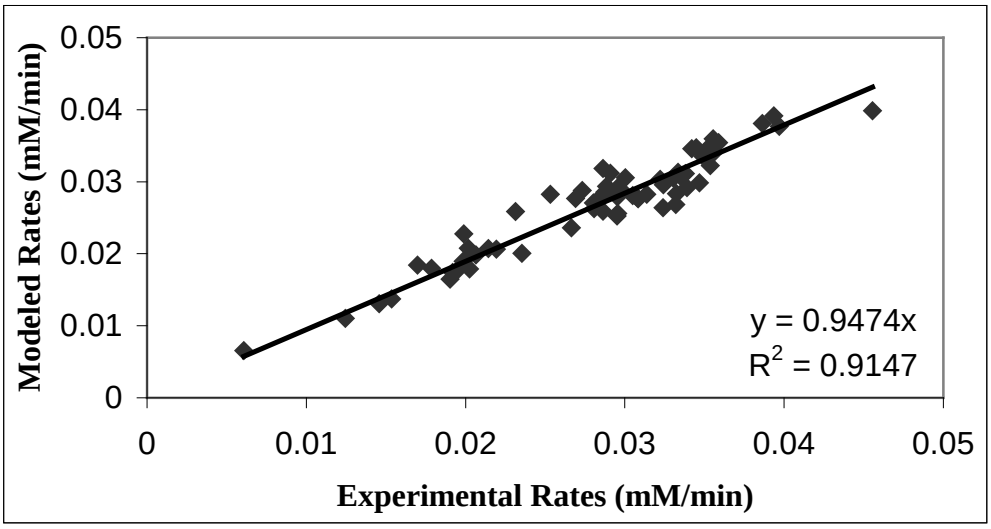

Figure 3.5 Correlation of Model and Experimental Values for all assays at (a) higher enzyme concentration (0.1663 U/mL) and (b) lower enzyme concentration (0.0405 - 0.0499 U/mL). Overall correlation for the entire data set is 97.5%.

3.5 REFERENCES

1. Novoa, W. B., Winer, A. D., Glaid, A. J., and Schwert, G. W. (1959). Lactic dehydrogenase. V. Inhibition by oxamate and by oxalate. J. Biol. Chem., 234, 1143.

2. DiSabato. G. (1968). Complexes of chicken heart lactic dehydrogenase with coenzymes and substrates. Biochem. Biophys. Res. Commun., 33, 688.

3. Gutfreund, H., Cantwell, R., McMurray, D. H., Criddle, R. S., and Hathaway, G. (1968). The kinetics of the reversible inhibition of heart lactate dehydrogenase through the formation of the enzyme–oxidized nicotinamide–adenine dinucleotide–pyruvate compound. Biochem. J., 106, 683.

4. Everse. J., Barnett, R. E., Thorne, C. J. R., and Kaplan, N.O. (1971). The formation of ternary complexes by diphosphopyridine nucleotide-dependent dehydrogenases. Arch. Biochem. Biophys. 143, 444.

5. Burgner, J. W., II, Ray, W. J., Jr. (1984). On the Origin of the Lactate Dehydrogenase Induced Rate Effect. Biochemistry 23, 3636-3648.

6. Wang, C. S. (1977). Inhibition of Human Erythrocyte Lactate Dehydrogenase by High Concentrations of Pyruvate: Evidence for the Competitive Substrate Inhibition. Eur. J. Biochem., 78, 569-574.

7. Fernandez-Santos, T., Lluis, C., Bozal, J. (1979). Journal of Molecular Catalysis, 5, 247-262.

8. McClendon, S., N. Zhadin, and R. Callender. (2005). The approach to the Michaelis complex in lactate dehydrogenase: the substrate binding pathway. Biophys. J., 89, 2024–2032.

9. Hewitt, C. O., Eszes, C. M., Sessions, R. B., Moreton, K. M., Dafforn, T. R., Takei, J., Dempsey, C. E., Clarke, A. R., and Holbrook, J. J. (1999). Protein Eng., 12, 491−496.

10. Bergmeyer, H.U., Bernt E., Hess B. (1974). Lactate Dehydrogenase. In: Methods of enzymatic analysis. Verlag Chemie, 3rd ed, Vol 2, 1986.

11. Burgner, J. W., II, Ainslie, G. R., Jr., Cleland, W. W., Ray, W. J., Jr. (1978). Bimodal Substrate Inhibition of Lactate Dehydrogenase. Factors Affecting the Enzyme in Vivo. Biochemistry, 17, 1646.

12. Alberty, R.A. (1953). The Relationship between Michaelis Constants, Maximum Velocities and the Equilibrium Constant for an Enzyme-catalyzed Reaction. J. Amer. chem. Soc., 75, 1928.

13. Zewe, V., and Fromm, H. J. (1962). Kinetic Studies of Rabbit Muscle Lactate Dehydrogenase. J. Biol. Chem., 237, 1668.

14. Wu C-Y, Chen S-T, Chiou S-H, Wang K-T. (1992). Kinetic analysis of duck ε-crystallin with L-lactate dehydrogenase activity: determination of kinetic constants and comparison of substrate specificity. Biochem. Biophys. Res. Commun., 186, 874–880.

15. Cleland, W.W. (1967). Enzyme Kinetics. Annu. Rev. Biochem. 36, 77-112.

CHAPTER 4

KINETIC INVOLVEMENT OF ACETALDEHYDE SUBSTRATE INHIBITION ON THE RATE EQUATION OF YEAST ALDEHYDE DEHYDROGENASE

(Matthew Warren Eggert, Mark E Byrne, Robert P Chambers, Applied Biochemistry and Biotechnology, under review April 6,2012)

Aldehyde dehydrogenase plays a crucial role of non-reversibly converting biologically toxic acetaldehyde to non-harmful acetate in many organisms. The NAD(P)+-dependent aldehyde dehydrogenase with characteristically broad substrate specificity is widely distributed in nature (1). Over the past decade and more, increasing effort has been placed on classifying and determining genetic variations of aldehyde dehydrogenase from diverse species and cellular tissue (2, 3). While organisms are dependent on many functional forms of ALDH for different aldehyde transformations, mitochondrial ALDH found in liver of mammals and mitochondrial ALDH from Saccharomyces cerevisae are the proteins responsible for most rapidly oxidizing acetaldehyde (4, 5).

Kinetic studies of aldehyde dehydrogenases from different species exhibit striking differences in the magnitude of binding constants such as Km for aldehyde (6, 7, 8) and in the requirement for exogenous sulfhydryl compounds and cations (1, 9-12). Early studies to elucidate the detailed mechanism of the enzymes with their substrates were limited, although it was known that all NAD(P)+-dependent aldehyde dehydrogenases followed a sequential mechanism, neither product being released before both substrates

have added. Freda and Stoppani then carried out studies with yeast aldehyde dehydrogenase using hydroxylamine inhibitor in the presence of coenzyme analogues to conclude that NAD(P)+ is added prior to aldehyde (13). Bradbury and Jakoby in efforts to also determine the ordered mechanism of yeast aldehyde dehydrogenase were led to believe NAD+ did not bind to free enzyme in the absence of aldehyde, as determined by equilibrium binding experiments and on the pattern of activity with mixed alternate substrates. However, they did conclude inhibition obtained with the product NADH was competitive with respect to NAD+ and uncompetitive with respect to aldehyde (14). More recently, structural imaging has revealed cofactor binding as an interaction involving a Rossman fold protein sequence that is common among all dehydrogenase families (15). Kinetic work by Dickinson has demonstrated the role of activating ions in assisting the yeast enzyme's conformational binding to cofactor, whereby increasing affinity 100 fold (16). Of additional kinetic significance, Milstein and Stoppani were aware of delayed kinetics due to high aldehyde concentrations and first proposed a substrate inhibition term based on the squared concentration of acetaldehyde (17). These binding interactions, especially those that lead to an inhibitory effect as substrate concentrations increase, can impact the utility of the enzyme when applied to larger biosystems. To successfully account for inhibiting enzyme complexes produced by high acetaldehyde, NADH, and combined cofactor with acetaldehyde, this chapter reports kinetic data bearing on the quantification of rate expression terms of the potassium activated yeast aldehyde dehydrogenase.

4.1 MATERIALS AND METHODS

4.1.1 Chemicals and Enzymes

All chemicals were purchased at the purest grade available from Sigma-Aldrich (St. Louis, MO) and Fluka (Milwaukee, WI). Lyophilized enzyme aldehyde dehydrogenase (AlDH, EC 1.2.1.5) from baker's yeast was also obtained from Sigma-Aldrich (St. Louis, MO). The enzyme had a specific activity of 1.9 U/mg (pH 8.0, 25°C).

4.1.2 Enzyme Activity and Kinetics

Aldehyde dehydrogenase activity was assayed spectrophotometrically at 340nm and 22 °C using a concentration of 0.2mM acetaldehyde and 1mM β-nicotinamide adenine dinucleotide hydrate (NAD+) as substrate and co-factor, respectively, in 200 mM-sodium, 90 mM potassium, 150mM phosphate buffer pH 7.8, which is a modification of a published procedure (18). One unit of AlDH activity was defined as the amount of enzyme converting 1.0 μmol of acetaldehyde per minute. The volumetric activity (mM min^{-1}) was defined as the enzyme activity per ml of enzyme solution for the free enzyme.

For kinetic determinations, a variety of substrate (acetaldehyde), cofactor (NAD), and product (NADH) concentrations using the aforementioned buffer and temperature were investigated. Kinetic effects of product acetate were not observed in experiment or found in literature. The kinetic experiments were divided into three sets wherein only two concentrations were varied per set while the initial concentration of the other components remained constant or zero. Aldehyde was studied in the presence of different concentrations of reduced and oxidized cofactor to understand correlating effects: i) acetaldehyde and cofactor substrate NAD concentrations were varied; ii) NADH and

NAD variants were tested at a peak concentration of acetaldehyde; iii) acetaldehyde and cofactor product NADH were studied to investigate inhibition of the adduct. A total of 72 different kinetic experiments were produced and repeated twice to eliminate possible error. From these results, 66 kinetic runs provided the basis for JMP statistical analysis and the other six were used for qualitative observations. Aldehyde concentrations up to 1.6mM were studied. Cofactor concentrations exceeding common biological amounts were also employed since higher concentrations are often more relevant for biotechnical catalysis. Concentrations of NAD ranged from 0.1-1.6mM, while NADH concentrations ranged from 0 to 0.45mM. The rates of reduction of NAD were carried out for 5 minutes, and the linear portion of the reaction progress curve was used to analyze the kinetics. Typically, the rates reported are from the first 15 seconds to 105 seconds, with concentrations from the median time (one minute) of the rate determination being used for kinetic analysis.

4.1.3 Development of Kinetic Rate Expression

In order to produce an accurate AlDH kinetic rate expression for reacting acetaldehyde and NAD to acetate and NADH, kinetic parameters were necessary for all enzymatic steps over the concentrations of interest. The simplest rate equation, in which dual substrates interact with the enzyme before any product is generated, follows (19):

$$\mathbf{v} = \frac{\mathbf{V_{max}(AB)}}{\mathbf{K_{ia}K_b + K_bA + K_aB + AB}} \tag{4.1}$$

where A is cofactor NAD concentration, B is the acetaldehyde concentration, and K_{ia}, K_a, and K_b are kinetic parameters, with K_{ia} denoting the dissociation of the cofactor substrate from the enzyme. The mechanism of reaction also initially involves cofactor

binding. Since most of the experimental data in this study is at inhibitory substrate regions, the literature value for K_b of 0.015mM was used (17). Data analysis suggested minimizing the $K_{ia}K_b$ term and a value of 0.12mM was settled upon for the K_{ia}.

4.1.4 Kinetic Expression Terms and Constant Determination

Determination of kinetic terms was first approached by utilizing classical plotting techniques, measuring inverse rates vs. substrate and/or inhibitory concentrations, in Microsoft Excel to verify linear or non-linear relationships. The linear relationships provided by the inverse rate verse concentration plots were interpreted into possible kinetic terms. Subsequently, multiple linear regressions were generated using JMP (version 8) statistical software from SAS Institute, Inc. (Cary, NC) using the rate data collected. Verification of denominator terms and initial estimates of inhibition constants for those terms were found by using the kinetic data at concentrations where that term had the most weighted significance in the kinetic rate expression.

4.2. RESULTS AND DISCUSSION

4.2.1 Substrate Inhibition of Aldehyde Dehydrogenase by Acetaldehyde and Acetaldehyde-Coenzyme Ternary Complexes

Preliminary experiments in our laboratory indicated that the enzyme is inhibited markedly by large acetaldehyde concentrations. Therefore, we determined the effect of increasing concentrations of acetaldehyde on AlDH. Experimental results indicate the highest rate is at approximately 0.2mM acetaldehyde. At concentrations tenfold larger than 0.2mM acetaldehyde, activity is less than 50% of the experimental maximum (Figure 4.1A). The fact that acetaldehyde inhibition occurs at such a small concentration

complicates the ability to determine an accurate binding constant. Literature values for kinetics of aldehyde dehydrogenase from Saccharomyces cerevisiae suggesting a Michaelis-Menten value below 0.05mM imply that the concentrations of acetaldehyde tested will begin to saturate the enzyme. Rates are expected to increase with growing acetaldehyde concentration; however, a peak is quickly reached, and the rate of reaction decreases with larger acetaldehyde concentrations. While the effect of acetaldehyde is apparent on the reaction rate, the amount of inhibition becomes largely dependent on the cofactor binding and formation of ternary complexes.

To further investigate the effect of ternary complexes formed by the acetaldehyde substrate, aldehyde dehydrogenase, and both coenzymes, kinetic experiments focused mainly on inhibiting acetaldehyde concentrations were analyzed. NAD cofactor concentrations were studied against inhibiting acetaldehyde concentration up to 1.6mM, nearly 100 times the Km. The cofactor NAD also effects the concentration at which inhibition from acetaldehyde occurs. The concentration of acetaldehyde for peak velocity of reaction shifts from 0.1mM to 0.2mM as NAD concentrations increases from 0.8mM to 1.6mM. Additionally, the rate rises as well with increasing initial NAD concentrations as seen in Fig 4.1B. Therefore, cofactor plays a significant role in mitigating the effect of aldehyde inhibition. Furthermore, higher concentrations of NAD are expected to be viable before any saturating effect occurs. The initial estimated value of Ka, which is obtained at peak velocity concentrations of acetaldehyde, is 0.52mM, slightly higher than reported range of values between 0.03-.44mM in literature (18). The linear correlation of velocity to NAD is observed from the inverse rate verse inverse NAD concentration plot (Fig 4.1C).

Complexity of the acetaldehyde substrate and NADH product inhibition was evaluated similarly. NADH concentration was varied from 0mM to as high as 0.4mM, while NAD concentration was held constant at 0.8mM. Kinetic experiments at lower concentrations of acetaldehyde, closer to peak rate concentration at or below 0.4mM, experienced little change in kinetic rate as the initial NADH concentration increased. In this subset of data, the NAD/NADH ratio was always greater than one. However, with more inhibiting initial concentrations of acetaldehyde, the kinetic rate was affected significantly by the presence of high levels of NADH (Figure 4.2A). The impact of a ternary complex, where NADH does not properly unbind from the enzyme and instead affects acetaldehyde-enzyme binding, becomes elucidated by the hampered rates. While acetaldehyde alone (1.6mM) as an inhibiting factor yields a relative rate around 38% of the maximum experimental rate, the result with 0.18mM initial NADH is 13% of the maximum experimental rate and further declines to 6.5% at 0.4mM NADH. The decline in catalytic rate with NADH can be directly observed against the various acetaldehyde concentrations (Figure 4.2B).

Because the presence of NADH can so significantly reduce the reaction rate, the effect of initial cofactor ratio was further evaluated. Concentration of initial acetaldehyde was 0.3mM. Little inhibition was observed for this concentration of acetaldehyde at the higher concentrations of NAD (Figure 4.3A). Inhibition, however, is quite apparent when the cofactor ratio of NADH to NAD exceeded a value of one. In fact the NADH effect is so large, the reaction rate is more than one magnitude (14 times) slower at a NADH/NAD ratio of 4 as compared to a ratio of 0.25. As a result, NADH inhibition is very pertinent to the reaction rate even when acetaldehyde inhibition would be less significant. Likewise,

the necessity of greater concentrations of NAD for an accelerated reaction is apparent (Figure 4.3B).

The inhibition effects noted illustrate the necessity for additional terms in the kinetic rate expression. Multiple linear modeling in the statistical software becomes a powerful tool for evaluating these new kinetic constants from the data. High concentrations of acetaldehyde have been shown to form a complex with the free enzyme, such that another kinetic parameter ($K_{I\text{-}Ald}$) was added as a squared substrate term to the general equation (Eq. 4.1). Additionally, the high acetaldehyde and high NADH inhibition effects suggest the presence of a ternary complex and the added kinetic parameter is $K_{I\text{-}Ald\text{-}NADH}$. The inhibition that arises at higher acetaldehyde concentrations is not attributed solely to the aldehyde. The NADH product forms a significant contribution and requires a term as well, $K_{I\text{-}NADH}$.

$$\mathbf{v} = \frac{\mathbf{V_{max}}(\mathbf{AB})}{\mathbf{K_{ia}K_b} + \mathbf{K_bA} + \mathbf{K_aB} + \mathbf{AB} + \frac{\mathbf{B^2}}{\mathbf{K_{I\text{-}Ald}}} + \frac{\mathbf{B^2Q}}{\mathbf{K_{I\text{-}Ald\text{-}NADH}}} + \frac{\mathbf{BQ}}{\mathbf{K_{I\text{-}NADH}}}} \tag{4.2}$$

The $K_{I\text{-}Ald}$ has been used in analysis of AlDH (17, 20). The $K_{I\text{-}Ald\text{-}NADH}$ term is utilized for the first time in regard to aldehyde dehyrogenase kinetics and is explored in detail. The $K_{I\text{-}NADH}$ term may also be seen as a reduction of cofactor product inhibition terms sometimes seen more commonly in reversible dehydrogenase reactions such as alcohol dehydrogenase (21).

Inversion of the rate expression allowed for a multiple linear regression against the assayed concentrations.

$$\frac{\mathbf{V_{max}}}{\mathbf{v}} = \frac{\mathbf{K_{ia}K_b}}{\mathbf{AB}} + \frac{\mathbf{K_a}}{\mathbf{A}} + \frac{\mathbf{K_b}}{\mathbf{B}} + \mathbf{1} + \frac{\mathbf{B}}{\mathbf{AK_{I\text{-}Ald}}} + \frac{\mathbf{BQ}}{\mathbf{AK_{I\text{-}Ald\text{-}NADH}}} + \frac{\mathbf{Q}}{\mathbf{AK_{I\text{-}NADH}}} \tag{4.3}$$

The three inhibition factors were regressed upon, using the JMP statistical software package, initially at experimental concentrations where the accompanying term of the kinetic factor carried the greatest weight. When analyzing the high acetaldehyde complex effects, the strongest linear correlation effect on reaction rate was that of the enzyme-aldehyde-NADH ternary complex, expressed by a combination of acetaldehyde concentration and cofactor ratio (Figure 4.4B). Likewise, a NADH product inhibition was also of notable importance, and the term was best linearly represented as the ratio of NADH to NAD (Figure 4.4C). Both terms reflect the competition of the cofactor forms for the binding site. The inhibition directly due to high acetaldehyde was correlated against the inverse of the NAD concentration (Figure 4.4A). This term suggests that the formation of a non-functional acetaldehyde-enzyme complex is likely to occur without the enzyme configuration being stabilized by the binding of the co-substrate.

While our initial value of K_a combined with literature values for K_{ia} and K_b form a suitable four term base equation, the limited data in the low substrate regions prevented a strong linear regression of K_a in terms of overall data, especially with a similar inverse relation to NAD as the three primary inhibition terms. Nevertheless, at best fit, the value for the NAD binding constant K_a was determined to be 0.251mM, corresponding closely to the early literature value of 0.14mM (17). Utilizing a preset value ensured that inhibitory regions, at which most of the data was collected, could be properly analyzed for term constants. Subsequent regressions using the entire data set in JMP provided final kinetic constants of 2.6 for $K_{I\text{-}Ald}$, 0.16 for $K_{I\text{-}NADH}$, and 0.027mM for $K_{I\text{-}Ald\text{-}NADH}$.

The final overall correlation coefficient between experimental and model kinetic expression rates (Eq. 4.3) is 91.5% (Figure 4.5). The correlation coefficient is strongest

for the varying NAD and NADH subset at 98.2%, the varying acetaldehyde and NAD set comprise a correlation of 95.2% between predicted and experimental rates, and a 91.1% correlation exists for the varying acetaldehyde and NADH set.

In 52 of the kinetic runs, the simulation rates exhibit from 0% to 20% error of difference from the experimental rates. Concentration runs with higher error occur at the lowest levels of substrate acetaldehyde where a literature value of K_b was applied in its place. Because acetaldehyde binds so readily at small concentrations, the observable reaction with time was also limited due to substrate being quickly reacted. Only at these conditions, the simulation tended to produce slightly slower rates than the measured values. For concentrations with the greatest amount of inhibition, the simulation provided excellent replication of experimental data.

4.3 CONCLUSIONS

Statistical software was a valuable tool in analyzing the three primary inhibiting factors effecting acetaldehye to acetate conversion by yeast aldehyde dehydrogenase. For the first time, the substrate-cofactor product ternary complex is accounted for at high concentrations of acetaldehyde and NADH. The enzyme rate is seen to drop as much as 40% with acetaldehyde inhibition alone and, with ternary complexes involved, can further diminish to nearly a fifteenth of maximum experimental velocity for our total set of data. The provided kinetic rate expression supplies a solid basis to evaluate aldehyde dehydrogenases in general as well as determine use of commercial yeast in enzymatic systems requiring oxidation of acetaldehyde compounds.

4.4 FIGURES

a)

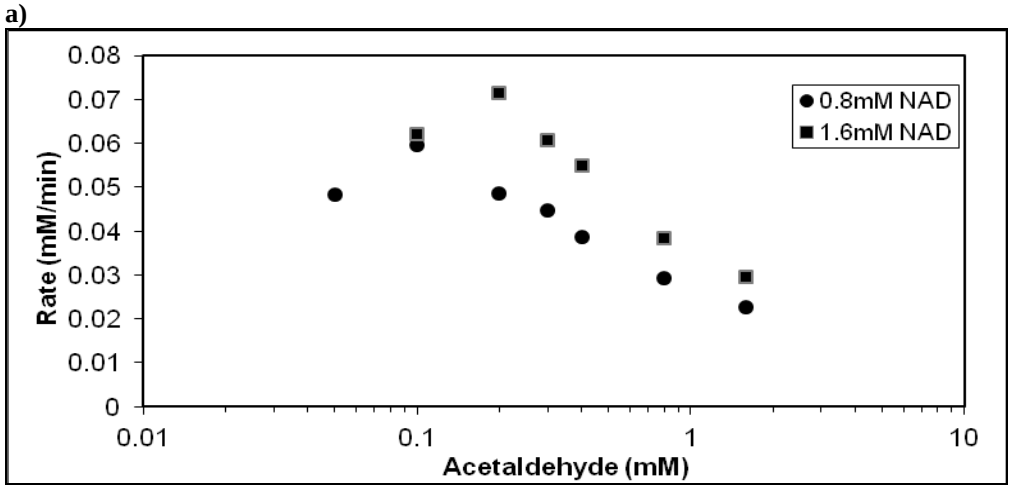

b)

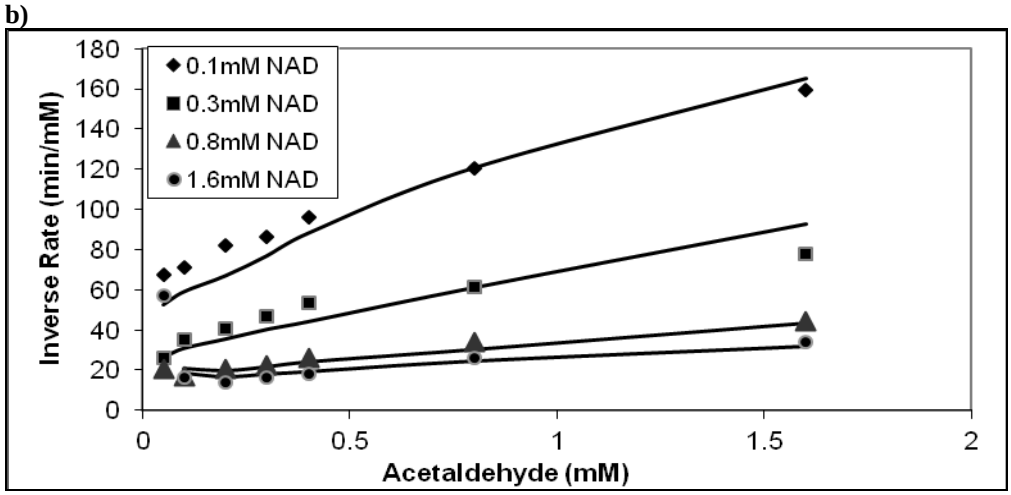

c)

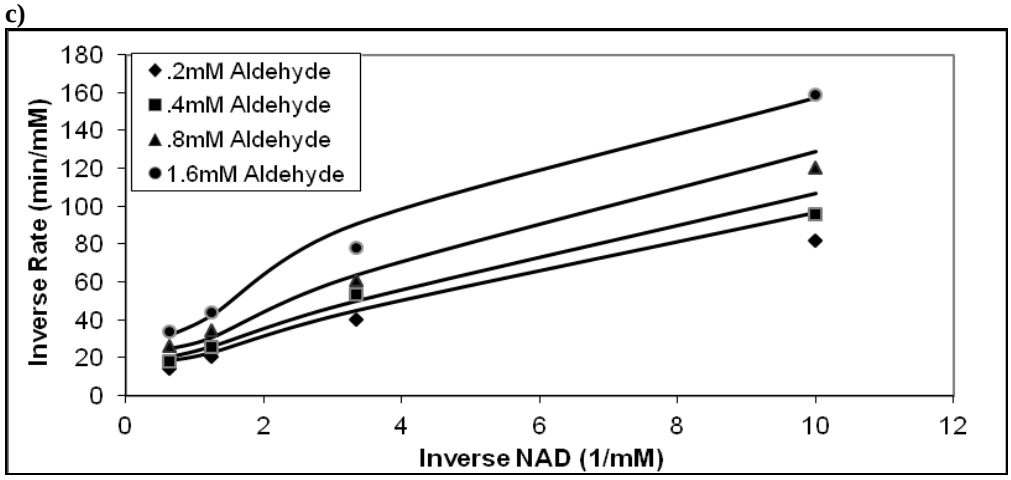

Figure 4.1 (a) Classic example of relative velocity versus acetaldehyde demonstrating substrate inhibition. (b) Reciprocal rate vs. acetaldehyde concentration plot demonstrating substrate inhibition. The higher concentrations of acetaldehyde create a linear relationship for the $K_{I\text{-}Ald}$ term. (c) Reciprocal rate vs. inverse NAD concentration representing the linear relationship of cofactor substrate on acetaldehyde inhibiton. Enzyme assay volumetric activity: 0.116 Units/mL. Solid lines depict kinetic expression (Eq. 4.3) predictions.

a)

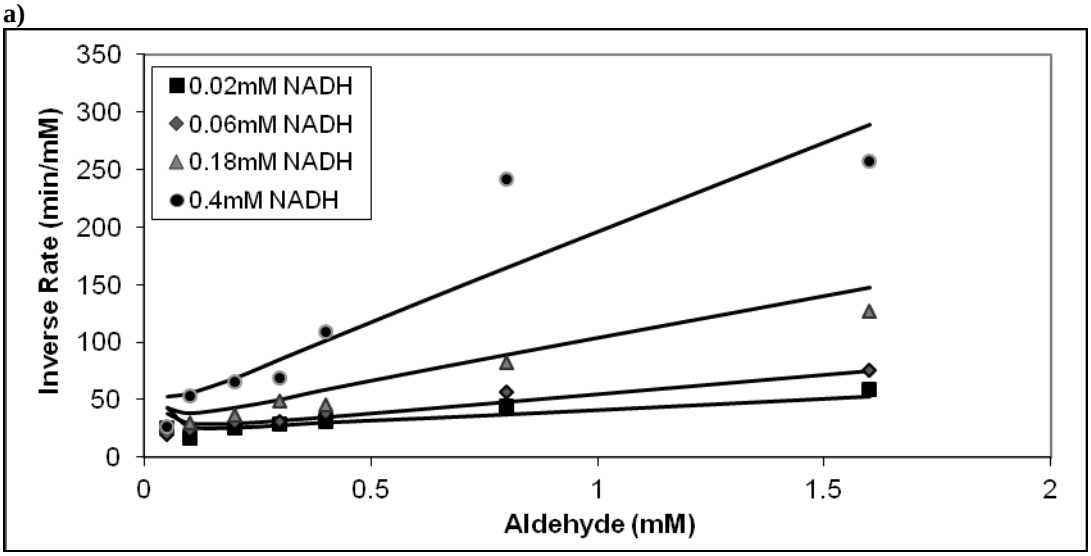

b)

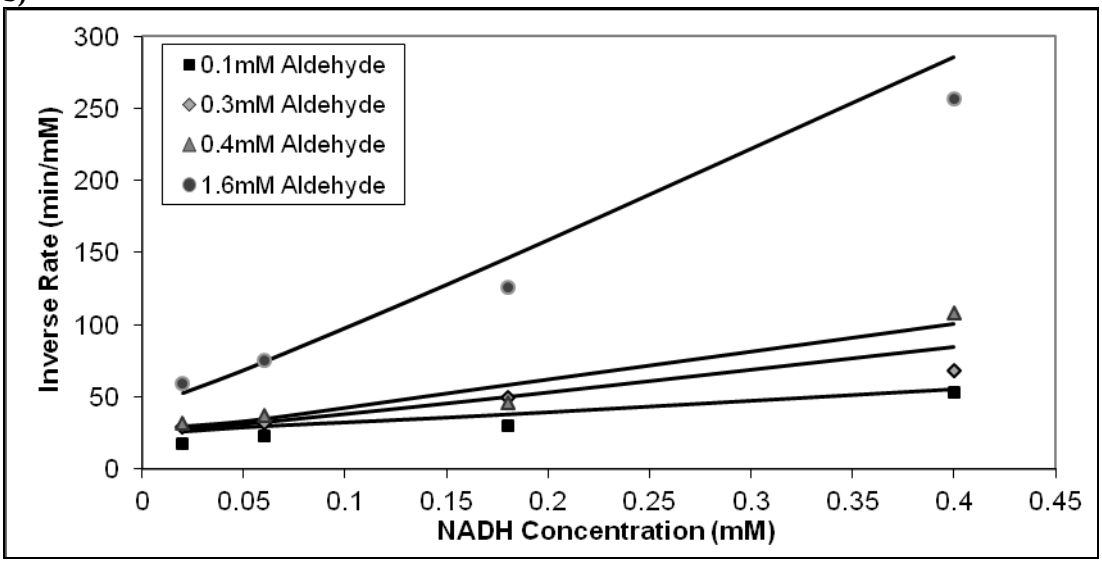

Figure 4.2 (a) Inverse rate vs. concentration of acetaldehyde in the presence of product cofactor. (b) Replot of Fig. 2a depicting increasing NADH concentration. Initial NAD concentration: 0.80mM. Enzyme assay volumetric activity: 0.116 Units/mL in each graph. Solid lines depict kinetic expression (Eq. 4.3) predictions.

a)

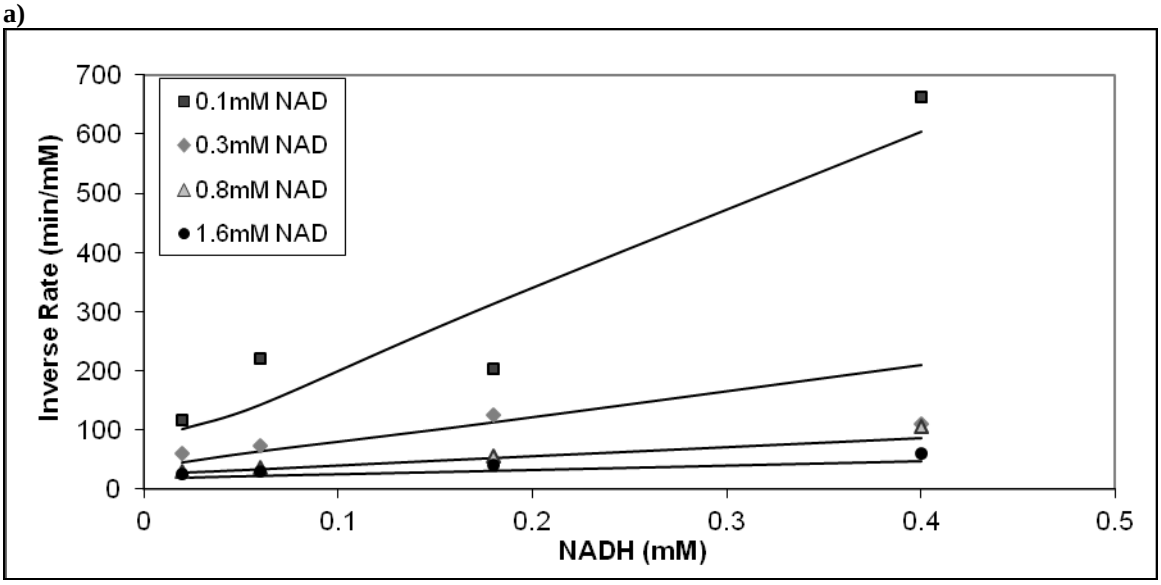

b)

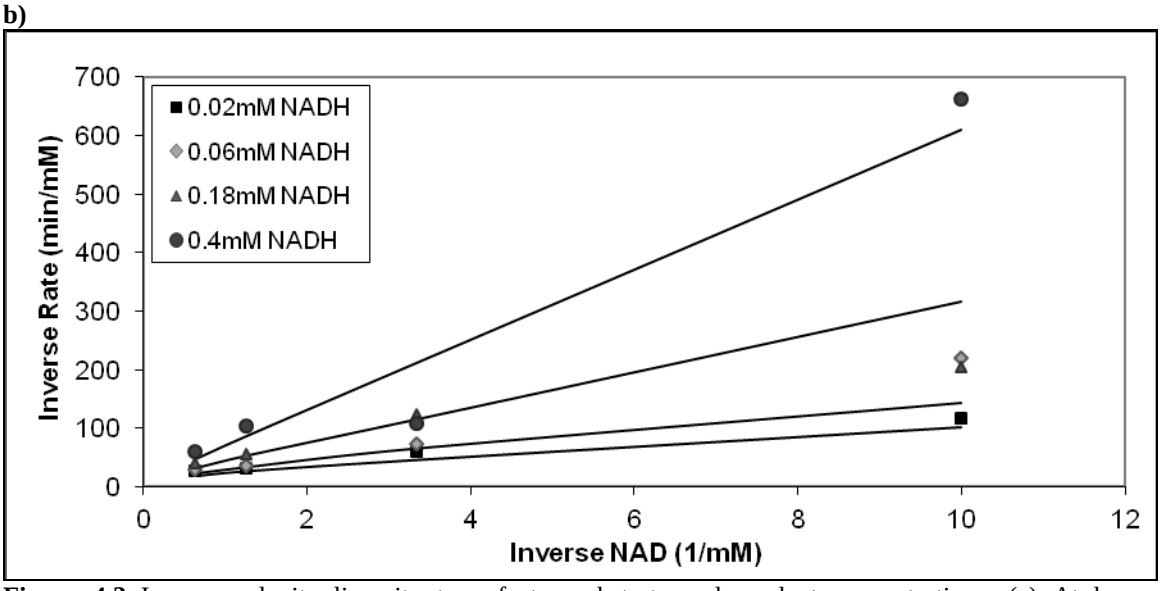

Figure 4.3 Inverse velocity linearity to cofactor substrate and product concentrations. (a) At lower concentrations of NAD, NADH demonstrates greater inhibition. (b) Replot of Fig. 3a depicting the relationship of inverse rate to inverse NAD. Enzyme assay volumetric activity: 0.116 Units/mL. Initial acetaldehyde concentration: 0.30mM. Solid lines depict model (Eq. 4.3) predictions.

a)

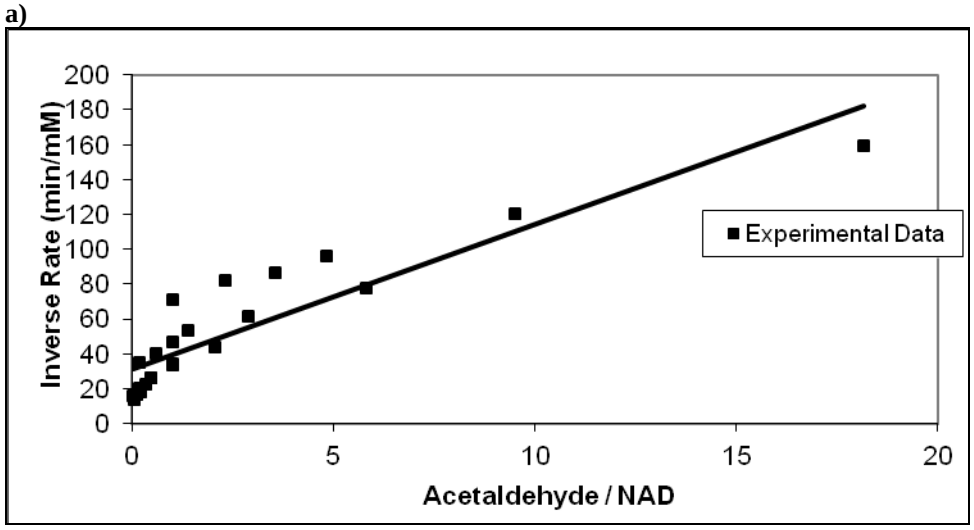

b)

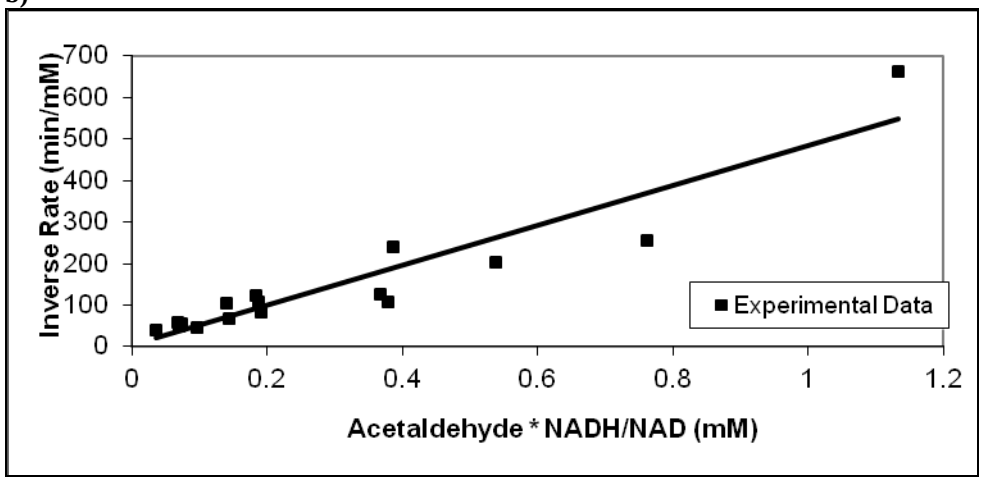

c)

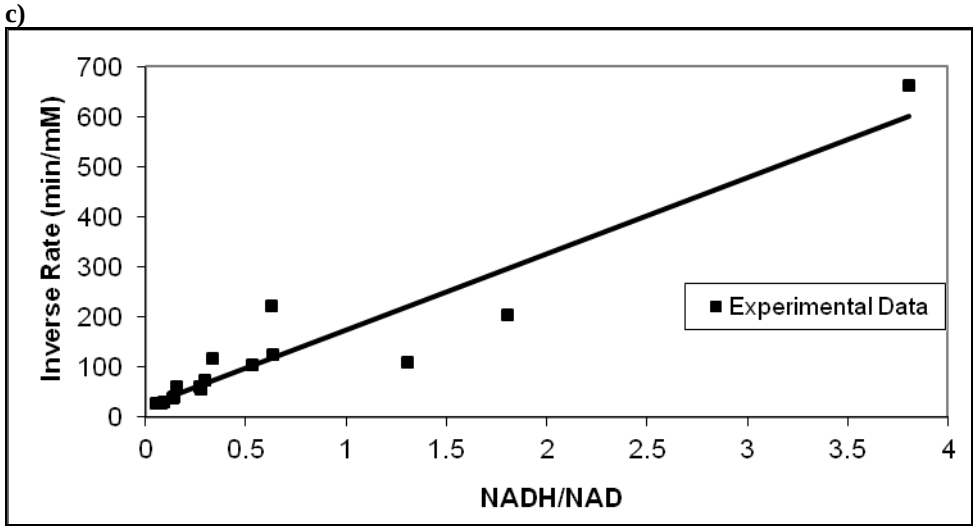

Figure 4.4 Linearity of inverse rate with respect to concentrations of inhibition terms. First approximations of kinetic constants can be drawn from linear least squares regression (lines) for (a) $K_{I\text{-}Ald}$ using data from Fig. 4.1, (b) $K_{I\text{-}Ald\text{-}NADH}$ using data from Fig.4. 2, and (c) $K_{I\text{-}NADH}$ featuring data from Fig. 4.3.

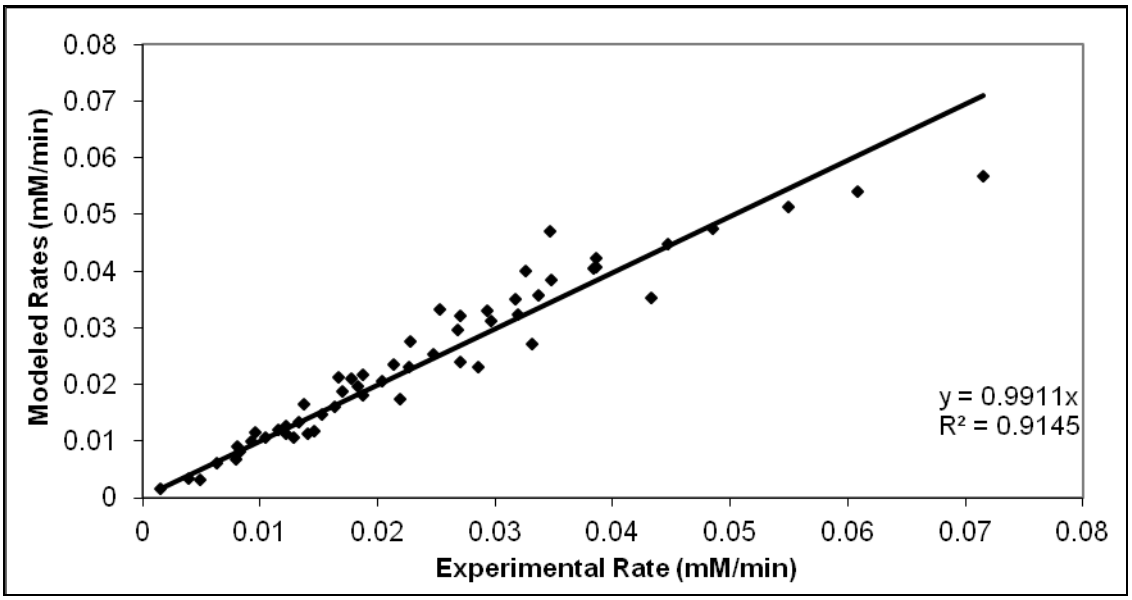

Figure 4.5 Correlation of Model and Experimental Values for all aldehyde dehydrogenase kinetic rate experiments.

4.5 REFERENCES

1. Jakoby, W. B. (1959). Aldehyde Dehydrogenase. The Enzymes (Boyer, P. D., Lardy, H., and Myrback, M.), 2nd Ed, Vol. 7, Academic Press, New York, 203-221.

2. Navarro-Avino, J.P., Prasad, R., Miralles, V.J., Benito, R.M., Serrano, R. (1999). A proposal for nomenclature of aldehyde dehydrogenases in Saccharomyces cerevisiae and characterization of the stress-inducible ALD2 and ALD3 genes. Yeast, 15, 829-842.

3. Pappa, A., Sophos, N.A., Vasiliou, V. (2001). Corneal and stomach expression of aldehyde dehydrogenases: from fish to mammals. Chem Biol Interact., 130-132(1-3):181-91.

4. Vasiliou, V., Pappa, A., Petersen, D.R. (2000). Role of aldehyde dehydrogenases in endogenous and xenobiotic metabolism. Chemico-Biological Interactions, 129 (1-2), 1-19.

5. Wang, M.F., Han, C.L., Yin, S.J. (2009). Substrate specificity of human and yeast aldehyde dehydrogenases. Chem Biol Interact., 178(1-3), 36-9.

6. Shum, G. T., and Blair, A. H. (1972). Aldehyde Dehydrogenases in Rat Liver. Can. J. Biochem., 50, 741-748.

7. Deitrich, R. A., Collins, A. C., and Erwin, V. G. (1972). Genetic Influence upon Phenobarbital-induced Increase in Rat Liver Supernatant Aldehyde Dehydrogenase Activity. J. Biol. Chem., 247, 7232-7236.

8. Ikawa, M., Impraim, C. C., Wang, G., and Yoshida, A. (1983). Isolation and characterization of aldehyde dehydrogenase isozymes from usual and atypical human livers. J Biol Chem. 258, 6282–6287.

9. Black, S. (1951). Yeast Aldehdye Dehydrogenase. Arch. Biochem. Biophys., 34, 86-97

10. Seegmiller, J.E. (1953). Triphosphopyridine nucleotide-linked aldehyde dehydrogenase from yeast. J. Biol. Chem., 201 (2): 629–37.

11. Dickinson, F. M. and Haywood, G.W. (1987). The role of the metal ion in the mechanism of the K+-activated aldehyde dehydrogenase of Saccharomyces cerevisiae. Biochem J., 247(2), 377–384.

12. Dickinson, F. M. (1996). The purification and some properties of the Mg(2+)-activated cytosolic aldehyde dehydrogenase of Saccharomyces cerevisiae. Biochem J. 315(2), 393–399.

13. Freda, C. E., and Stoppani, A. O. M. (1970). Kinetics of bovine liver aldehyde dehydrogenase. Effect of coenzyme and aldehyde structure. Enzymologia, 38, 225-242.

14. Bradbury, S. L., and Jakoby, W. B. (1971). Ordered Binding of Substrates to Yeast Aldehyde Dehydrogenase. J. Biol. Chem., 246, 1834-1840.

15. Liu, Z.-J., Sun, Y.-J., Rose, J., Chung, Y.-J., Hsiao, C.-D., Chang, W.-R., Kuo, I., Perozich, J., Lindahl, R., Hempel, J., and Wang, B.-C. (1997). The first structure of an aldehyde dehydrogenase reveals novel interactions between NAD and the Rossmann fold. Nature Structural Biology, 4, 317 – 326.

16. Dickinson, F.M. (2003). Conformational changes and activation of yeast aldehyde dehydrogenase by various agents. Chem Biol Interact., 143-144, 169-74.

17. Milstein, S. and Stoppani, A. O. M. (1958). Essential Role of Thiol Groups in Aldehyde Dehydrogenases. Biochim. biophys. Acta, 28, 218.

18. Bostian, K.A. and Betts, G.F. (1978). Rapid purification and properties of potassium-activated aldehyde dehydrogenase from Saccharomyces cerevisiae. Biochemical Journal, 173, 773-786.

19. Alberty, R.A. (1953). Mechanisms of Enzyme Action. J. Amer. chem. Soc., 75, 1928.

20. Wang, X., Mann, C.J., Bai, Y., Ni, L., Weiner, H. (1998). Molecular cloning, characterization, and potential roles of cytosolic and mitochondrial aldehyde dehydrogenases in ethanol metabolism in Saccharomyces cerevisiae. J Bacteriol.,180(4):822-30.

21. Cleland, W.W. (1967). The statistical analysis of enzyme kinetic data. Annu. Rev. Biochem., 36, 77-112.

CHAPTER 5

ANALYSIS OF THE THREE DEHYDROGENASE SYSTEM

A multi-enzyme system (MES) containing the soluble enzymes alcohol (ADH), acetaldehyde (ALDH) and lactic (LDH) dehydrogenases, linked together by cofactor NAD, was investigated for improving the rate of alcohol metabolism. Conversion of ethanol as well as acetaldehyde is paramount in maintaining proper physical and chemical function of the body. Both substances have toxic effects within the body, primarily in the central nervous system. By these ends, ADH is the necessary catalyst for ethanol conversion to acetaldehyde. Subsequently, ALDH facilitates the cleanup of acetaldehyde by converting the substance to non-toxic acetate. LDH and pyruvate function as a substrate pumped cofactor regenerator (SPCR) effectively cycling NAD from its reduced form generated during the bi-substrate reactions of the previous two enzymes. An analysis of the scale up from the single ADH enzyme to combinations of ADH with ALDH or LDH followed by the complete three enzyme combination illustrate the improved capability in ethanol conversion afforded by the MES.

5.1 MATERIALS AND METHODS

5.1.1 Chemicals and Enzymes

Buffer salts, sodium phosphate monobasic and dibasic as well as potassium phosphate, were purchased from Fluka (Sigma-Aldrich, Buchs, Germany). Lyophilized enzymes alcohol dehydrogenase (ADH, EC 1.1.1.1), aldehyde dehydrogenase (ALDH, EC 1.2.1.5) from yeast Saccharomyces cervisiae as well as L-lactate dehydrogenase Type XI (LDH, EC 1.1.1.27) from rabbit's muscle were readily available and bought from Sigma-Aldrich (St. Louis, MO). Activites of the enzymes were listed on each label as having a specific activity of 451 U/mg (pH 8.8, 25°C), 2.1 U/mg (pH 8.0, 25°C), and 891 U/mg (pH 7.5, 37°C), respectively. Additionally, enzyme cofactors β-Nicotinamide adenine dinucleotide, disodium salt, its reduced form β-NADH, and substrates ethanol (95%), acetaldehyde (98%), and pyruvate were obtained from Sigma (St. Louis, MO). Ethanol, acetaldehyde, and lactate assay kits for use in multi-enzyme studies were from R-Biopharm (Dormstadt, Germany).

5.1.2 Enzyme Activity Assays

Individual enzyme activities were assayed spectrophotometrically at 340nm by measuring the stoichiometric conversion of NADH at 22 °C in a 200 mM-sodium, 90 mM potassium, 150mM phosphate buffer at pH 7.8. Each enzyme is reacted at substrate concentrations following published procedure modified for buffer conditions (1-3). One unit of activity was defined as the amount of enzyme converting 1.0 μmol of substrate per minute. The volumetric activity (mM min^{-1}) was defined as the enzyme activity per ml of enzyme solution for the free enzyme. The rates of reduction of NAD were carried out for 5-10 minutes and recorded utilizing either a Gilford Spectrophotometer 250 for 3mL

cuvette assays or a Biotek Synergy HT for 6mL assays in a Nunc 6-well plate. The linear portion of the reaction progress curve was used to analyze the activity. Typically, the rates reported are from the first minute and a half of concentration change.

5.1.3 Multi-Enzyme Concentration Assay

In the three enzyme system, substrate conversions were determined experimentally by halting the reaction and measuring the time specific concentration using the aforementioned assay kits. After a desired length of time, 100µL reaction samples were taken from a 15mL combined free enzyme assay mixture and quickly heated to 80°C to denature the enzymes and prevent further reaction. These samples were then diluted as necessary and tested in triplicates to ascertain the amount of each substrate present utilizing its corresponding assay kit.

5.1.4 Method of Simulation

Single and multi-enzyme simulations of reactant and product change were generated by applying the rate equations to a simultaneous Visual Basic Program in Microsoft Excel. A step-wise procedure was used to calculate the instantaneous rate of each enzyme followed by the corresponding change in concentration of each component. A thousand iterations were performed and values outputted for each minute over a one hour time scale. The full Visual Basic algorithm can be seen in Appendix B. Corresponding simulations were matched with three enzyme experiments to determine accuracy and elucidate optimal reaction environments.

5.2 INDIVIDUAL ENZYME KINETICS

Evaluation of the multienzyme system effectiveness was started by performing kinetic studies on the individual enzymes present in the system. Analysis of component conversion, i.e. concentrations of ethanol, acetaldehyde, pyruvate, NAD, NADH, acetate and lactate, in the multienzyme system cannot be done by simple means over the course of the entire reaction. Required techniques would involve gas chromatography with flame ionization detection for ethanol and acetaldehyde while acetate and lactate would still necessitate use of enzymatic methods similar to use of the assay kits (4). Real-time and short period end-point analyses suffer practical complications. Therefore, the performance of *each* enzyme served as a benchmark in forming a computer simulation of the three enzyme system. Following a Bi-Bi substrate mechanism equation proposed by Wratten and Cleland, Michaelis-Menten rate constants were determined for the enzymes in our pH and buffer system (5).

5.2.1 Alcohol Dehydrogenase Kinetic Studies

Beginning with alcohol dehydrogenase, the initial concentrations of ethanol, NAD, acetaldehyde, and NADH were found to significantly affect the initial rate of the reversible reaction. The conversion rate for ethanol increased with increasing concentrations of ethanol itself (Figure 5.1). Similarly, as NAD concentrations were augmented, the reaction rate rose. However, the presence of acetaldehyde and NADH inhibited ADH (Figure 5.2). This product inhibition is best reflected using an inverse rate vs. inverse substrate Lineweaver-Burke plot (Figure 5.3). In two substrate enzyme reactions, these plots demonstrate the effect on rate based on substrate and the substrate's corresponding inhibition product. Utilizing a series of Lineweaver-Burke plots,

assembled from various concentrations of reactants and products, and then performing non-linear regression methods, rate constants for each of the ADH components were determined for the eleven term denominator of the Wratten-Cleland equation (6).

$$\mathbf{v} = \frac{\mathbf{V_{max}}\left(\mathbf{AB} - \mathbf{PQH^{+}/K_{eq}}\right)}{\mathbf{K_{ia}K_b} + \mathbf{K_bA} + \mathbf{K_aB} + \mathbf{AB} + \frac{\mathbf{K_{ia}K_bQ}}{\mathbf{K_{iq}}} + \frac{\mathbf{K_{ia}K_bK_aP}}{\mathbf{K_{iq}K_p}} + \frac{\mathbf{K_{ia}K_bPQ}}{\mathbf{K_pK_{iq}}} + \frac{\mathbf{K_bK_qAP}}{\mathbf{K_{iq}K_p}} + \frac{\mathbf{K_pBQ}}{\mathbf{K_{iq}}} + \frac{\mathbf{ABP}}{\mathbf{K_{ip}}} + \frac{\mathbf{K_{ia}K_bBPQ}}{\mathbf{K_pK_{iq}K_{ib}}}} \quad (5.1)$$

Keq (mM)	Kia (mM)	Kb (mM)	Ka (mM)	Kiq (mM)	Kq (mM)	Kp (mM)	Kip (mM)	Kib (mM)
8E-09	0.2735	49.439	0.2978	0.0487	0.113	0.78	0.624	51.24

Variables A and B represent concentrations of substrates NAD and ethanol, while P and Q reflect their products formed acetaldehyde and NADH. K-values express association values reflective of the Michaelis-Menten constants, and Ki-values denote the dissociation concentrations relative to product formation. The equilibrium, Keq, and reversibility of the reaction are also dependent upon the proton concentration of the buffer solution. Because acetaldehyde and NADH have been identified as inhibitors, the necessity exists for minimizing this impact on the catalytic rate of alcohol dehydrogenase.

5.2.2 Aldehyde Dehydrogenase Kinetic Studies

In the three enzyme system, aldehyde dehydrogenase is responsible for non-reversibly converting the toxic acetaldehyde to the non-harmful acetate. ALDH's purpose also doubles as the enzyme crucial for removing much of the inhibition constraints of the system. Unlike the beneficial impact substrate concentration has on the rate of reaction

for ADH, ALDH experiences an effect known as substrate inhibition from acetaldehyde. Additionally, NADH is observed to also have product inhibitory effects. Moreover, the presence of NADH was found to amplify any inhibition effect produced by acetaldehyde. The finalized rate equation for ALDH is provided in Chapter 4. Again, taking into account the forms of inhibition to which ALDH is subject, the MES's viability relies on the enzyme operating at concentrations that are not detrimental to its performance. With acetaldehyde and NADH being kept to a minimum, the ADH and ALDH reactions are effective.

5.2.3 Lactate Dehydrogenase Kinetic Studies

Lactate dehydrogenase's role in the three enzyme system is that of co-factor NAD recycler. By converting the produced NADH from the former two enzymes, the enzyme further removes inhibition barriers to the ethanol and acetaldehyde catalysis and ultimately maintains equilibrium for the system. Whereas large amounts of more expensive co-factor protein would be necessary to metabolize ethanol without the addition of LDH, the use of the enzyme allows for simply the addition of carbohydrate pyruvate instead. However, similarly to aldehyde dehydrogenase, lactate dehydrogenase also is affected by substrate inhibition at larger concentrations of pyruvate, a problem that is again exacerbated by a dual substrate / product cofactor inhibition as seen in Chapter 3 along with the kinetic rate equation. The pyruvate inhibition may be unavoidable in the three enzyme system initially, but the system is more benefited by the maintained concentrations of cofactor.

5.2.4 Single Enzyme Kinetic Analysis

In order to demonstrate the kinetic impact that inhibiting terms have over the rate of each enzyme, the rate equations were cross-studied against their basic enzyme rate equations. The basic reaction mechanism for enzymes involving two substrates, in which both interact with the enzyme before dissociation of either product, a simple rate equation is obeyed (7):

$$\mathbf{v} = \frac{\mathbf{V_{max}(AB)}}{\mathbf{K_{ia}K_b + K_bA + K_aB + AB}} \tag{5.2}$$

where A is reduced cofactor concentration, B is the substrate concentration, and Kia, Ka, and Kb are kinetic parameters, with Kia denoting an inhibition constant. The mechanism of reaction also involves a sequence of cofactor binding initially. By plotting out the rate vs. the primary inhibiting chemical reactant, the magnitude of the involvement the inhibiting term plays within the rate equation becomes clear.

For alcohol dehydrogenase, acetaldehyde product inhibition exerts a significant effect such that the conversion of ethanol is eventually halted. In the base scenario, the rate would be independent of the product concentration. The dual role of double product inhibition by both acetaldehyde and NADH concentration is exhibited by the rate ratio of inhibited rate vs. the uninhibited rate formulated from each rate equation. With inhibition, the rate of reaction is reduced by half when 0.27mM of acetaldehyde is present without any NADH. With the addition of as little as 0.1mM NADH, the rate is at 50% of maximum with only 0.1mM acetaldehyde present. Up to 2mM acetaldehyde, inhibition is so strong that only 10% of the enzyme activity is possible regardless of NADH (Figure

5.4). Although inhibition generates a strong effect, typically equilibrium alone will halt the reaction after the production of 0.15mM acetaldehyde and NADH.

In both aldehyde dehydrogenase and lactate dehydrogenase, the substrates, acetaldehyde and lactate, respectively, are the primary inhibitors affecting the enzyme catalyst. Under uninhibiting circumstances, substrate can be added until the rate reaches a plateau rate relative to the amount of enzyme. With inhibition, a peak rate, or true maximum velocity (Vmax), is reflected as an inflection point followed by a decline in activity associated with the substrate inhibition. For ALDH, the peak rate occurs at 0.2mM acetaldehyde, while in LDH, the peak concentration of pyruvate is 4.3mM (Figure 5.5).

The dual substrate/product inhibition effect can be observed in both the ALDH and LDH enzymes as well (Figure 5.6). With very small increases in NADH concentrations, the effect of aldehyde substrate inhibition can be observed to be augmented. While half activity exists with 2mM acetaldehyde when no NADH is initially present, the volumetric rate is similar at 0.75mM acetaldehyde when only 0.1mM NADH is present. Likewise, the rate of pyruvate conversion by LDH is half of the uninhibited case with 30mM pyruvate and no initial NAD concentration. When 2mM NAD is introduced, the initial rate is halved with as little as 10mM pyruvate concentration. Both results indicate that it is critical to maintain low cofactor product should high concentrations of substrate be present. Otherwise, if cofactor is necessary to the reactions in larger quantities, the reaction is likely to experience a steeper decline in activity with increased substrate.

5.3 TWO ENZYME KINETIC ANALYSIS

Two enzyme simulations were conducted to further evaluate concentration inhibition as well as equilibrium barriers that the system might incur. Specifically, by pairing ADH and ALDH, it was desired to find the extent of acetaldehyde inhibition. Likewise, ADH and LDH were evaluated to determine the concentration effects of cofactor and pyruvate on the combination. Reaction rates of kinetic equations with and without their inhibiting terms were compared to determine the specific impact of those terms to the overall progress of ethanol conversion.

With excess NAD, acetaldehyde inhibition only became evident in the low enzyme concentration ADH-ALDH system at larger initial concentrations of the aldehyde (Figure 5.7). Moreover, the majority of inhibition was linked to substrate inhibition present in the ALDH. Conversion rates of acetaldehyde grew exponentially larger in comparison to non-inhibited rates as acetaldehyde concentrations increased beyond 0.1mM. Below 1mM acetaldehyde, the system was able to eventually remove the acetaldehyde within an hour at half the rate of the uninhibited scenario. Still, overall ethanol conversion was restricted. In fact, above 0.5mM initial concentration of acetaldehyde, the process was controlled by equilibrium, and ADH was incapable of converting ethanol until ALDH could reduce the acetaldehyde below onset inhibition concentration (Figure 5.8). Once acetaldehyde reached kinetically favorable concentrations, the maximum ethanol conversion became limited primarily due to the buildup of NADH rather than any product inhibition from the acetaldehyde.

In a cofactor limited system involving ADH-LDH, ethanol conversion to acetaldehyde was restricted by the amount of pyruvate available to regenerate the

cofactor (Figure 5.9). Without inhibition, ethanol conversion remained rapid until pyruvate concentrations were exhausted. The ethanol conversion typically matched the amount of pyruvate available. NADH concentrations remained below concentrations of 0.05mM for the duration of the reaction. When cofactor regeneration halted, product acetaldehyde prevented further conversion of ethanol. This demonstrates the significance of lactate dehydrogenase to the system. LDH enables its enzyme counterpart alcohol dehydrogenase to operate beyond equilibrium. With inhibition, the overall ethanol conversion is tremendously affected by acetaldehyde product inhibition and to a lesser degree by pyruvate substrate inhibition. ADH rates are more than 10 fold slower than the non-inhibited kinetic counterparts. Peak conversion of ethanol exists when pyruvate substrate inhibition remains lowest. At concentrations up to 44mM pyruvate, ADH rates are half that of the runs with little pyruvate inhibition.

The effect of cofactor amount and ratio of NAD/NADH were also studied in the ADH-LDH system to evaluate LDH's ability to recycle cofactor. In nearly all cases, LDH demonstrated the capability of rapidly converting NADH to NAD such that the ratio favored NAD. Overall, increasing amounts of total cofactor favored greater conversions of ethanol.

5.4 THREE ENZYME KINETICS

5.4.1 Kinetic Analysis

Similar concentrations and enzyme ratios employed in the two enzyme analysis were applied to the three enzyme system to observe the true efficacy of the system. The

change in kinetic influence of similar acetaldehyde concentrations and pyruvate concentrations are demonstrated (Figures 5.10-5.12).

Initially, a system defined by large concentrations of acetaldehyde and NADH substance and having equal ratio of units among the three enzymes exhibits high inhibition among the ADH and ALDH enzymes, with an additional reversible nature of ADH to remove acetaldehyde from the process. Deetz et al. has supported the notion of a significant reverse reaction effect, noting a 5 to 50 times greater preference for acetaldehyde to ethanol conversion by ADH (8). We find for both the inhibited enzymes, the aldehyde terms play a significant role. In ALDH, the combined substrate-product term accounts for 90% of the inhibition. LDH demonstrates its normal substrate inhibition but is by far the fastest catalyst in the forward direction, beginning to quickly eliminate the initial concentrations of NADH. As the ratio of NADH to NAD diminishes, ALDH is able to speed up its catalysis. Even at these low enzyme concentrations, within five minutes, half the acetaldehyde has been removed and only 3% of the initial NADH remains. At this point the ALDH rate has increased 20 fold due to the enormous decline in aldehyde-NADH inhibition. The reverse ADH Reaction rate has reduced nearly the same degree as equilibrium is approached. Simultaneously, NADH product inhibition terms become insignificant. LDH rates decline as its substrate-product inhibition term dominates. Ethanol peaks as acetaldehyde concentrations approach levels where substrate inhibition on ALDH becomes non-apparent. ALDH rates reach their highest, and LDH rates again climb with NADH consumption by ADH, which lessens the pyruvate-NAD inhibition term. Eventually the system equilibrates with a cofactor ratio dependent on

LDH enzyme amount. ADH and ALDH become substrate limited with minor NADH product inhibition, while substrate inhibition terms of LDH remain present but impotent.

In the same system with only an increased LDH enzyme concentration, the NADH removal is accelerated; however, the pyruvate-NAD term grows 3-5 times larger. The presence of more NAD limits ADH reversibility and temporarily allows the persistence of acetaldehyde in the system. This indicates ADH may in fact be more effective in removing acetaldehyde. Nevertheless, once ALDH removes a significant quantity of acetaldehyde, the lack of NADH reduces inhibition effects on ADH and ALDH enough to counter the remaining aldehyde inhibition. The system equilibrates to a lower concentration of NADH which translates to double enzyme rates in comparison to the former enzyme ratio.

5.4.2 Experimental vs. Simulation Comparison of Multi-Enzyme Kinetics and Three Enzyme Optimization

Similarity in trend and correlation among data between experimental and simulation MES concentrations suggest a well defined set of ADH-ALDH-LDH enzyme kinetics (Figures 5.13-5.14). 45% conversion of ethanol according to simulation compared to 35% conversion based on experiment occurs in 20 minutes (Figure 5.15). This rate is more than enough to reduce BAC from 0.10% to under legal limits. Based on a compartmentalized human pharmacological model of ethanol and acetaldehyde, Umulis et al. suggest a rate of 80 minutes for 20% conversion from peak BAC of 0.078% (9). Extrapolated up to 0.10% BAC, over 100 minutes would be required. Over an hour the rate of our multiple enzyme system is roughly 7 times or more faster than alcohol removal by the human body. The uninhibited models indicate excessive conversions of

ethanol despite enormous acetaldehyde buildup (Figure 5.16, 5.18). This conversion of ethanol may be desirable but it fails to account for the dependence on cofactor regeneration by LDH which is impacted by high concentrations of pyruvate. Additionally, acetaldehyde is assumed to convert at a more rapid rate and the buildup of acetaldehyde is not seen as a barrier. On the contrary, the levels of acetaldehyde would be extremely toxic. In reality, very little buildup of toxic by-product acetaldehyde occurs as the aldehyde intermediate is non-detectable experimentally. Furthermore, simulations only reveal accumulation of acetaldehyde when ALDH is at its minimum ratio in comparison to the other enzymes (Figure 5.17). Ideally, the levels of aldehyde are less than inhibiting concentration at the majority of enzyme concentrations. LDH's role as cofactor regenerator and removal of NADH inhibitor is critical to maintain desirable activity rates among ADH and ALDH. With these considerations in mind, a MES ratio having 30%:20%:50% ADH:ALDH:LDH of total units yields the optimum conversion of ethanol for standard initial concentrations of system components.

5.5 CONCLUSIONS

The combinatorial analysis of enzyme kinetics and three enzyme simulation for the alcohol, aldehyde, lactate dehydrogenase system reveals the extended extensive effect that inhibitor acetaldehyde and cofactor concentration place on the system. Ultimately, the system operates to remove concentrations of NADH followed by any initially inhibitory concentration of acetaldehyde before a progressive rapid conversion of ethanol occurs. Nevertheless, with a fixed amount of enzyme protein, we report that ethanol can be efficiently removed in vitro at pH similar to human intestinal environment at rates seven times faster. At well balance ratios of enzyme, experimental evidence confirmed the accuracy of simulations. The simulations ultimately are instrumental in the further design of pharmaceutically relevant formulation of enzymes for ethanol metabolism.

5.6 FIGURES

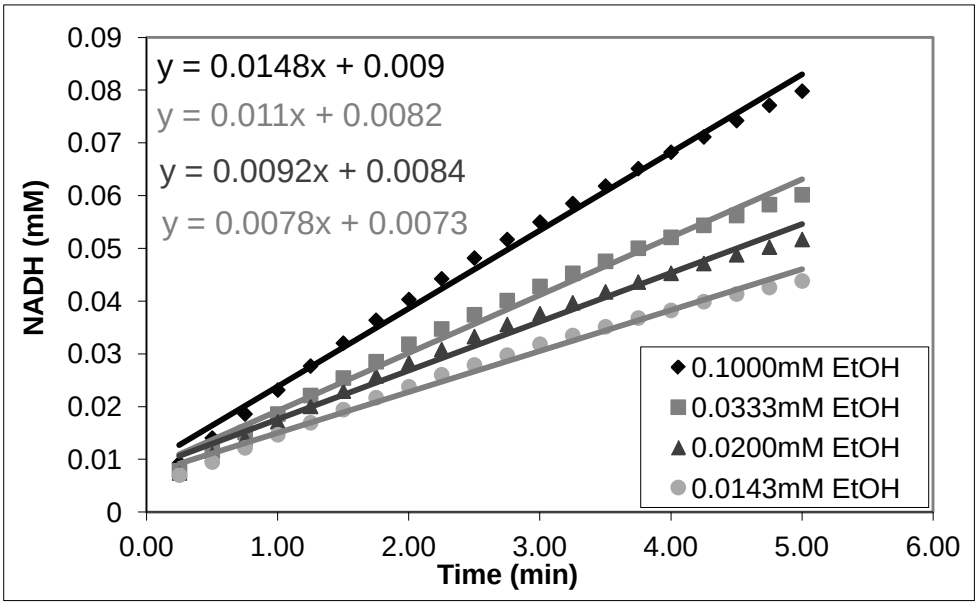

Figure 5.1: Kinetic studies of Alcohol Dehydrogenase demonstrating reaction rate (slope) for increasing initial concentrations of ethanol. Enzyme assay volumetric activity: 0.0308 units ADH/mL; NAD concentration: 0.58mM.

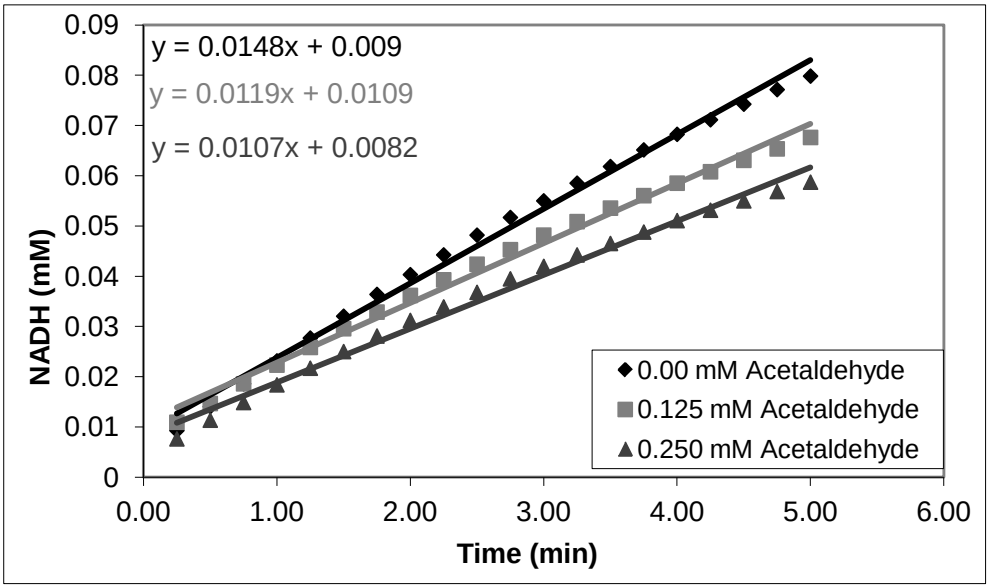

Figure 5.2: Kinetic Studies of alcohol dehydrogenase demonstrating reaction rate decreases (slopes) for increasing concentrations of acetaldehyde. Enzyme assay volumetric activity: 0.0308 units ADH/mL; Initial NAD concentration: 0.58mM; Initial Ethanol concentration: 0.10mM.

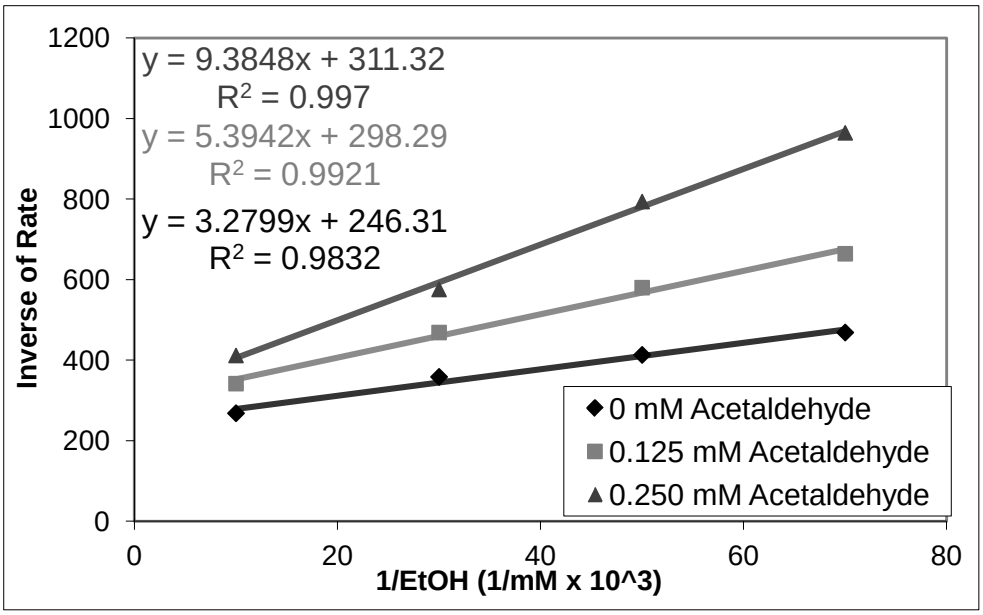

Figure 5.3: Lineweaver-Burke plot showing acetaldehyde product inhibition's impact on reaction rate for different ethanol concentration. Enzyme assay volumetric activity: 0.0308 units ADH/mL; Initial NAD concentration: 0.58mM

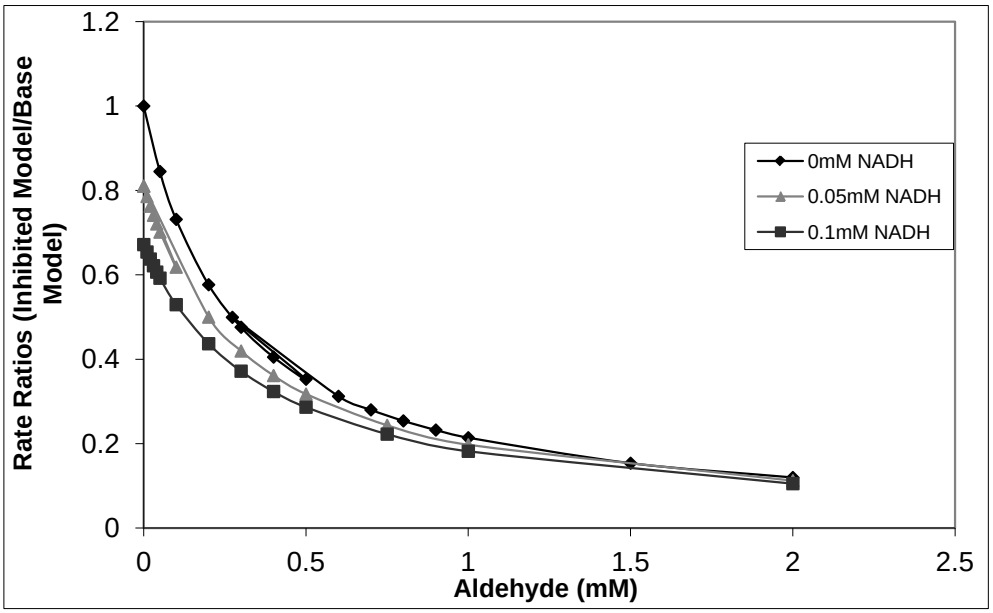

Figure 5.4: Alcohol Dehydrogenase rate ratio of predicted rate of the full term equation over the predicted rate of the base term equation at various product concentrations of acetaldehyde and NADH according to concentrations of 0.05 ADH units/mL, 22mM Ethanol, 1mM NAD, and pH = 7.8.

a)

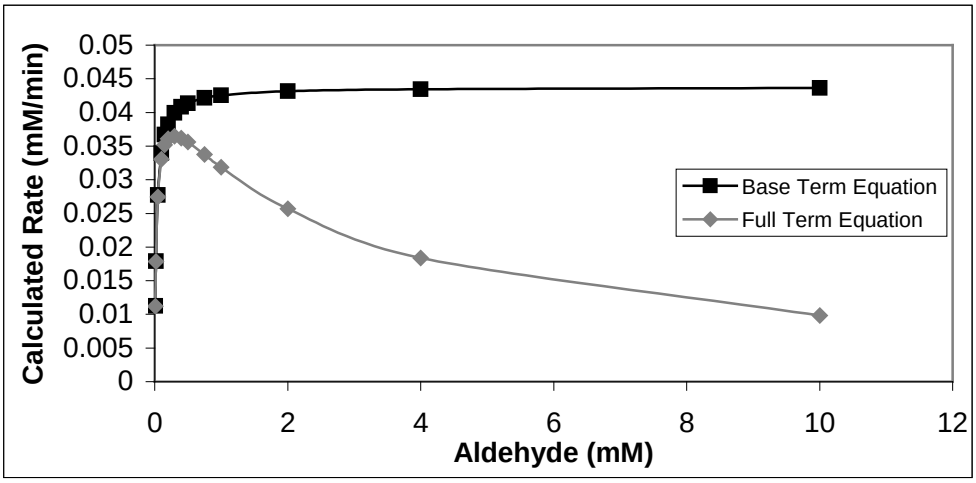

b)

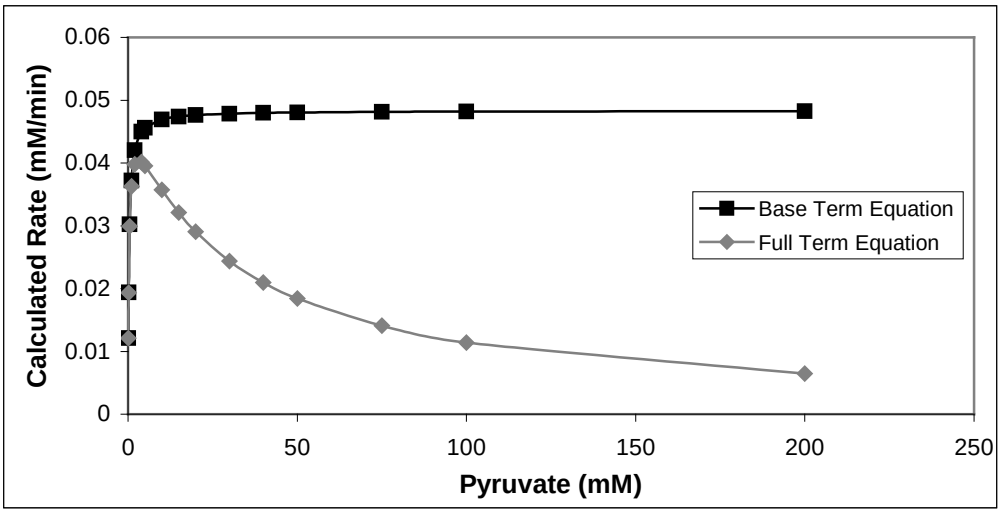

Figure 5.5: Comparisons of substrate inhibition effect on initial rate using the base term model and full term equation. (a) Aldehyde dehydrogenase at concentrations of 0.05 ALDH units/mL, 1mM NAD, no products, and pH = 7.8. (b) Lactate dehydrogenase at 0.05 LDH units/mL, 0.33mM NADH, no products, and pH = 7.8.

a)

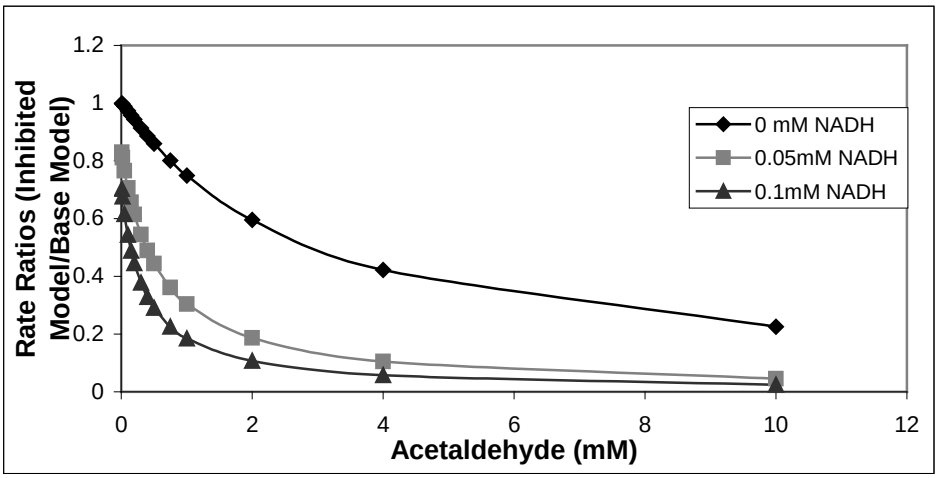

b)

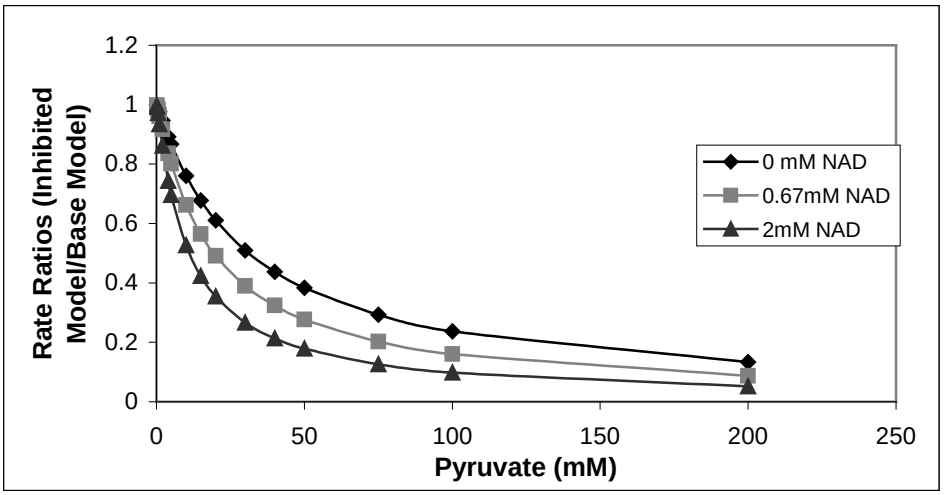

Figure 5.6: Rate ratio of predicted rate of the full term equation over the predicted rate of the base term equation involving substrate-product inhibition complexes. (a) Aldehyde dehydrogenase according to concentrations of 0.05 ALDH units/mL, 1mM NAD, and pH 7.8 and (b) Lactate dehydrogenase according to concentrations of 0.05 LDH units/mL, 0.33mM NADH, and pH 7.8

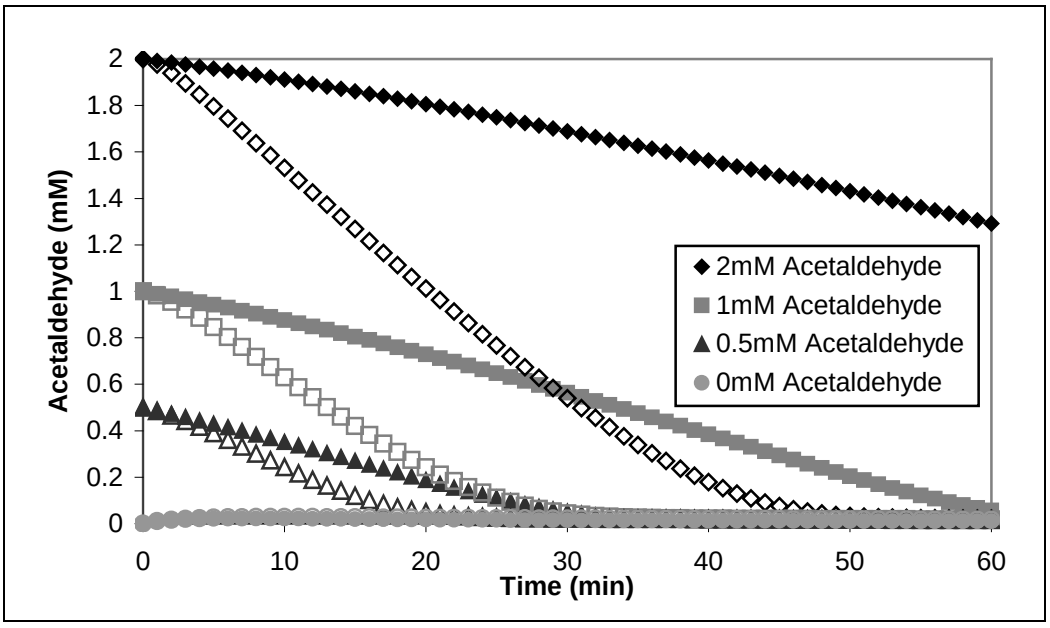

Figure 5.7: Concentration profile of acetaldehyde in a two enzyme system consisting of alcohol dehydrogenase and acetaldehyde dehydrogenase at different starting concentrations of acetaldehyde. Initial Concentrations: 22mM Ethanol, 5mM NAD, 0.05 Units/mL ADH, 0.05 Units/mL ALDH, and pH 7.8. Solid points represent the complete model with full inhibition while hollow points depict the four term base models with no inhibition present.

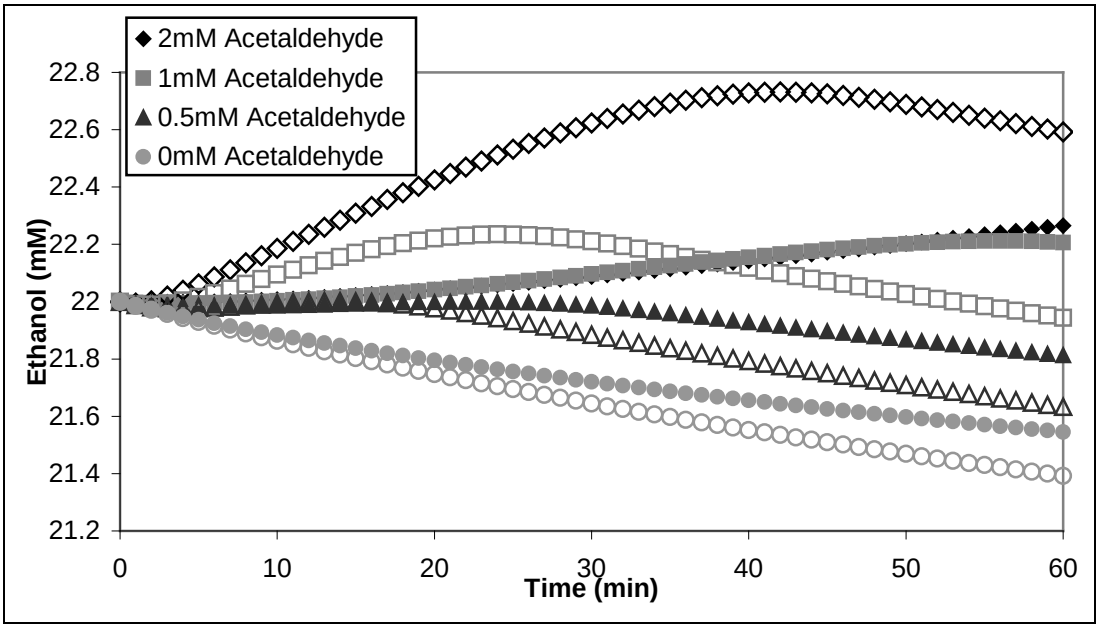

Figure 5.8: Concentration profile of ethanol in a two enzyme system consisting of alcohol dehydrogenase and acetaldehyde dehydrogenase at different starting concentrations of acetaldehyde. Initial Concentrations: 22mM Ethanol, 5mM NAD, 0.05 Units/mL ADH, 0.05 Units/mL ALDH, and pH 7.8. Solid points represent the complete model with full inhibition while hollow points depict the four term base models with no inhibition present.

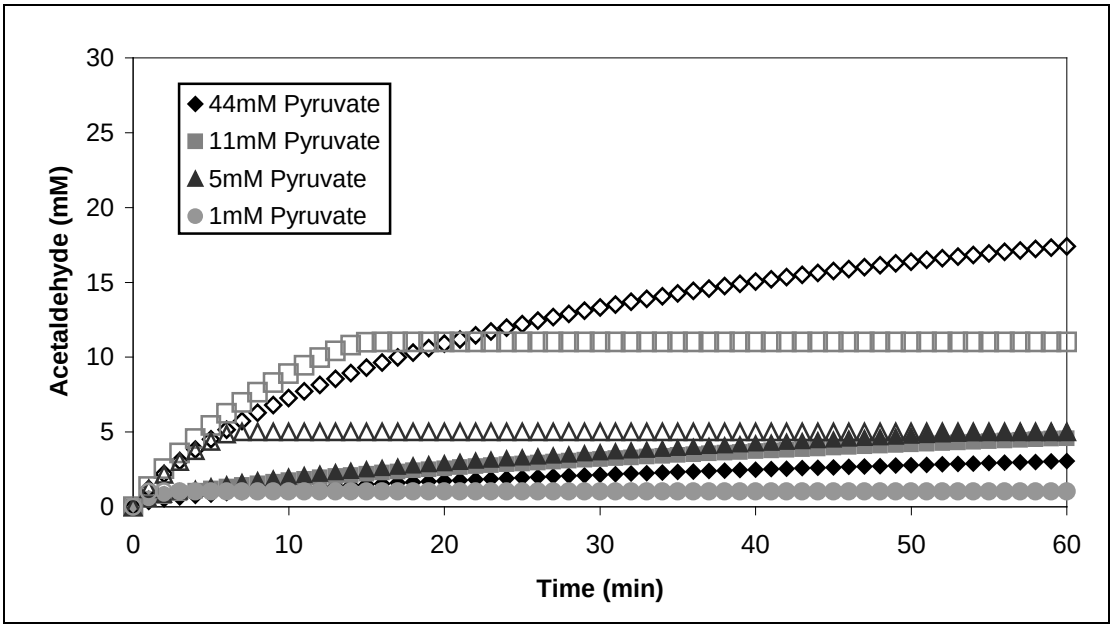

Figure 5.9: Concentration profile of acetaldehyde in a two enzyme system consisting of alcohol dehydrogenase and lactate dehydrogenase at different starting concentrations of pyruvate. The increase in acetaldehyde concentration reflects the equimolar decrease in ethanol concentration. Initial Concentrations: 22mM Ethanol, 2mM NAD, 5 Units/mL ADH, 5 Units/mL ALDH, and pH 7.8. Solid points represent the complete model with full inhibition while hollow points depict the four term base models with no inhibition present.

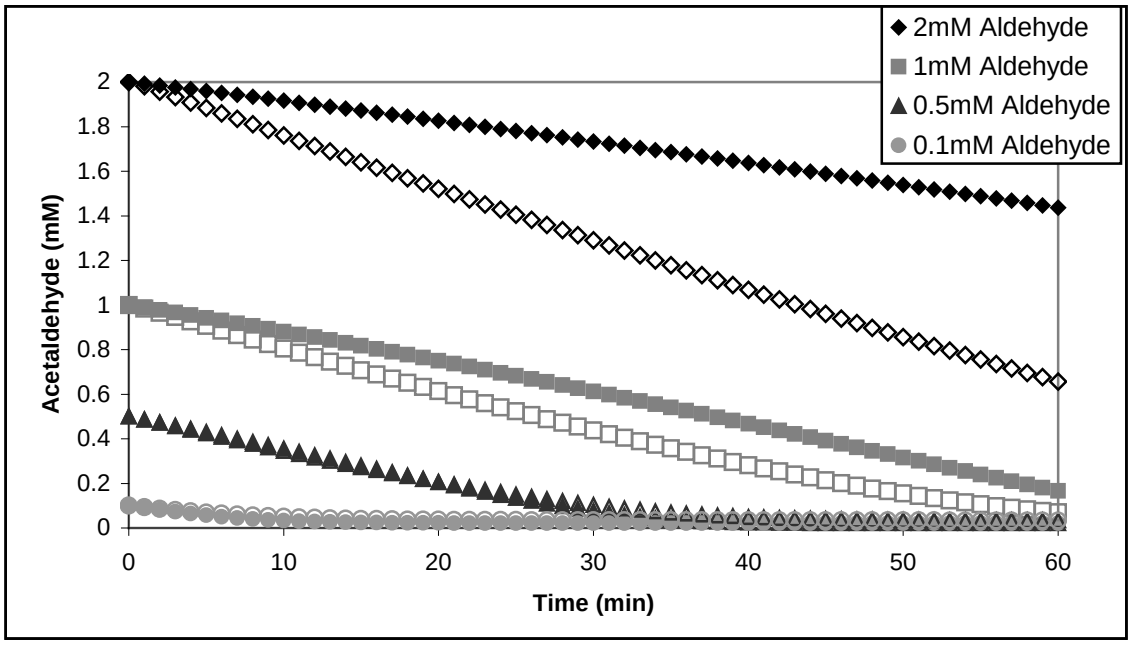

Figure 5.10: Concentration profile of acetaldehyde in the three enzyme system consisting of alcohol, acetaldehyde, and lactate dehydrogenases at different starting concentrations of acetaldehyde. Initial Concentrations: 22mM Ethanol, 5mM NAD, 5mM Pyruvate, 0.05 Units/mL ADH, 0.05 Units/mL ALDH, 0.05 Units/mL LDH, and pH 7.8. Solid points represent the complete model with full inhibition while hollow points depict the four term base models with no inhibition present.

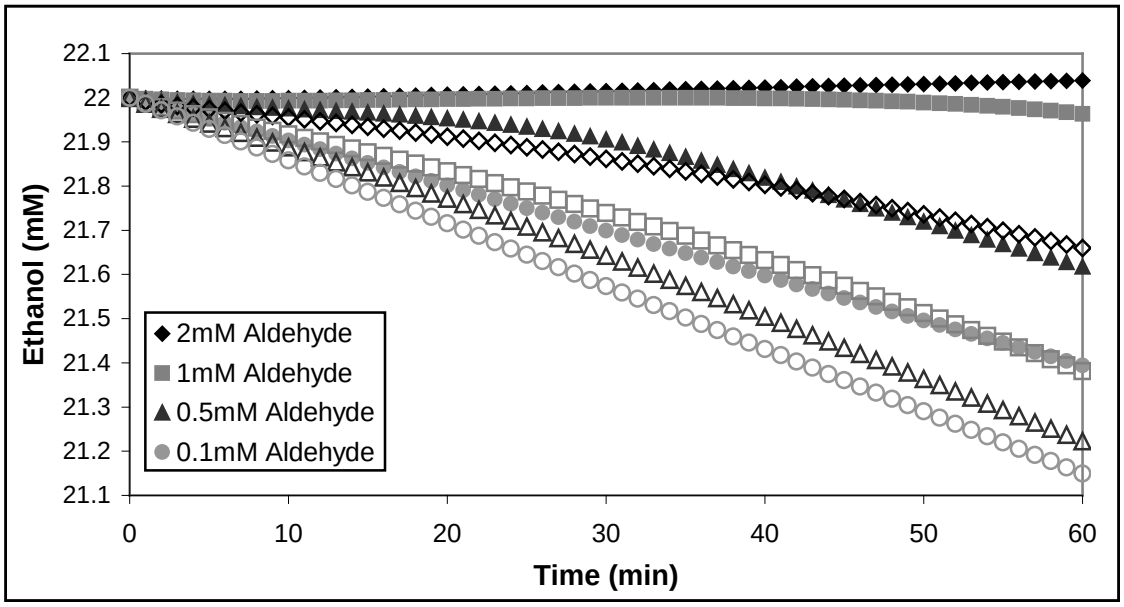

Figure 5.11: Concentration profile of ethanol in the three enzyme system consisting of alcohol, acetaldehyde, and lactate dehydrogenases at different starting concentrations of acetaldehyde. Initial Concentrations: 22mM Ethanol, 5mM NAD, 5mM Pyruvate, 0.05 Units/mL ADH, 0.05 Units/mL ALDH, 0.05 Units/mL LDH, and pH 7.8. Solid points represent the complete model with full inhibition while hollow points depict the four term base models with no inhibition present.

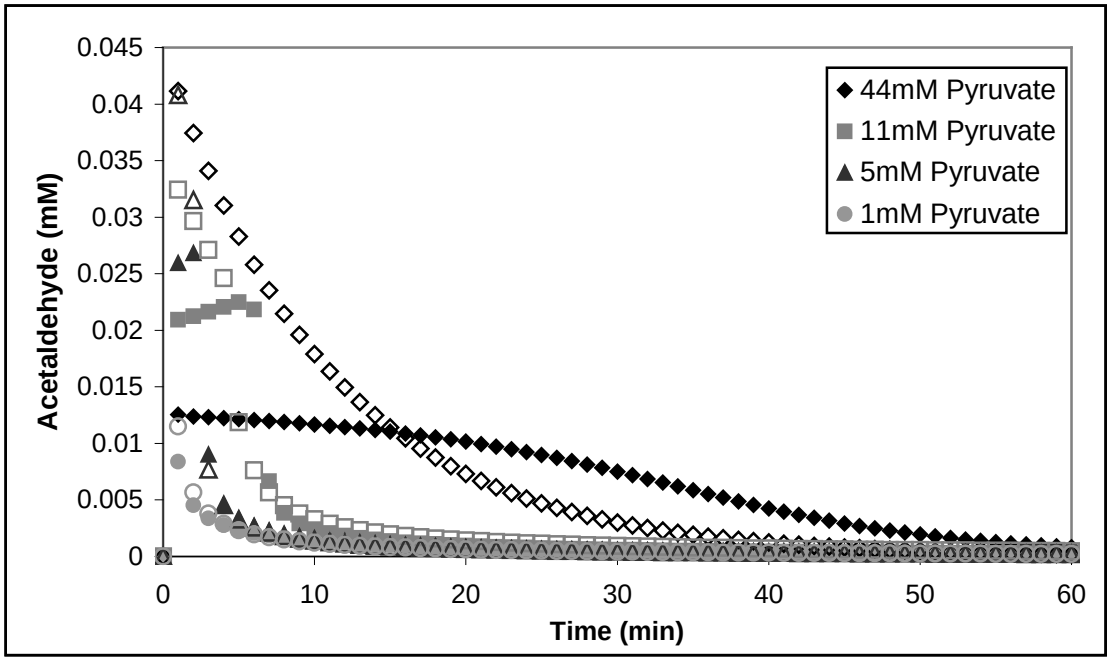

Figure 5.12: Concentration profile of acetaldehyde in the three enzyme system consisting of alcohol, acetaldehyde, and lactate dehydrogenases at different starting concentrations of pyruvate. Initial Concentrations: 22mM Ethanol, 5mM NAD, 5mM Pyruvate, 0.05 Units/mL ADH, 0.05 Units/mL ALDH, 0.05 Units/mL LDH, and pH 7.8. Solid points represent the complete model with full inhibition while hollow points depict the four term base models with no inhibition present.

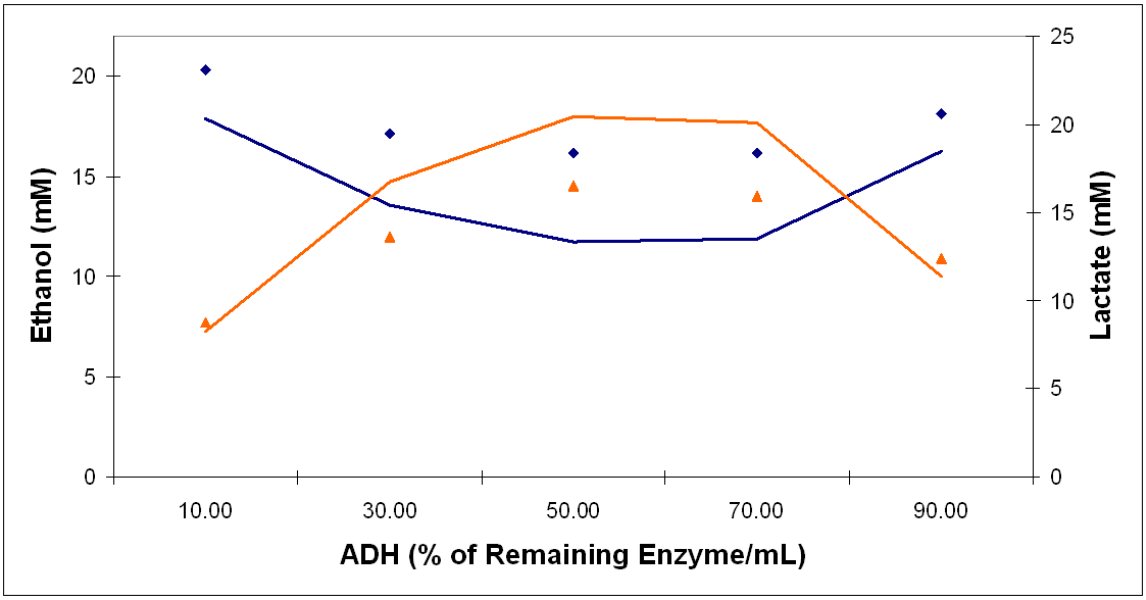

Figure 5.13: Substrate Concentrations at 20 Minutes in the Three Enzyme System with LDH Accounting for 30% of the Total Enzyme Units. Initial Concentrations: 21 Combined Enzyme Units / mL, 22mM Ethanol, 44mM Pyruvate, 1mM NAD, and pH = 7.8. Ethanol Experimental Values (♦) and Simulation (—). Lactate Experimental Values (▲) and Simulation (—).

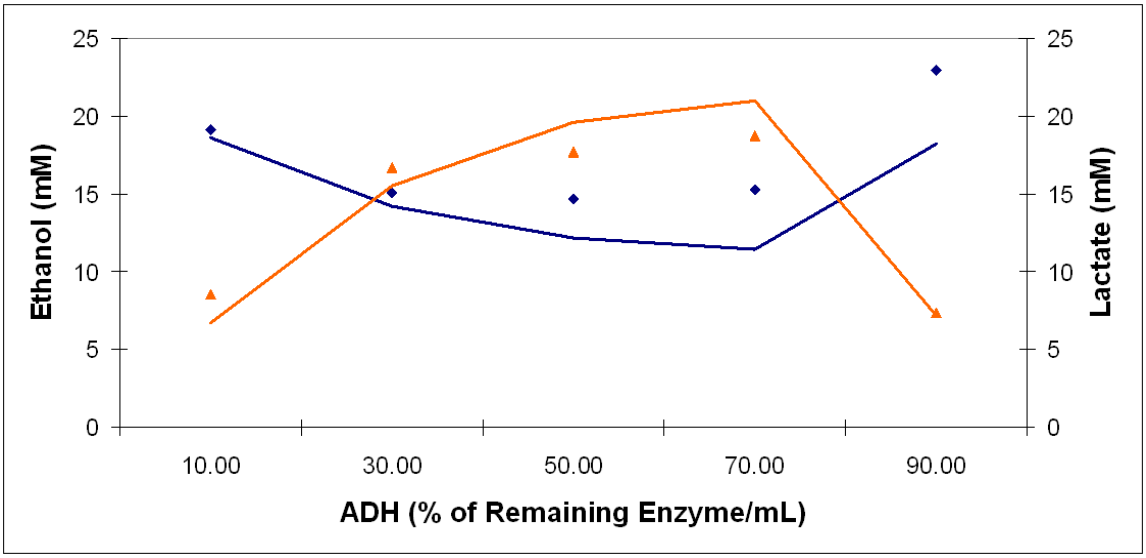

Figure 5.14: Substrate Concentrations at 20 Minutes in the Three Enzyme System with LDH Accounting for 50% of the Total Enzyme Units. Initial Concentrations: 21 Combined Enzyme Units / mL, 22mM Ethanol, 44mM Pyruvate, 1mM NAD, and pH = 7.8. Ethanol Experimental Values (♦) and Simulation (—). Lactate Experimental Values (▲) and Simulation (—).

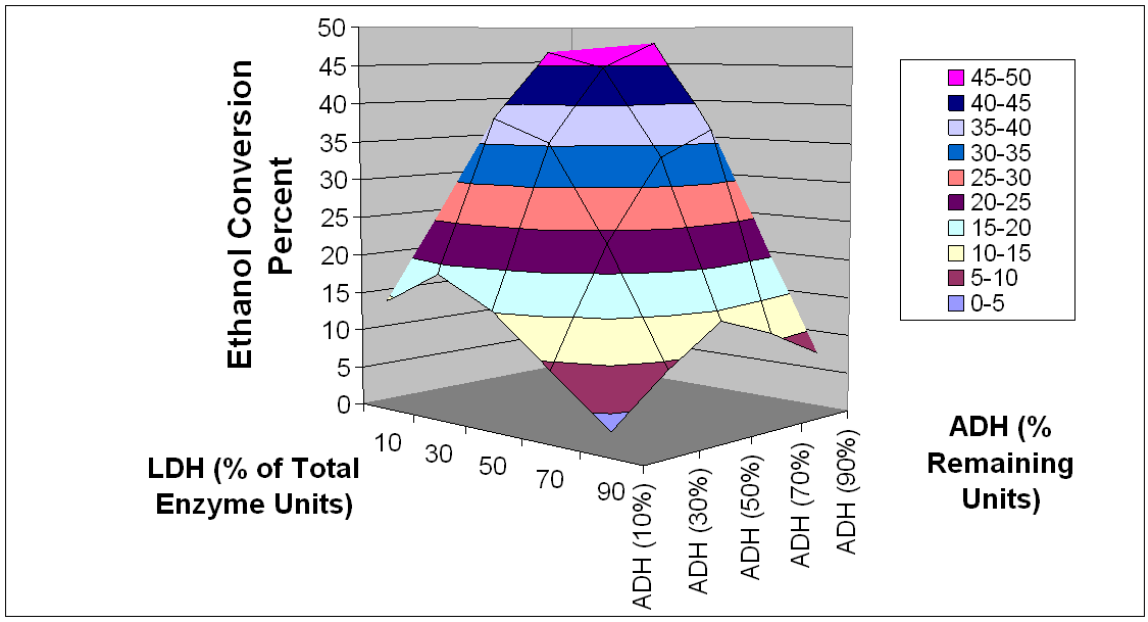

Figure 5.15: Simulation of Ethanol Conversion Percent Achieved at 20 Minutes in the Three Enzyme System, based on 21 Total Units of Enzyme per Each Milliliter of Reaction Solution. Initial Concentrations: 22mM Ethanol, 44mM Pyruvate, 1mM NAD, and pH = 7.8.

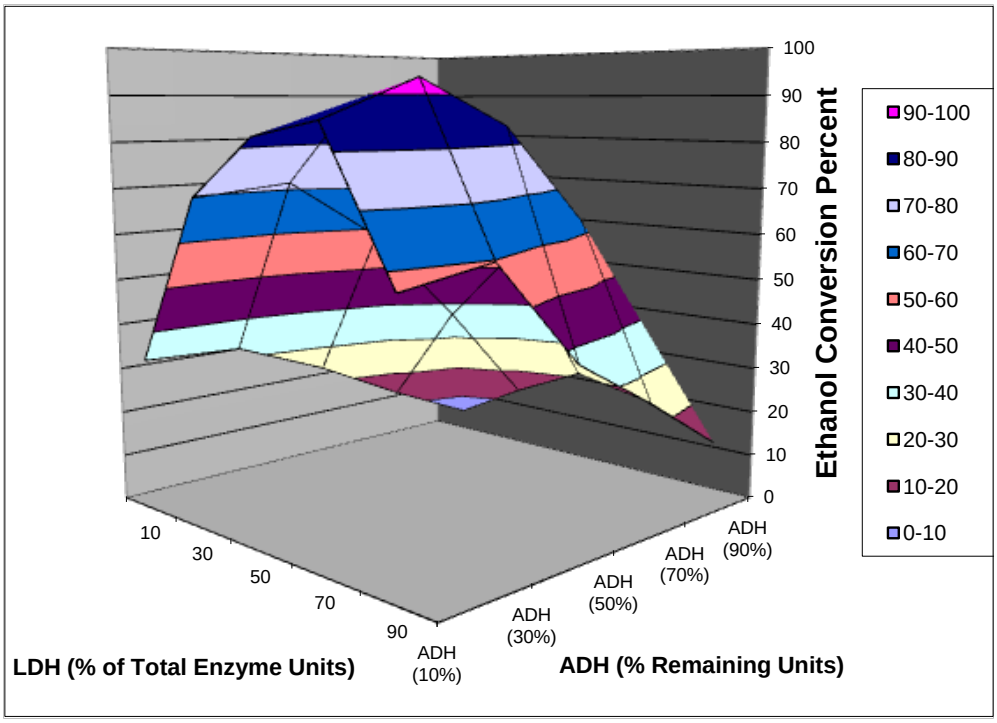

Figure 5.16: Unihibited Simulation of Ethanol Conversion Percent Achieved at 20 Minutes in the Three Enzyme System, based on 21 Total Units of Enzyme per Each Milliliter of Reaction Solution. Initial Concentrations: 22mM Ethanol, 44mM Pyruvate, 1mM NAD, and pH = 7.8.

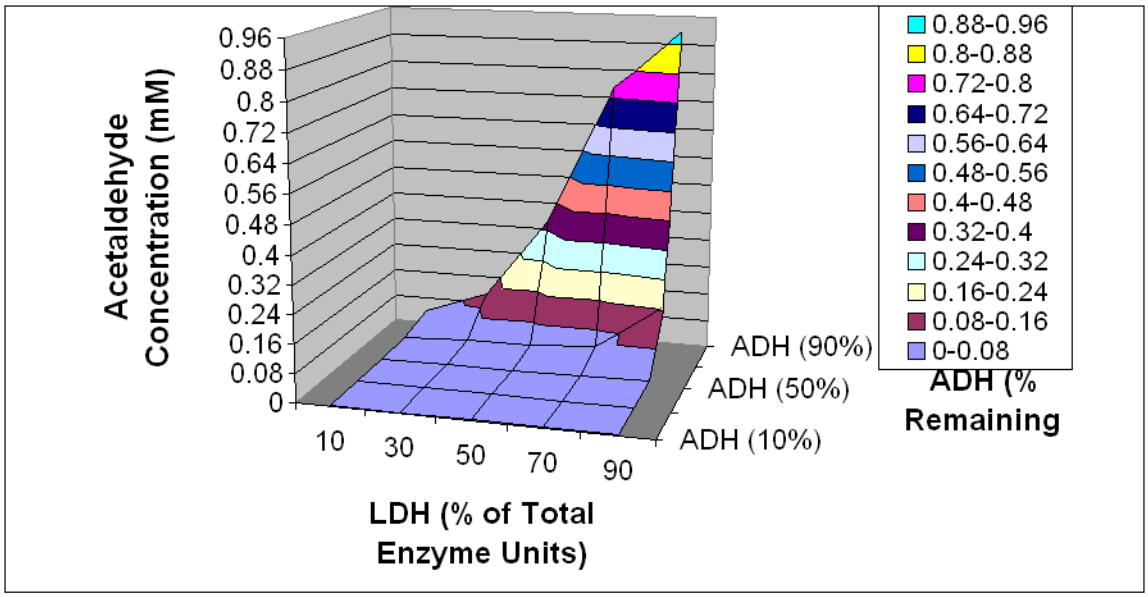

Figure 5.17: Simulation of Acetaldehyde Concentration Achieved at 20 Minutes in the Three Enzyme System, based on 21 Total Units of Enzyme per Each Milliliter of Reaction Solution. Initial Concentrations: 22mM Ethanol, 44mM Pyruvate, 1mM NAD, and pH = 7.8.

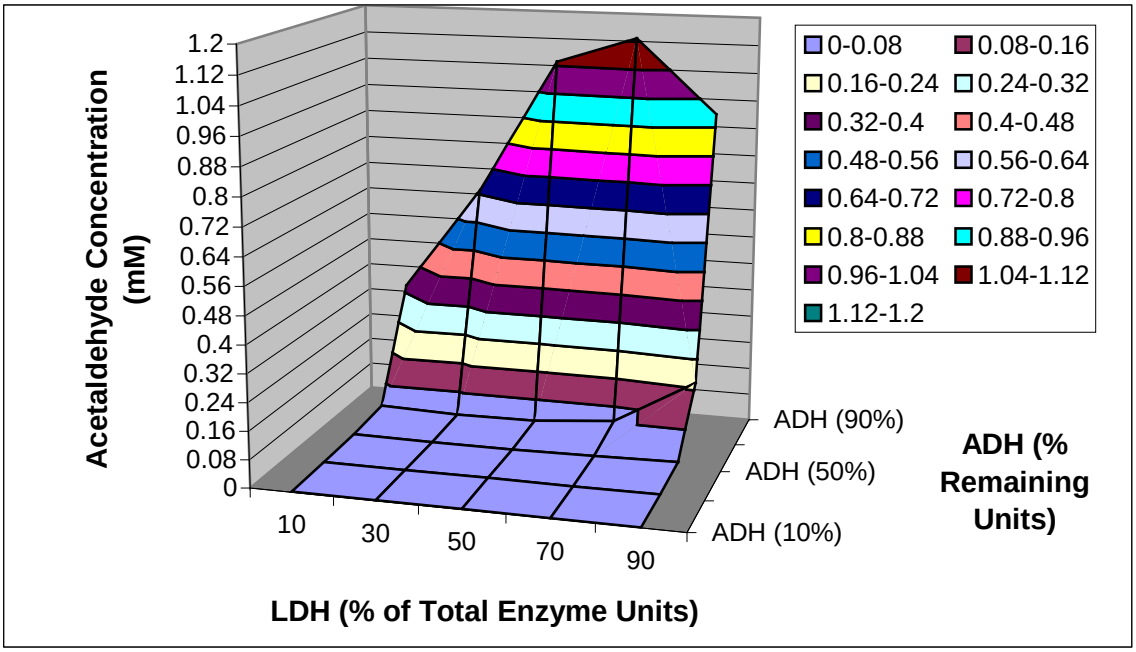

Figure 5.18: Unihibited Simulation of Acetaldehyde Concentration Achieved at 20 Minutes in the Three Enzyme System, based on 21 Total Units of Enzyme per Each Milliliter of Reaction Solution. Initial Concentrations: 22mM Ethanol, 44mM Pyruvate, 1mM NAD, and pH = 7.8.

5.7 REFERENCES

1. Bostian, K.A. and Betts, G.F. (1978). Rapid purification and properties of potassium-activated aldehyde dehydrogenase from Saccharomyces cerevisiae. Biochemical Journal 173, 773-786.

2. Bergmeyer, H.U., Bernt E., Hess B. (1974). Lactate Dehydrogenase. Methods of enzymatic analysis.

3. Kagi, J. H. R. & Vallee, B. L., (1960). The role of zinc in alcohol dehydrogenase. J. Biol. Chem. 235, 3188-3192.

4. Tangerman, A. (1997). Highly sensitive gas chromatographic analysis of ethanol in whole blood, serum, urine and fecal supernatants by the direct injection method. Clinical Chemistry, 43, 1003–1009.

5. Wratten, C.C., and Cleland, W.W. (1963). Product inhibition studies on yeast and liver alcohol dehydrogenases. Biochemistry, 2, 935.

6. Cleland, W.W. (1967). The statistical analysis of enzyme kinetic data. Annu. Rev. Biochem., 36, 77-112.

7. Alberty, R.A. (1953). Mechanisms of Enzyme Action. J. Amer. chem. Soc., 75, 1928.

8. Deetz, J. S., Luehr, C. A., & Vallee, B. L. (1984). Human liver alcohol dehydrogenase isozymes: reduction of aldehydes and ketones. *Biochemistry, 23*, 6822–6828.

9. Umulis, D.M., Gurmen, N.M., Singh, P., Fogler, H.S. (2005). A physiologically based model for ethanol and acetaldehyde metabolism in human beings. Alcohol, 35 (1), 3-12.

CHAPTER 6

INCORPORATION OF ALCOHOL DEHYDROGENASE BY COVALENT CONJUGATION INTO pH SENSITIVE PEG-g-MAA HYDROGEL

Immobilization of biologically active species has been studied for some time as a means of increasing functional capability. Industrially, the process is important due to the ease of product separation, reuse of the enzyme, and no unfavorable side reactions. An emergent use of hydrogel polymer networks are toward pharmaceutical applications, predominantly as carriers for delivery of drugs, peptides, or proteins. The choice of the support and the method of immobilization play a crucial role in governing enzymatic reactions. Synthetic polymers such as polyacrylamide, poly(hydroxyethyl methacrylate), and crosslinked copolymers offer stiffness as well as internal mass-transfer resistance. Moreover, in regards to bioactive proteins, hydrogels offer a support structure capable of protecting the protein against environmental conditions capable of causing denaturization, unfolding of the protein into a non-useful state.

Alcohol dehydrogenase (ADH), a complex redox enzyme, contains four subunits bound to zinc and a sensitive sulfhydryl group essential for its activity (1). The immobilization of ADH onto numerous supports was reported in the literature (2–5). Various techniques like covalent binding, crosslinking, and entrapment of ADH were used for these immobilizations (6, 7). Specifically, covalent binding of enzymes involves the chemical conversion of a functional group of the polymer through a multifunctional

group reagent, prior to the coupling of the enzyme, while entrapment of an enzyme is performed by polymerizing an aqueous solution containing monomers and the enzyme in the presence of a crosslinking agent. Studies of the stability or activity of immobilized enzymes showed that immobilization leads to deviation from their native form in terms of activity (8-12).

Here, we undertook the immobilization of functionalized yeast ADH through covalent coupling utilizing a pegylated gel, specifically, poly(methacrylic acid- grafted-ethylene glycol). This hydrogel is capable of a reversible responsive action to the acidity of its environment due to temporary physical cross-links provided by hydrogen bonding between carboxylic acid pendent groups of PMAA and etheric groups of PEG grafts (13). Ultimately, the system may be capable of delivering vital detoxification proteins in a cell-like microreactor assembly to the intestines of vertebrate organisms where it may be useful in metabolizing ethanol.

6.1 MATERIALS AND METHODS

6.1.1 Materials

Buffer salts, sodium phosphate monobasic and dibasic as well as potassium phosphate, were purchased from Fluka (Sigma-Aldrich, Buchs, Germany). Citrate buffer salt as well as Tris-HCl 1M buffer solution was procured from Fisher Bioreagents (Fair Lawn, NJ). Lyophilized enzyme alcohol dehydrogenase (ADH, EC 1.1.1.1) from Saccharomyces cerevisiae was also bought from Sigma-Aldrich (St. Louis, MO). Activity of the enzyme was listed on the label as having a specific activity of 451 U/mg (pH 7.5, 37°C). Additionally, enzyme cofactor β-nicotinamide adenine dinucleotide disodium salt was obtained from Sigma (St. Louis, MO). Substrate ethanol (95%), acryloyl chloride

(98%), sodium chloride (NaCl), ethyl ether, and Sephadex G-25 were also purchased from Sigma (Miwaukee, WI) Hydrogel monomer methacrylic acid (MAA) was obtained from Sigma (Milwaukee, WI), while methoxy-terminated poly(ethylene glycol) monomethacrylate (PEGMA) with PEG molecular weight 200 and poly(ethylene glycol) dimethacrylate (PEG200DMA) crosslinker were obtained from Polysciences, Inc (Warrington, PA).

6.1.2 Enzyme activity assays

Alcohol dehydrogenase activity was assayed spectrophotometrically at 340nm and 22 °C using a concentration of 20mM ethanol and 1mM β-nicotinamide adenine dinucleotide, disodium salt (NAD; ε_{340} = 6.22 mM^{-1} cm^{-1}) as substrate and co-factor in 200 mM sodium, 90 mM potassium, 150mM phosphate buffer, pH 7.8, which is a modification of a published procedure (14). One unit of ADH activity was defined as the amount of enzyme converting 1.0 μmol of ethanol per minute. The volumetric activity ($mM\ min^{-1}$) was defined as the enzyme activity per ml of enzyme solution for the free enzyme. The rates of reduction of NAD were carried out for 5-10 minutes and recorded utilizing either a Gilford Spectrophotometer 250 for 3mL cuvette assays or a Biotek Synergy HT for 6mL assays in a Nunc 6-well plate. The linear portion of the reaction progress curve, where applicable, was used to analyze the activity. It should be noted, nevertheless, that given the inhibitory nature of ADH relative to its product acetaldehyde, generated curves were often non-linear, especially for the free enzyme over five minutes and longer. Typically, the rates reported are from the first minute and a half of concentration change.

6.1.3 Enzyme Functionalization Procedure

Alcohol dehydrogenase (380 label units, 0.87mg) was dissolved into 1.8mL of the sodium, potassium phosphate buffer described previously to achieve an approx. 218 IU/mL enzyme solution. Following the procedure of Bille, acryloyl chloride diluted in ethyl ether (6.5mM) was added to the enzyme solution at a 25 mole ratio (20µL) of AC to concentration of enzyme and reacted for 30 minutes in a 4°C ice bath under gentle stirring (15). Subsequently, an activity assay was performed using 0.75 label units of reacted enzyme per milliliter of assay solution.

6.1.4 Purification of Functionalized Enzyme

Separation of the enzyme from excess acryloyl chloride was done by passing the reacted enzyme sample through a 6mL gel column of Sephadex G-25. The acrylated ADH is eluted using 0.1M NaCl, 0.1M Tris-HCl Buffer (pH 6.5). The filtrate was collected in 16-0.5mL samples and analyzed at 280nm using UV spectroscopy to determine the presence of functionalized and/or unfunctionalized enzyme.

6.1.5 Hydrogel Formation

Hydrogels were prepared from 1:1 molar ratios of MAA/PEG200MA. After bringing the monomers to room temperature, the monomers were mixed and sonicated for 5 minutes. One or two percent mole fractions crosslinking agent of PEG200DMA was added, and the mixture was sonicated again. A 50% by weight equimolar methanol / water solution was applied as solvent to the monomer mixture followed by a repeated sonication. The polymer solution was then bubbled under nitrogen for 15 minutes to remove dissolved oxygen. Photoinitiator Irgacure 184 was added to the monomer solution at about 5% of total mass, and the mixture was swirled briefly in a vial until all

initiator had dissolved. About 8% by volume of purified functionalized enzyme, depending upon the enzyme concentration, was added to monomer solution to achieve an estimated 10 label units per milliliter of mixture, which was given a brief final sonication. The enzyme-enriched monomer solution was then injected between clamped glass slides with a 0.8mm Teflon spacer. Following two minutes of exposure to UV light at 10mW/cm^2, a crosslinked hydrogel was produced. A 0.45mL doughnut shaped disc (4.5 label units total) was cut out and washed a sodium, potassium phosphate buffer solution at pH=7.8 for 2.5 hours until swelling was complete and polymerization solvent was replaced with buffer. The disc was then be submerged in an assay solution, employing an estimated 0.75 gel units of enzyme per milliliter assay, in a six-well plate for reading in a Synergy Biotek reader.

6.1.6 Gel Swelling

Sample 10mm diameter discs of hydrogel were vacuum oven dried to consistent mass over a period of 36hrs. The samples were then allowed to swell in McIlvaine buffer solutions at a higher (7.4), medium (4.0), and lower (2.0) pH values to determine mass swelling ratio and dynamic swelling profiles.

6.1.7 ADH Ultraviolet Exposure Investigation

A buffered solution of Free enzyme ADH was clamped between glass plates with a 0.8mm Teflon spacer. Volume of the plates was 2mL, and enzyme concentration was 10UI/mL (label units). These plates were exposed to UV light from a Novacure photometer arranged normal to the plate at intensities of 10mW/cm^2 while temperature was controlled with a cold plate for 0.5°C runs. Upon removal from the light source, the UV bombarded free enzyme was added to an assay (0.75 units/mL) to attain activity.

6.1.8 pH Cycling Activity

Standard assay concentrations were used to determine pH effect in neutral, moderately acidic, and low pH McIlvaine buffers as noted above. Three gels of similar composition, 2% crosslinker PEG200DMA and 4.5units ADH/mL gel, were prepared for use in each buffer. Initial activity of the gel was investigated by submerging doughnut discs into pH buffer with standard assay concentration following polymerization and pre-swelling at the desired initial pH for 90 minutes. These gels were placed in one pH buffer for a one hour period before being placed in the alternate pH buffer. A pH shift was performed twice and enzyme activity was monitored each half hour by utilizing a fresh assay of standard substrate concentration in the desired pH buffer.

6.2 ADH INVESTIGATION

6.2.1 UV influence on activity of ADH

One of the primary objectives in conjugating an active protein to a polymer matrix is to preserve the activity of the protein by protecting its tertiary structure. Because the formation of a MAA/PEGMA hydrogel requires UV-initiated free radical polymerizations, experiments were performed in order to reduce the influence of UV degradation of alcohol dehydrogenase, in which the ultraviolet light supplies energy that disrupts the protein bonds and causes unfolding. UV exposure time, UV intensity, temperature, and presence of cofactor NAD to protect the enzyme active site were all analyzed to produce enzyme conjugated gels with minimal activity loss. Possibly the greatest effect was seen to occur based on UV exposure time and penetration of UV light through the polymer template.

Generally, hydrogels undergo UV free-radical polymerization by placing monomer solution between glass plates with 0.80mm Teflon spacers. The monomer solution is exposed to UV light with 10mW/cm^2 intensity for duration up to 15 minutes, ensuring complete polymerization. However, prolonged exposure of the enzyme to the UV light for this duration has been demonstrated to eliminate nearly all enzyme activity (Figure 6.2). ADH activity is reduced to half after 10 minutes and diminishes to 15% of original free enzyme activity by 15 minutes. Thermal studies of the exothermic polymerization reaction also revealed maximum temperatures of 37°C as a potential cause for degradation. Nevertheless, isothermal studies at 0.5°C (Figure 6.1) as well as using NAD to protect the active enzyme sites proved to have little impact.

Decreases in enzyme activity occurred even at cold temperature polymerization. Based on 30 sec exposure, no significant difference with temperature was observed, and approx. a 7.5% drop in activity occurred. However, at 60 sec and beyond, the enzyme that was maintained at 0.5 Celsius seemed to retain about 5% more of its original activity in comparison to the enzyme at room temperature, i.e. 88% vs. 81.6% at 60 seconds of UV light and 76.6% vs. 71.2% at 90 seconds of UV light. In regards to isothermal reactions specifically, the rate decrease with time varies no more than 6% when comparing remaining activity among the non-isothermal room temperature UV exposure and that of the 0.5°C constant temperature runs. Conclusively, the most sufficient means of retaining activity is minimizing UV exposure time, meaning the ultraviolet light is most damaging to the enzyme's protein structure in our process. Using a dynamic scanning calorimeter to monitor heat flow, the time for complete polymerization was determined to be 90 seconds at 10mW/cm^2 intensity. Therefore, the enzymes do not need

to be exposed to the UV for more than two minutes in order for covalent bonding to the hydrogel matrix to occur. Again, for a two minute polymerization period, the minimum activity loss through 90 seconds is 25-29% (Fig. 6.1), while the maximum activity loss through five minutes is 37% (Fig. 6.2).

6.2.2 Hydrogel Formation Impact on ADH activity

Following the UV experimentation, activity testing was conducted for each phase in the production of matrix-bound ADH. The activity following each step was standardized, or compared, to the activity achieved by the equivalent of 0.75 unit/mL of free ADH enzyme in a 20mM ethanol, 1mM NAD, sodium-potassium-phosphate buffer assay at pH 7.8. Following the procedure of acryloyl chloride multi-point functionalization of ADH, which can interfere with the active site, the activity was still 93% of the original enzyme activity. Previous procedures utilizing more excessive concentrations of acryloyl chloride had the effect of removing all enzyme activity. Then, filtration through the Sephadex G-25 column provided four eluent samples with strong traces of protein (Figure 6.3). Volatile traces of the acryloyl chloride could be detected in the subsequent eluent. The curve suggests a majority of the ADH was recovered in 2.4mL of Tris-HCl buffer eluent, accounting for nearly 80% of original protein concentration. Standardization of ADH on a units/mL basis further identifies the amount of protein with a max concentration of approximately 145 units/mL. Another activity assay measurement found the rate to be 52% in comparison to the original free enzyme. This volumetric activity indicates that more than half of the active enzyme remained after possible denaturization and filtration loss. Finally, the hydrogel was prepared according to procedure. The creation of the doughnut shaped hydrogel disc allowed the Biotek's

UV spectrometer to read through the solution of the 6-well flat bottom dish once the disk has been placed in the assay. Comparison of initial slope for the ADH hydrogel to the original free enzyme demonstrated that the covalently bound ADH still possesses an encouraging amount of activity, i.e. 6.07μM/min/mL unswollen gel(Figure 6.4).

6.2.3 Swelling Studies

Employment of a loosely crosslinked pH-sensitive hydrogel provides two strategies to protecting the ADH protein and ensuring its activity. The 1% crosslinking of the monomer chains allowed significant mass swelling based on pH as much as 8 times increase in mass over dry state at pH=7.4 (Figure 6.5a). An aqueously swollen gel provides uptake of substrate for the enzyme to react; moreover, the open structure of the polymer matrix removes diffusion limitations of reactant which could potentially suppress ADH activity. Conversely, at a lower pH of 4.0, the mass size of the hydrogel is nearly a quarter of the mass at the higher pH environment. This contraction of the hydrogel provides a shield to the already covalently bound and stabilized protein against the acidic environment and proteolytic enzymes that can cause protein denaturization.

The speed at which the pendant PEG chains complex with the backbone polymeric structure due to the pH environment is another significant characteristic of the system. Due to the use of a short molecular weight PEG chain, the degree of complexation was limited, as per Lowman and Peppas work, allowing for speedier equilibrium swelling verse other polymer compositions (14). Dynamic volume swelling studies indicate a doubling in volume from the dry state to the pH 2.0 equilibrium within an hour. A subsequent quadrupling of volume occurs due to a buffer pH change of 2.0 to 7.4. Equilibrium, however, requires nearly a three hour period, corresponding to an

extended influx of substrate during a potential ingestion period. Conversely, an immediate increase in the ionic interaction of the chains again at low pH 2.0 produces a rapid collapse. The volume decreases as much as 90% within an hour toward the pH 2.0 equilibrium (Figure 6.5b).

6.2.4 pH and Stability testing of ADH activity in hydrogel vs. free enzyme

The most vital performance factor of the conjugate system involves the enzyme activity within the hydrogel polymer at conditions similar to biological acidity. We have established the enzymatic conversion of ethanol proceeds slower within the polymer at pH 7.4 (Figure 6.6a). At a pH of 2.0, similar to stomach acidity, the greatest success of the hydrogel in maintaining protein function is exhibited in the fact that activity exists. Typically, no activity is observed of the alcohol dehydrogenase at a pH lower than 5. However, a reaction rate of 1.75μM ethanol/minute is observed for the ADH-loaded hydrogel in pH 2.0 buffer. This rate compares well with the activity of the gel that was submerged in the pH 7.4 buffer: 2.17μM ethanol/minute (Figure 6.6a).

In studies evaluating multiple pH shifts, the integrity of the gel became quite important. Activity was consistent for each 30 minute assay at individual pH for the first hour. More satisfyingly, rates increased when shifting both lower pH gels to the neutral 7.4 pH (Figure 6.6b); although, activity loss began to become more significant over the second hour. Additionally, the gels that complexed from high pH to lower pH began to develop stress fractures. Upon subsequent reexpansion of the gel to pH 7.4, and in part due to shaking of the well plates to ensure mixing in the Biotek, the gels began to break apart and interfere with the UV absorbance in the well plate. Nevertheless, the gel that experienced the double pH shift from 2.0 to 7.4 and then back to 2.0 maintained 87% of

activity, i.e. activities of 0.75µM ethanol/min, 0.95µM ethanol/min, and 0.61µM ethanol/min respectively for each pH, providing promising activity to the enhanced gel despite the pH environment. Optimization of the polymer network will lead to polymers with better properties.

6.3 CONCLUSIONS

Herein, we have described the process for immobilization of alcohol dehydrogenase, primarily through covalent attachment, to a pH sensitive hydrogel and studied bioactive qualities of the hybrid structure. Although the system suffers from activity loss, especially during polymerization due to UV and the steric restriction of the protein, the enzyme does remain active throughout various pH environments. Specifically, alcohol dehydrogenase demonstrates reversible activity as a result of the diffusion afforded by the complexed state of the hydrogel structure. Future investigation may show the hydrogel capably provides support for concerted activity among multiple enzymes.

6.4 FIGURES

a)

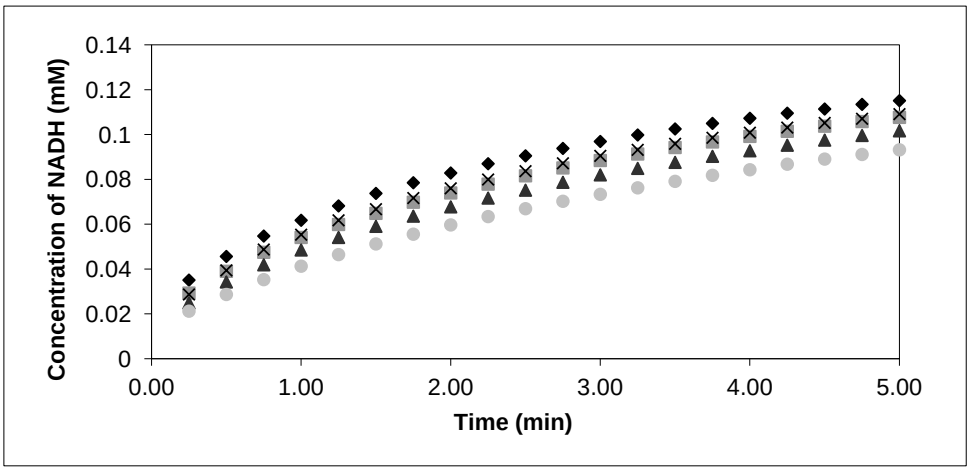

b)

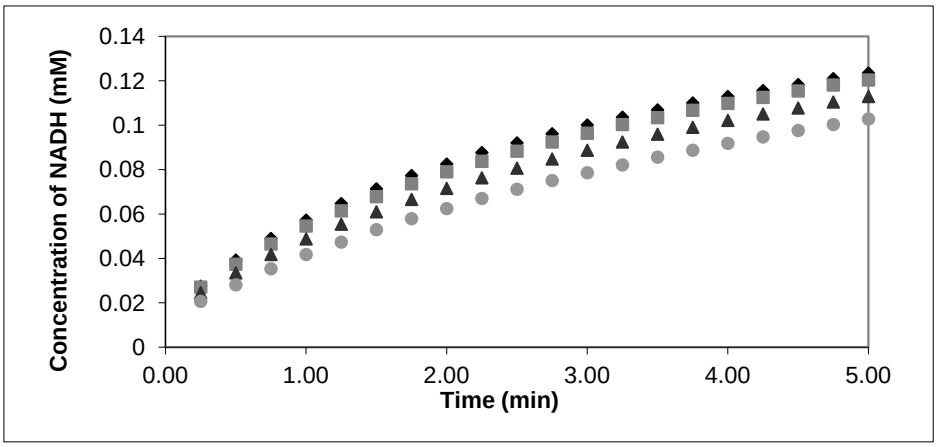

Figure 6.1: (a)Effect of UV exposure on free alcohol dehydrogenase enzyme activity at 0.5°C up to duration of necessary polymerization time. Free Enzyme at room temperature of 22°C (♦); At 0.5°C: No UV exposure (**x**), 30 seconds (■), 60 seconds (▲), and 90 seconds (●) of UV exposure. (b) Effect of UV on ADH activity at room temperature of 22°C up to duration of necessary polymerization time. No UV exposure (♦), 30 seconds (■), 60 seconds (▲), and 90 seconds (●) of UV exposure.

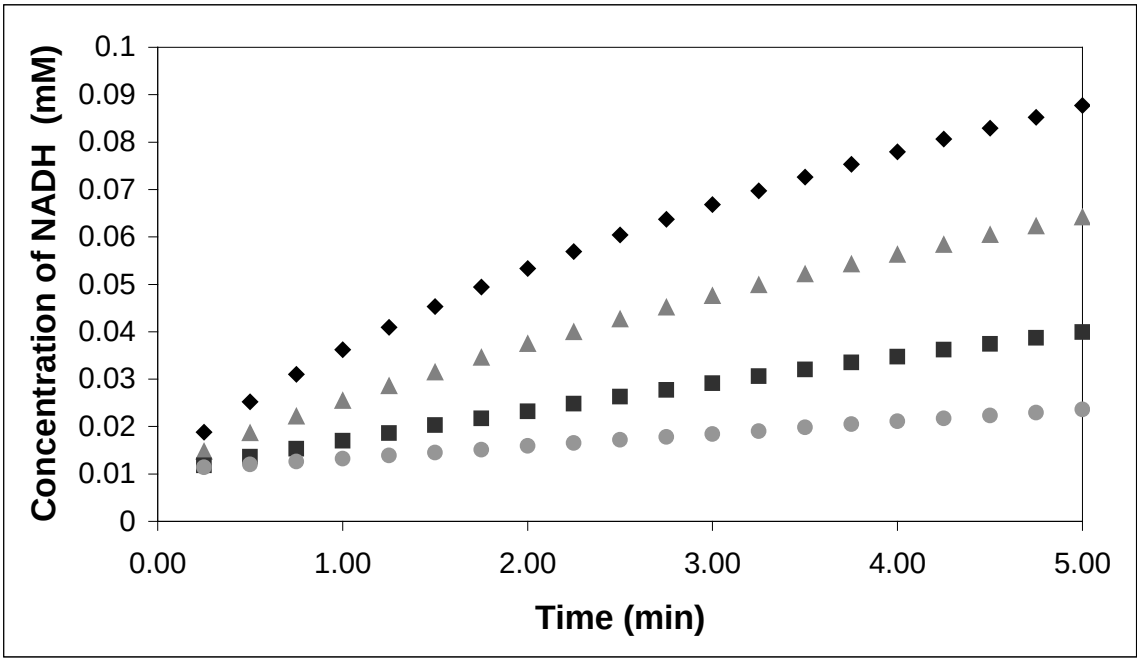

Figure 6.2: Effect of extended UV exposure on free alcohol dehydrogenase activity at room temperature of 22°C. No UV exposure(♦), 5 minutes (▲), 10 minutes (■), and 15 minutes (●) of UV exposure.

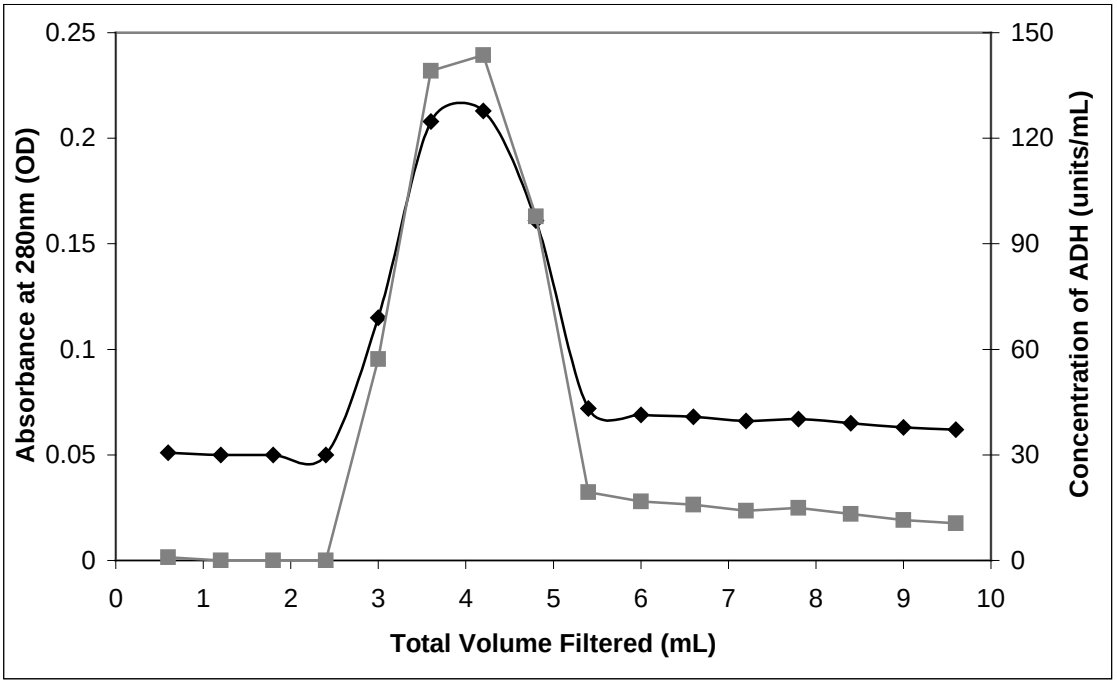

Figure 6.3: Detection of filtered alcohol dehydrogenase samples (0.6mL) from Sephadex G-25 column. Optical density measurements using UV spectroscopy at 280nm wavelength (♦), standardized concentration of protein for each sample(■).

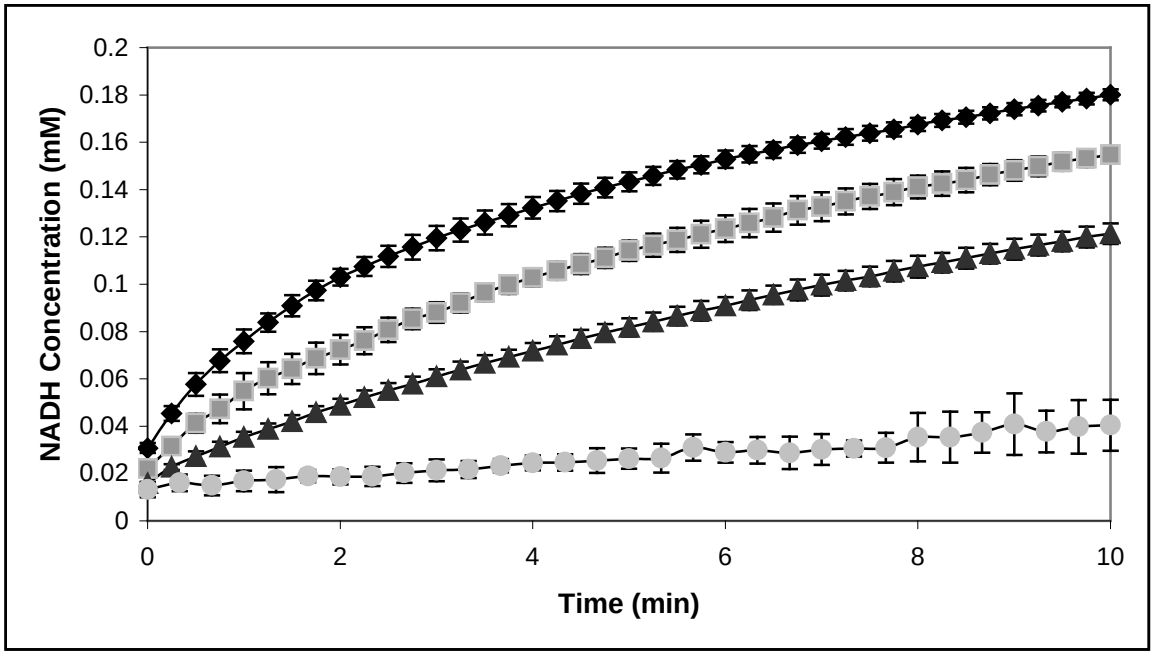

Figure 6.4: Activity Analysis of ADH during fabrication of the enzyme conjugated hydrogel matrix. Initial Concentrations: 0.75 ADH units/mL assay, 20mM Ethanol, 1mM NAD, and pH = 7.8. Enzyme Form: Free (♦), Functionalized (■), Filtered (▲), and Conjugated (●).

a)

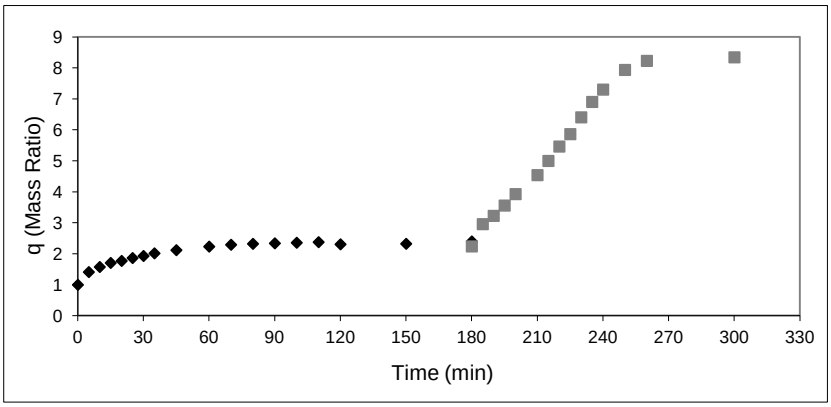

b)

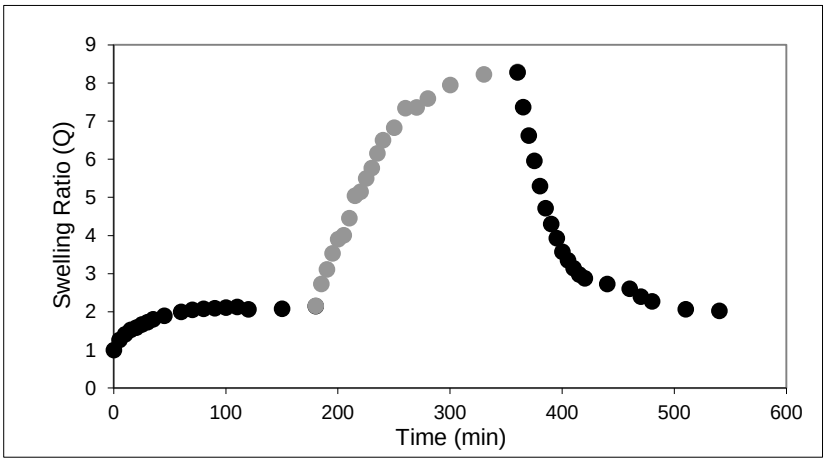

Figure 6.5: (A) Mass swelling ratio of the MAA/PEGMA hydrogel matrix due to pH changes. pH = 4.0(♦) followed by continued buffer acquisition at pH = 7.4 (■).
(B) Dynamic Volume Swelling of pH responsive hydrogel with 2% crosslinker beginning from dry state. pH = 2.0 (●), pH = 7.4 (●). Upon a pH switch from 7.4 to 2.0. The polymer structure collapses by 50% within 30 minutes.

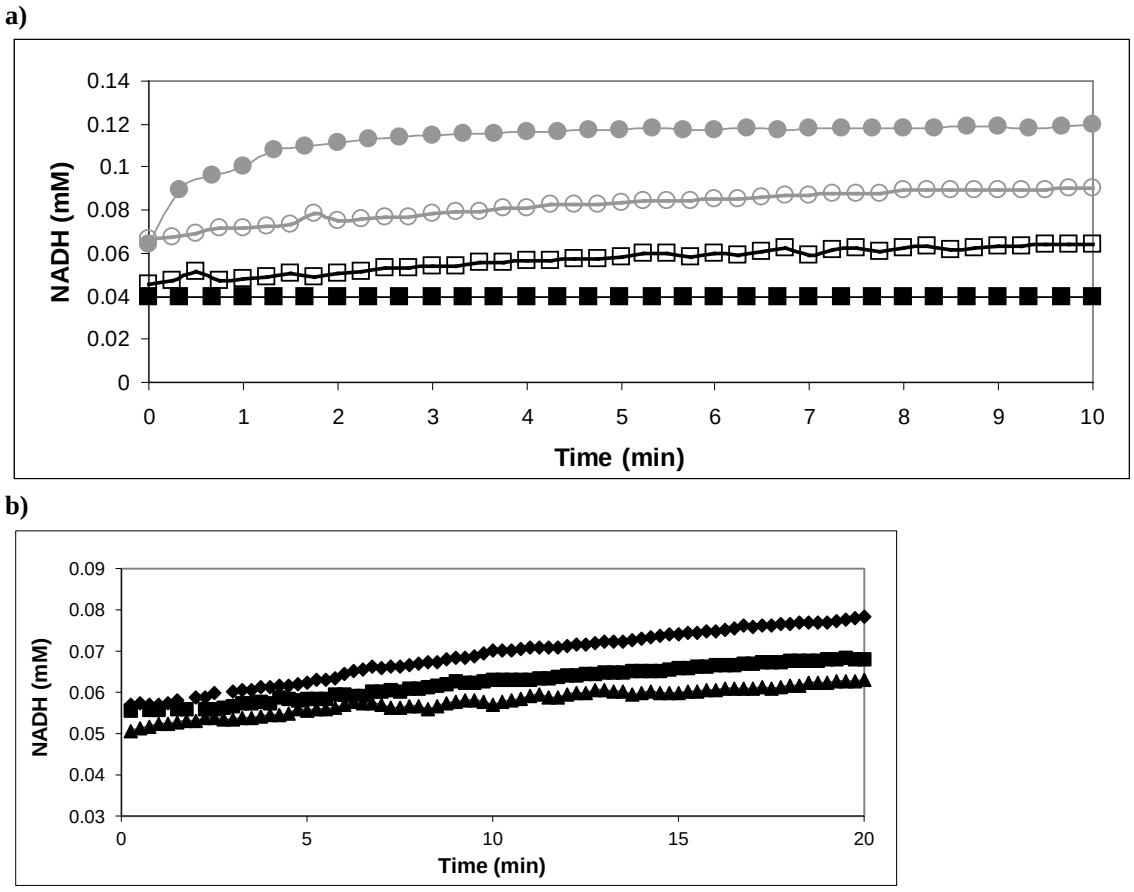

Figure 6.6: Activity Analysis of ADH comparing polymer conjugated and free enzyme in different McIlvaine pH buffers. Assay Initial Concentrations: 0.75 ADH units/mL assay, 20mM Ethanol, 1mM NAD. (A) pH 7.4, Free Enzyme (●); pH 2.0, Free Enzyme (■). Hollow shapes depict activity of gel-conjugated ADH at pH 7.4 and pH 2.0. (B) Gel Conjugated ADH submersed in pH 7.4 initially (♦), pH 2.0 initially, (■), and gel experiencing a shift from pH 2.0 to pH 7.4 (▲).

6.5 REFERENCES

1. Braden, C. I., Jornvall, H., Eklund, H., Furugren, H. (1975). In Enzymes, 3rd ed.; Bayer, P. D., Ed.; Academic:
New York, Vol. 2, p 103.

2. Kelly, N., Flynn, A. and Johnson, D. B. (1977), Preliminary investigations on the immobilization of yeast alcohol dehydrogenase. Biotechnology and Bioengineering, 19: 1211–1213.

3. Bille, V. and Remacle, J. (1986), Simple-kinetic descriptions of alcohol dehydrogenase after immobilization on tresyl-chloride-activated agarose. European Journal of Biochemistry, 160: 343–348.

4. Wheeldon IR, Campbell E, Banta S. (2009). A chimeric fusion protein engineered with disparate functionalities-enzymatic activity and self-assembly. J. Mol. Biol. 392:129–42

5. Zhi-de Zhou, Gui-yin Li, Yuan-jian Li. (2010). Immobilization of Saccharomyces cerevisiae alcohol dehydrogenase on hybrid alginate-chitosan beads. International Journal of Biological Macromolecules 47, 21-26.

6. S. Miyamoto, T. Murakami, A. Saiti and J. Kimura, (1991). Development of an amperometric alcohol sensor based on immobilized alcohol dehydrogenase and entrapped NAD+**,** *Biosens. Bioelectron.* 6, 563.

7. Juan M. Bolivar, Lorena Wilson, Susana Alicia Ferrarotti, Jose M. Guisan, Roberto Fernandez-Lafuente, Cesar Mateo. (2006). Improvement of the stability of alcohol dehydrogenase by covalent immobilization on glyoxyl-agarose, Journal of Biotechnology 1251, 85-94.

8. Haynes, C. A., Norde, W. J. (1995). Structures and stabilitys of adsorbed proteins. Colloid Interf Sci, 169, 313.

9. Steadman, B. L., Thompson, K. C., Middaugh, C. R., Matsuno, K., Vrona, S., Lawson, E. Q., Lewis, R. V. (1992). The effects of surface adsorption on the thermal stability of proteins. Biotechnol Bioeng, 40, 8.

10. Basinska, T., and Slomkowski, S. (1995). Attachment of horseradish peroxidase (HRP) onto the poly(styrene/acrolein) latexes and onto their derivatives with amino groups on the surface; activity of immobilized enzyme. Colloid Polym Sci, 273, 431.

11. Geluk, M. A, Norde, W., van Kalsbeek, H. K. A. I., van't Riet, K. (1992). Adsorption of lipase from *Candida rugosa* on cellulose and its influence on lipolytic activity. Enzyme Microbiol Technol, 14, 748.

12. Kondo, A.; Urabe, T.; Yoshinaga, K. (1996). Adsorption activity and conformation of α-amylase on various ultrafine silica particles modified with polymer silane coupling agents. Colloids Surfaces A: Physicochem and Engr Asp, 109, 129.

13. Lowman, A.M. and Peppas, N.A. (1997). Analysis of the Complexation/Decomplexation Phenomena in Graft Copolymer Networks. Macromolecules *30* (17), 4959-4965.

14. Kagi, J. H. R. & Vallee, B. L. (1960). The role of zinc in alcohol dehydrogenase. J. Biol. Chem. 235, 3188-3192.

15. Bille V, Plainchamp D, Remacle J. (1987). Affinity and stability modifications of immobilized alcohol dehydrogenase through multipoint copolymerization, Biochimica et Biophysica Acta, 915, 393-398.

16. Koji Nakamura, Robert J. Murray, Jeffrey I. Joseph, Nicholas A. Peppas, Mariko Morishita, Anthony M. Lowman. (2004). Oral insulin delivery using P(MAA-g-EG) hydrogels: effects of network morphology on insulin delivery characteristics. Journal of Controlled Release 95, 589-599.

CHAPTER 7

CONCLUSIONS AND FUTURE DIRECTION

In this work, our research has shown the very successful development of a three enzyme system that is useful at optimized enzyme concentrations for the metabolism of ethanol at rates that exceed human detoxification by nearly seven times. For the purpose of immediate ethanol conversion from blood alcohol content of 0.10% to legal limits and for zero toxic bi-product acetaldehyde buildup, the multi-enzyme system requires as little as 10-20 minutes, and complete ethanol conversion is possible within an hour. With the development of kinetic equations for yeast aldehdye dehydrogenase and rabbit muscle lactate dehydrogenase, we have produced simulations that very accurately, even with the presence of inhibiting substrate and product concentrations of acetaldehyde, pyruvate, and cofactor, reflect in vitro effectiveness of our multi-enzyme microreactor. The simulation promotes the efficient performance of concerted activity of the enzymes due to the prevention of inhibiting concentrations. Based on our source of enzymes, we have determined an optimum enzyme ratio of 30%:20:%:50% ADH:ALDH:LDH. Also, we have concluded that ADH conjugation to a poly(methacrylic acid- grafted-ethylene glycol) hydrogel can serve as a prime biocompatible carrier with bioactivity unseen in typically acidic, hydrolyzing environments. The ADH gel in an acidic (pH 2.0) environment maintains an active rate around 53% of the rate of an enzyme gel in normal

(pH 7.4) conditions. Upon reversing the pH environment of the gel, the active rate still matches 71% of the original gel activity.

Moving forward, this biohybrid hydrogel system may provide effectual means of developing a multi-immobilized enzyme hydrogel that produces concerted activity similar to our in-vitro and simulated multi-enzyme system. Some potential research goals are establishing maximum load concentrations. Subsequently, gel kinetics may be studied to determine binding and diffusion limitations. Diffusion limitations may then lead to studies into optimization of the polymer network. Moreover, alternate enzyme sources provide opportunity for greater activity and emerging metabolic engineering strategies offer potential for reduced inhibition through gene knockout and easy production of protein through recombination methods.

APPENDIX A

BUFFERS, ASSAYS, and STANDARDIZATIONS

Buffer Composition:

Buffer solution was typically prepared prior to kinetic experiments in quantities of about 220mL and was kept refrigerated before use for no more than 10 days. Masses of 2.84g of sodium phosphate dibasic and 1.74g of potassium phosphate dibasic salts were dissolved in 200mL of distilled water. 1.38g sodium phosphate monobasic salt was mixed in 50mL distilled water to produce a 200mM solution. The monobasic solution was slowly titrated using a burette into the beaker with the dibasic solution under continual stirring. The pH was monitored with a Fisher Accumet Basic AB15Plus Meter. Beginning at 9.1 pH, the dibasic solution became the desirable 7.8 pH after the addition of 17-20mL of the monobasic sodium phosophate at 22±1 °C. The resulting concentration of buffer was usually in the range of 200 mM-sodium, 90 mM potassium, 150mM phosphate. The buffer solution was utilized for all enzyme assay and reagent stock solutions.

NADH and ADH Standardization:

Because all enzyme catalysis in this work involves cofactor oxidation of NADH and reduction of NAD, rates of reaction can be observed spectrophotometrically at 340nm utilizing a Gilford Spectrophotometer. A standardization curve of β-Nicotinamide adenine dinucleotide, reduced disodium salt, purchased from Sigma-Aldrich (St. Louis, MO), at various concentrations in buffer solution was produced to determine the extinction coefficient according to the Gilford device using a single cuvette. The extinction coefficient is 4.997 millimolar. The extinction coefficient on the Synergy Biotek instrument is 3.182 millimolar for a 6-well plate configuration.

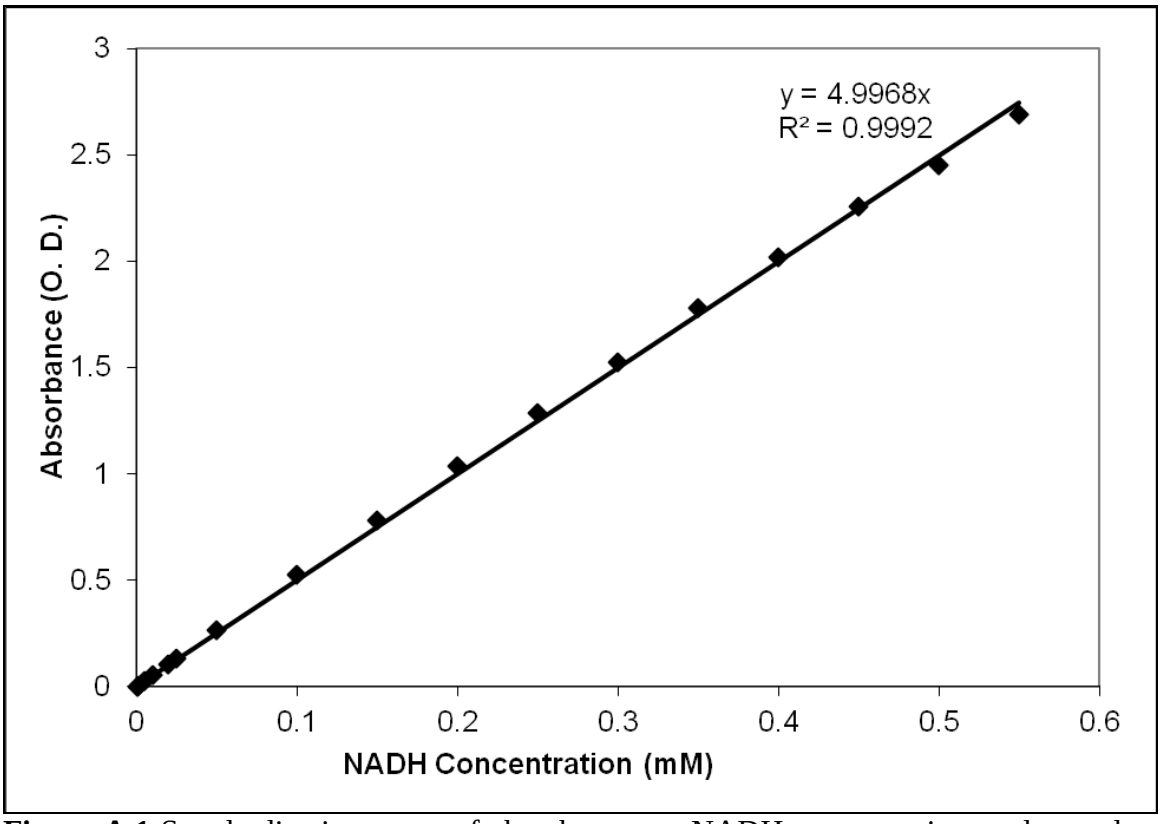

Figure A.1 Standardization curve of absorbance vs. NADH concentration as detected at 340nm wavelength on the Gilford Spectrophotometer.

A standardization curve of yeast aldehyde dehydrogenase purchased from Sigma-Aldrich (St. Louis, MO), at various concentrations in buffer solution was produced to determine the unit per milliliter concentration of the protein measured at 280nm UV wavelength on the Synergy Biotek device using a 96-well plate configuration. The curve was used to determine protein concentration of ADH following filtration procedures

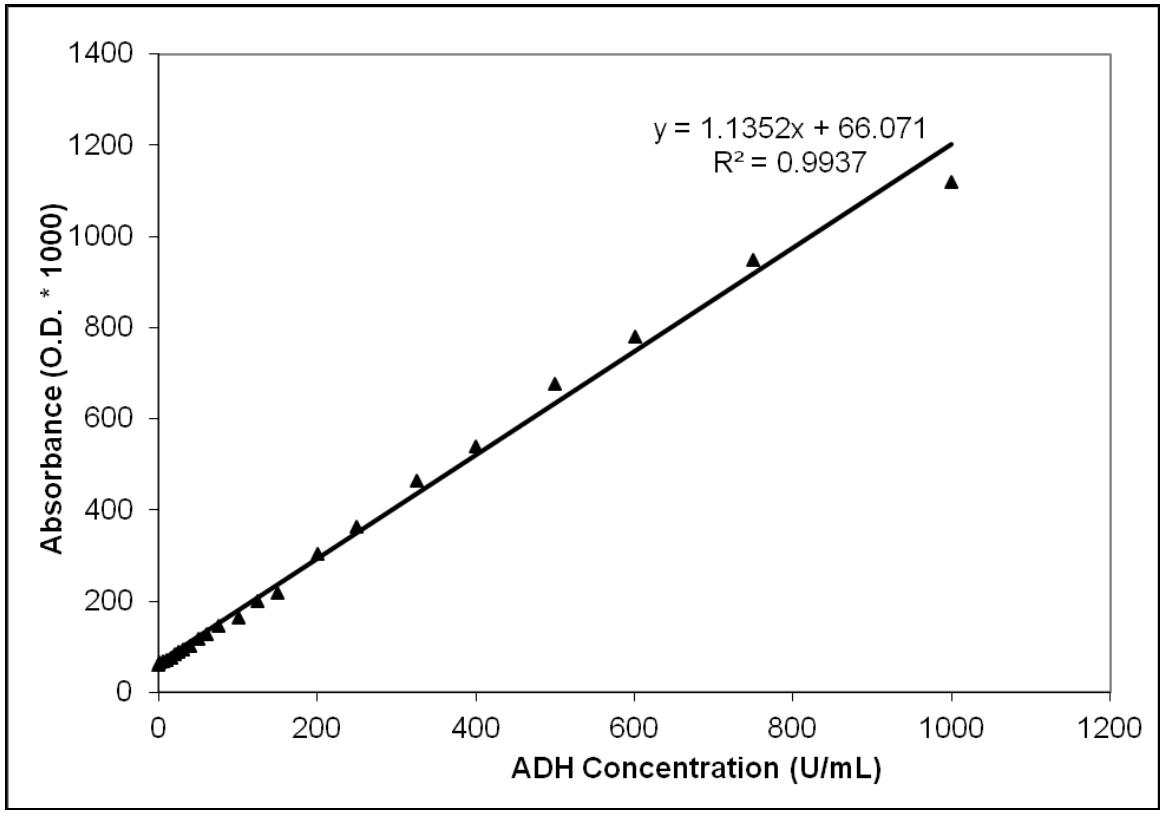

Figure A.2 Standardization curve of ADH bottle unit concentration vs. absorbance in the Synergy Biotek device at 280nm wavelength.

Enzyme Activity Assays - LDH:

Before taking enzyme kinetic data, stock solution of L-lactate dehydrogenase (LDH, EC 1.1.1.27) was assayed regularly to ascertain activity under experimental conditions (pH 7.8, 22±1 °C) versus reported activity of units/mg listed on the Sigma-Aldrich bottle label. Assay conditions called for a concentration of 2.3mM pyruvate and 0.12mM NADH as substrate and co-factor at pH 7.5 and 37°C following a modified published procedure (see Chapter 3). Stock solutions of substrates were prepared separately in buffer solution according to amount and concentration necessary for the kinetic study being conducted. Bovine serum albumin was excluded. The assay mixture was prepared using a total 3mL of solution. Upon adding LDH stock solution to attain 0.075 units/mL, based on the label amount weighed out on a Sartorius microbalance, the cuvette was promptly covered with Teflon film, shaken 2-3 times, and placed in the holding cell of a Gilford spectrophotometer. Initial reading was observed 15 seconds after addition of enzyme to the assay and every 15 seconds thereafter. Optical density values, reported by the spectrophotometer with absorbance set to 340nm, were recorded into a prepared excel spreadsheet. The rate determinations were carried out for 5 minutes or more. A control assay without enzyme present was also performed to account for natural deprotonation of NADH over the course of the 5-minute assay. Excel macros were used to convert absorbance to NADH concentrations using the established extinction coefficient of the cofactor. Absorbance and concentration of NADH was plotted vs. time whereby initial steady-state rates (mM/min) were determined from the linear portions of reaction progress curves. LDH activity, translated to units/mL, relative to the purified enzyme bottle label was usually calculated to be in the range of 45-60% activity at the buffer

conditions. Similar activities were observed for yeast ADH and ALDH purchased from Sigma-Aldrich according to the assay concentrations provided in the previous chapters. These enzymes had linear slopes for the increase of NADH concentration. These activities were necessary for adjusting simulated rate kinetics with experimental rate kinetics.

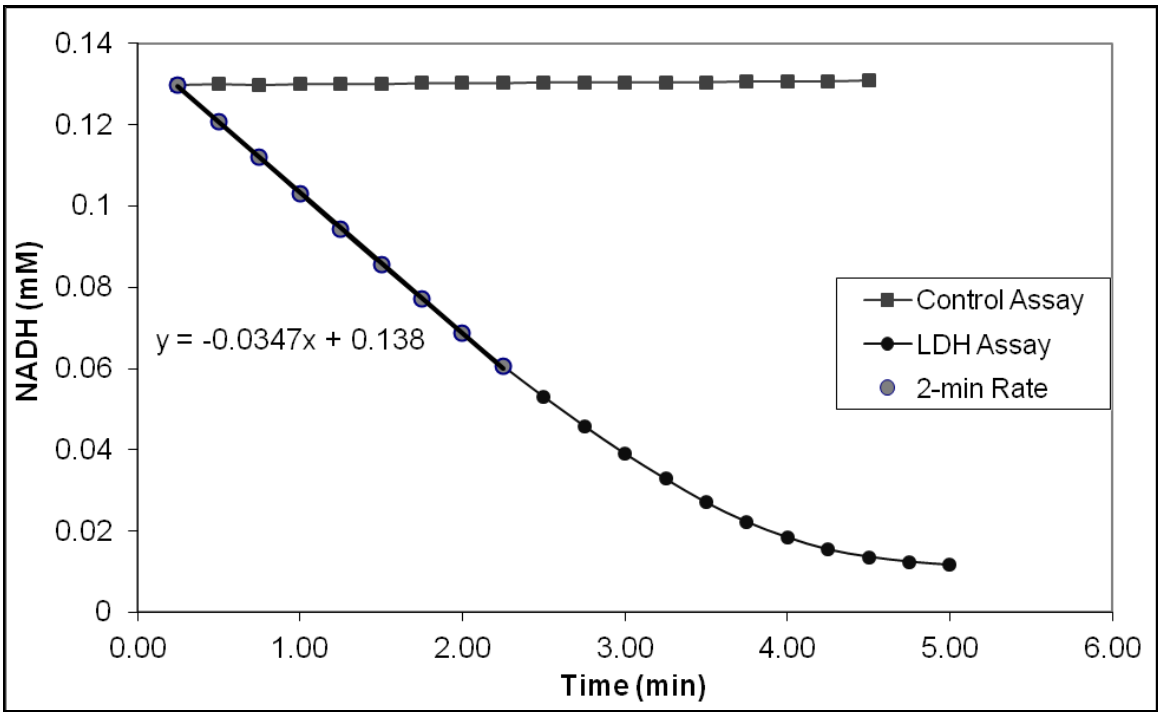

Figure A.3 Rate activity determination for l-lactate dehydrogenase based on the linear decrease of NADH concentrations. The actual rate is 0.0347mM/min compared to the 0.075 bottle units/mL ([=] mM/min) used. This correlates to a 46.3% activity at the tested conditions.

APPENDIX B

VISUAL BASIC THREE ENZYME SIMULATION

```
Sub threeEnzyme()
    Dim NAD As Double
    Dim EtOH As Double
    Dim Acetaldehyde As Double
    Dim Acetate As Double
    Dim NADH As Double
    Dim Pyruvate As Double
    Dim Lactate As Double
    Dim pH As Double
    Dim H As Double
    Dim t As Double
    Dim time As Double
    Dim step As Double
    Dim adh_rate As Double
    Dim aldh_rate As Double
    Dim ldh_rate As Double
    Dim i As Long
    Dim timestep As Double
    Dim count As Long

    pH = Range("B2")
    NAD = Range("B6")
    EtOH = Range("B7")
    Acetaldehyde = Range("B8")
    Acetate = Range("B9")
    NADH = Range("B10")
    Pyruvate = Range("B11")
    Lactate = Range("B12")
    time = Range("B14")

    H = (10 ^ -pH) * 1000


    step = 0.001
    timestep = 0
    count = 1
```

```
    Do
        Range("A18").Offset(count, 0) = timestep
        Range("B18").Offset(count, 0) = NAD
        Range("C18").Offset(count, 0) = EtOH
        Range("D18").Offset(count, 0) = Acetaldehyde
        Range("E18").Offset(count, 0) = NADH
        Range("F18").Offset(count, 0) = Pyruvate
        For i = 1 To 1000

            adh_rate = adh(NAD, EtOH, Acetaldehyde, NADH, H)
            aldh_rate = aldh(NAD, Acetaldehyde, Acetate, NADH)
            ldh_rate = ldh(NADH, Pyruvate, Lactate, NAD, H)

            NAD = NAD - (adh_rate + aldh_rate - ldh_rate) * step
            EtOH = EtOH - (adh_rate) * step
            Acetaldehyde = Acetaldehyde + (adh_rate - aldh_rate) * step
            Acetate = Acetate + (aldh_rate) * step
            NADH = NADH + (adh_rate + aldh_rate - ldh_rate) * step
            Pyruvate = Pyruvate - (ldh_rate) * step
            Lactate = Lactate + (ldh_rate) * step
            timestep = timestep + step
        Next i
        count = count + 1
    Loop While timestep < time
End Sub

Function adh(A As Double, B As Double, P As Double, Q As Double, H As Double) As
Double
'A: NAD+
'B: Ethanol
'P: Acetaldehyde
'Q: NADH
'H: Proton
    Dim Ka As Double
    Dim Kb As Double
    Dim Kp As Double
    Dim Kq As Double
    Dim Kia As Double
    Dim Kib As Double
    Dim Kip As Double
    Dim Kiq As Double
    Dim Keq As Double
    Dim Vmax As Double
    Dim FirstTerm As Double
    Dim SecondTerm As Double
```

```
    Dim ThirdTerm As Double
    Dim FourthTerm As Double
    Dim FifthTerm As Double
    Dim SixthTerm As Double
    Dim SeventhTerm As Double
    Dim EighthTerm As Double
    Dim NinthTerm As Double
    Dim TenthTerm As Double
    Dim EleventhTerm As Double
    Dim Denominator As Double
    Dim Numerator As Double

    Keq = 0.000000008
    Ka = 0.2978 '0.074
    Kb = 49.439 '130
    Kp = 0.78 '0.78
    Kq = 0.113 '0.108
    Kia = 0.2486 * 1.1 '0.61
    Kib = 51.24 '43
    Kip = 0.624 '0.67
    Kiq = 0.0177 * 2.75 '0.018
    Vmax = Range("B3")

    FirstTerm = Kia * Kb
    SecondTerm = Kb * A
    ThirdTerm = Ka * B
    FourthTerm = A * B
    FifthTerm = (Kia * Kb * Q) / Kiq
    SixthTerm = (Kia * Kb * Kq * P) / (Kiq * Kb)
    SeventhTerm = (Kia * Kb * P * Q) / (Kp * Kiq)
    EighthTerm = (Kb * Kq * A * P) / (Kiq * Kp)
    NinthTerm = (Ka * B * Q) / Kiq
    TenthTerm = (A * B * P) / Kip
    EleventhTerm = (Kia * Kb * B * P * A) / (Kp * Kiq * Kib)

    Denominator = FirstTerm + SecondTerm + ThirdTerm + FourthTerm + FifthTerm +
SixthTerm + SeventhTerm + EighthTerm + NinthTerm + TenthTerm + EleventhTerm
    Numerator = 0.5 * Vmax * ((A * B) - (Q * P * H) / Keq)

    adh = Numerator / Denominator

End Function
Function aldh(A As Double, B As Double, P As Double, Q As Double) As Double
'A: NAD+
'B: Acetaldehyde
```

```
'P: Acetate
'Q: NADH
    Dim Ka As Double
    Dim Kb As Double
    Dim Kp As Double
    Dim Kq As Double
    Dim Kia As Double
    Dim Kib As Double
    Dim Kip As Double
    Dim Kiq As Double
    Dim Kibb As Double
    Dim Kibbq As Double
    Dim Vmax As Double
    Dim FirstTerm As Double
    Dim SecondTerm As Double
    Dim ThirdTerm As Double
    Dim FourthTerm As Double
    Dim FifthTerm As Double
    Dim SixthTerm As Double
    Dim SeventhTerm As Double
    Dim EighthTerm As Double
    Dim NinthTerm As Double
    Dim TenthTerm As Double
    Dim EleventhTerm As Double
    Dim TwelfthTerm As Double
    Dim ThirteenthTerm As Double

    Dim Denominator As Double
    Dim Numerator As Double

    Ka = 0.14
    Kb = 0.015
    Kp = 0
    Kq = 0
    Kia = 1.2
    Kib = 0
    Kip = 0
    Kiq = 6.173
    Kibb = 2.55
    Kibbq = 0.02693

    Vmax = Range("B4")
    FirstTerm = Kia * Kb
    SecondTerm = Kb * A
    ThirdTerm = Ka * B
```

```
    FourthTerm = A * B
    FifthTerm = 0
    SixthTerm = 0
    SeventhTerm = 0
    EighthTerm = 0
    NinthTerm = Kiq * B * Q
    TenthTerm = 0
    EleventhTerm = 0
    TwelfthTerm = (B ^ 2) / Kibb
    ThirteenthTerm = (B ^ 2 * Q) / Kibbq

    Denominator = FirstTerm + SecondTerm + ThirdTerm + FourthTerm + FifthTerm +
SixthTerm + SeventhTerm + EighthTerm + NinthTerm + TenthTerm + EleventhTerm +
TwelfthTerm + ThirteenthTerm
    Numerator = 0.4 * Vmax * (A * B)

    aldh = Numerator / Denominator
End Function

Function ldh(A As Double, B As Double, P As Double, Q As Double, H As Double) As
Double
'A: NADH
'B: Pyruvate
'P: Lactate
'Q: NAD+
    Dim Ka As Double
    Dim Kb As Double
    Dim Kia As Double
    Dim Kip As Double
    Dim Keq As Double
    Dim FirstTerm As Double
    Dim SecondTerm As Double
    Dim ThirdTerm As Double
    Dim FourthTerm As Double
    Dim FifthTerm As Double
    Dim SixthTerm As Double
    Dim SeventhTerm As Double
    Dim EighthTerm As Double
    Dim NinthTerm As Double
    Dim TenthTerm As Double
    Dim EleventhTerm As Double
    Dim Denominator As Double
    Dim Numerator As Double

    Ka = 0.0107
```

```
    Kb = 0.301
    Kia = 0.00842
    Kip = 487.33
    Kib = 29.91
    Kibq = 97.47
    Keq = 1284
    Vmax = Range("B5")

    FirstTerm = Kia * Kb
    SecondTerm = Kb * A
    ThirdTerm = Ka * B
    FourthTerm = A * B
    FifthTerm = P / (Kip)
    SixthTerm = B ^ 2 * A / Kib
    SeventhTerm = B ^ 2 * Q / (Kibq)
    EighthTerm = 0
    NinthTerm = 0
    TenthTerm = 0
    EleventhTerm = 0

    Denominator = FirstTerm + SecondTerm + ThirdTerm + FourthTerm + FifthTerm +
SixthTerm + SeventhTerm + EighthTerm + NinthTerm + TenthTerm + EleventhTerm
    Numerator = 0.65 * Vmax * ((A * B) - (Q * P * H) / Keq)

    ldh = Numerator / Denominator
End Function
```